UNCLASSIFIED

AD NUMBER

AD450077

NEW LIMITATION CHANGE

TO

Approved for public release, distribution unlimited

FROM

Distribution authorized to U.S. Gov't. agencies and their contractors; Administrative/Operational Use; SEP 1964. Other requests shall be referred to Air Force Weapons Laboratory, Attn: WLRC, Kirtland AFB, NM 87117.

AUTHORITY

AFWL ltr, 29 Apr 1985

THIS PAGE IS UNCLASSIFIED

UNCLASSIFIED

AD. 450077

DEFENSE DOCUMENTATION CENTER

FOR

SCIENTIFIC AND TECHNICAL INFORMATION

CAMERON STATION ALEXANDRIA. VIRGINIA

UNCLASSIFIED

WL TDR-64-91

A QUASI-STATIC THEORY OF SOIL-STRUCTURE INTERACTION

September 1964
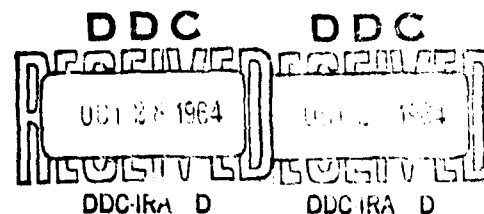
TECHNICAL DOCUMENTARY REPORT NO. WL TDR-64-91

Research and Technology Division
AIR FORCE WEAPONS LABORATORY
Air Force Systems Command
Kirtland Air Force Base
New Mexico

DDC

DDC

OCT 2 1964

DDC-IRA D

DDC IRA D

3.078

Project No 1080, Task No. 108003

by
R...

)

Research and Technology Division
Air Force Systems Command
AIR FORCE WEAPONS LABORATORY
Kirtland Air Force Base
New Mexico

Research and Technology Division
Air Force Systems Command
AIR FORCE WEAPONS LABORATORY
Kirtland Air Force Base
New Mexico

DDC AVAILABILITY NOTICE

Qualified requesters may obtain copies of this report from DDC.

ABSTRACT

This study treats the effect of the interaction between underground structures and the surrounding soil in reducing the loads transmitted to the structure, the so-called "arching" phenomenon.

A continuum theory of soils proposed by G. A. Geniev is applied to a quasi-static, plane-strain problem of arching. The basic partial differential equations are shown to form a hyperbolic set and are solved by the method of characteristics. Consistent stress and velocity fields are obtained.

Comparison with available experimental results shows that the Geniev theory underestimates the surface pressure required for failure of an underground structure in relatively dense granular soils. The source of this difficulty is explained and an approximate method of overcoming it is presented.

A simplified extension to a theory taking account of inertia of the soil and unsteady motions is treated in an appendix.

PUBLICATION REVIEW

This report has been reviewed and is approved.

J. E. JOHNSON
Lt   USAF
Project Officer

THOMAS J LOWRY, JR.   WILLIAM H. STEPHENS
Colonel   USAF   Colonel   USAF
Chief, Civil Engineering Branch   Chief, Research Division

TABLE OF CONTENTS

iii

TABLE OF CONTENTS (CONTD)

LIST OF FIGURES

v

LIST OF FIGURES (CONTD)

1. INTRODUCTION TO THE SOIL-STRUCTURE INTERACTION PROBLEM

1.1 Object and Scope

The purpose of the main part of this report (Chapters 1-6) is to investigate the applicability of a continuum theory of granular media to the problem of soil-structure interaction of underground structures. The problem essentially involves a determination of the effect of "arching"[1,2] in granular soils on the pressure transmitted to a buried structure when the ground surface is subjected to a loading in the form of an air overpressure such as would result from the detonation of a high-yield nuclear device.

The air overpressure loading is assumed to result from an air burst occurring either high above the ground surface or near the ground surface with a superseismic velocity of propagation of the pressure wave, so that only the air-induced pressure need be considered. The air-over-pressure loading is assumed to vary slowly with time and to be uniformly distributed over an infinitely large area as far as the underground structure is concerned. A pressure distribution of this type is adequate for an introductory study. For the truly dynamic problem a more realistic pressure distribution is needed. In the superseismic case the pressure wave propagates downward through the soil inclined at an angle to the ground surface;[3] however for simplicity the pressure wave is assumed to propagate vertically downward with the wave front parallel to the ground surface.

The soil is considered to be a homogeneous, isotropic, granular material having some cohesion and satisfying the Coulomb-Mohr failure criterion which states that slip or failure occurs at a point when the shear stress on some place through the point is equal to the sum of the cohesion and a function of the normal stress acting on the same plane. On no plane

1

can the shear stress exceed this sum. The function of the normal stress is taken to be a constant, namely, the tangent of the angle of internal friction ϕ, times the normal stress. The fact that the failure criterion depends on the hydrostatic part of the stress tensor and not simply on the deviatoric part, as is the case in the theory of plasticity for metals, adds an important complication to the problem as will be seen later.

The structure to be considered is a long, rectangular plate, simply supported at the edges. It is assumed that the length-width ratio of the plate is large, so that conditions of plane strain will prevail away from the ends of the long side. It follows from these assumptions that the behavior of the structure may be considered to be that of a beam, and the problem may be formulated in two-dimensional plane strain.

The depth of burial of the underground structure is in the shallow range with the maximum depth of interest on the order of twice the span length. It is in this range of depths that the effect of arching in the soil is expected to be a maximum. Although the attenuation of free-field air-overpressure by the soil may be significant in this range,[4] only the redistribution of pressure caused by soil-structure interaction will be considered in determining the pressure transmitted to the structure.

An important effect of the soil on the nature of the pressure wave, particularly for dynamic studies, leads to an increase in the rise time of the pressure pulse as the wave propagates downward through the soil[5,6]. This increased rise time tends to reduce dynamic effects.

1.2 Summary of Previous Work

One of the earliest studies of the soil-structure interaction problem to appear in the literature was Terzaghi's "Trap Door" experiment.[17]

2

With a simple device he showed that a small downward movement of an underground structure results in a large decrease in the intensity of pressure applied to the structure. This type of behavior is of interest for the design of tunnel liners or large underground conduits as well as the design of underground blast-resistant structures.

Several methods have been used to evaluate the effect of soil-structure interaction on underground structures subjected to air-blast loadings. One study was made by considering the soil to be an ideal elastic material.[8] Spherical and cylindrical models were treated by considering a uniformly distributed, radially symmetric pressure, and using equations of equilibrium and compatibility from the theory of elasticity. The method was applied to shapes of structures other than spherical by considering the compressibility of the structure, that is, the change in volume due to externally applied loads.

Another approach considered only the Rankine passive earth pressure developed by the soil as a flexible two-hinged arch moved into the soil mass.[9] The problem was reduced to a single-degree-of-freedom system consisting of a lumped mass restrained by a weightless spring with the configuration being defined by the radial deflection of the arch at the quarter-point of the arch rib. For all arches considered, the response was found to occur in the plastic, or yielded, part of the assumed elastic-plastic resistance diagram for the soil.

A more realistic approach utilizing the classical Rankine earth pressure theory has been made by considering both the active and passive states of stress in the soil and the different soil masses entering into the response as the arch deflects.[3] In this case, the structure consisted of four rigid,

3

massless bars connected by rotation resisting springs. In determining the dynamic response of the two-degree-of-freedom system, the masses were assumed to be concentrated at the bar connections. The blast overpressure acting on the ground surface of the soil failure wedge was taken into account in determining the total resistance of the soil mass.

A dynamic analysis based on the formation of vertical slip planes in the soil between the structure and the ground surface and a uniform distribution of vertical stress on horizontal sections has been made for pseudo-steady state air overpressure.[10] In this analysis the failure mass of soil is considered to undergo a rigid body motion along with the structure. In this theory no account is taken of the propagation of the pressure wave through the soil or the associated dynamic soil-structure interaction.

4

1.3 Notation

A list of primary symbols used in the first six chapters is summarized for convenience in the following.

a_x, a_y = components of acceleration in the x and y directions

H = depth of burial of structure

K = ratio of horizontal to vertical stress at a point in the soil

k = soil cohesion in units of stress

L = span length of structure

p_o = intensity of overpressure at the ground surface

q = intensity of pressure loading on the structure

r, θ = polar coordinates

v_x, v_y = components of velocity in the x and y directions

X, Y = intensities of body force in the x and y direction

x, y = rectangular coordinates

α = direction of the velocity vector measured counterclockwise from the positive x-axis in rectangular coordinates

$\bar{\alpha}$ = direction of the velocity vector measured counterclockwise from the positive radius vector in polar coordinates

β = direction of the maximum principal stress measured counterclockwise from the positive x-axis in rectangular coordinates

$\bar{\beta}$ = direction of the maximum principal stress measured counterclockwise from the positive radius vector in polar coordinates

γ = $\pi/4 - \varphi/2$. Physically, the inclination of possible slip planes to the direction of principal stress

ϵ_x, ϵ_y = components of strain in the x and y directions

$\dot{\epsilon}_x, \dot{\epsilon}_y$ = components of strain-rate in the x and y directions

γ_{xy} = shear strain

$\dot{\gamma}_{xy}$ = shear strain rate

5

ξ, η = rectangular coordinates on the characteristic plane

ρ = density of the soil mass per unit volume

σ_x, σ_y = components of stress in the x and y directions

τ_{xy} = shear stress

σ_1, σ_2 = principal stress

σ_n, τ_n = normal stress and shear stress on failure plane

σ_v = combined stress and velocity variables

φ = angle of internal friction of the soil

X = angle between the x-axis and the characteristic curve

6

2. DYNAMIC THEORY OF GRANULAR MEDIA

2.1 Assumptions

The theory of the dynamics of granular media to be presented in this and the next two chapters follows that of G. A. Geniev[11]. In applying this theory to the problem of soil dynamics, it is assumed that the soil will benave as a continuous and homogeneous granular medium having a shearing resistance consisting of the cohesion, which is assumed to be a constant independent of the stress state at a point, and internal friction, which is assumed to be a linear function of the mean normal stress.

It has been shown by experiment[1] that the resistance to slip along a plane through a typical point in the medium is given by

$$|\tau_n| = \sigma_n \tan \varphi + k \qquad (2.1.1)$$

where σ_n, τ_n = the normal and tangential components of the stress vector acting at the point,

φ = the angle of internal friction,

k = the cohesion.

Planes in the soil medium on which the relation

$$\max \left[|\tau| - (\sigma_n \tan \varphi + k) \right] = 0 \qquad (2.12)$$

is satisfied are called slip planes. At any point in a region of slip there are two planes along which slip may occur. The one along which slips actually occur is called the "active slip plane."

When equilibrium is destroyed, a velocity field resulting from the relative motion of the soil particles is set up in the soil. It is assumed

that this velocity field will satisfy the equation of continuity from the theory of continuous media. It is further assumed that when flow occurs the stress components may be expressed in terms of the strain rates.

As stated in Chapter 1, the two-dimensional plane problem will be considered in which the stress components σ_x, σ_y, τ_{xy} and the velocity components v_x and v_y are expressed as functions of the space variables x and y and the time t. Since relatively large displacements are expected, the problem has been formulated in Eulerian coordinates so that the motion is expressed in terms of the components of the velocity field rather than the displacements of the particles. After a complete velocity solution has been obtained, the particle displacements may be found by direct integration.

2.2 Equations of Motion

Figure 2.1 shows an infinitesimal element of the soil medium which is in a state of flow and which is acted upon by the direct stresses σ_x and σ_y and the shear stress τ_{xy}. The sign convention adopted here takes compressive stresses positive, so that the inward normal stress acting on a surface of the element shown in Fig. 2.1 is positive if the inward normal to the surface is in the direction of the negative coordinate axis. Positive shearing stress on a surface acts in the negative direction of one coordinate axis when the inward normal to the surface acts in the negative direction of the other coordinate axis. This sign convention is opposite to the usual convention in the theory of elasticity; however, it is convenient since the normal stresses usually encountered in soils are compressions.

If X and Y are the intensities of the body force and ρ is the mass per unit volume, the equation of motion in the x-direction of the element in Fig. 2.1 is:

8

$$\rho \, X \, dx \, dy - (\sigma_x + \frac{\partial \sigma_x}{\partial x} \, dx) \, dy + \sigma_x \, dy - (\tau_{xy} + \frac{\partial \tau_{xy}}{\partial y} \, dy) \, dx$$

$$+ \, \tau_{xy} \, dx = \rho \, dx \, dy \, a_x$$

where a_x is the acceleration of the element in the x-direction. This equation may be written as

$$X - \frac{1}{\rho} (\frac{\partial \sigma_x}{\partial x} + \frac{\partial \tau_{xy}}{\partial y}) = a_x \qquad (2.21)$$

Similarly, the equation of motion in the y-direction yields

$$Y - \frac{1}{\rho} (\frac{\partial \tau_{xy}}{\partial x} + \frac{\partial \sigma_y}{\partial y}) = a_y \qquad (2.2.2)$$

In Eulerian coordinates the acceleration terms a_x and a_y in Eqs. (2.2.1) and (2.2.2) are expressed as functions of the velocity components, v_x and v_y by

$$a_x = \frac{\partial v_x}{\partial t} + v_x \frac{\partial v_x}{\partial x} + v_y \frac{\partial v_x}{\partial y} \qquad (2.2.3)$$

$$a_y = \frac{\partial v_y}{\partial t} + v_x \frac{\partial v_y}{\partial x} + v_y \frac{\partial v_y}{\partial y} \qquad (2.2.4)$$

Using these expressions, the equations of equilibrium become

$$X - \frac{1}{\rho} (\frac{\partial \sigma_x}{\partial x} + \frac{\partial \tau_{xy}}{\partial y}) = \frac{\partial v_x}{\partial t} + v_x \frac{\partial v_x}{\partial x} + v_y \frac{\partial v_x}{\partial y} \qquad (2.2.5)$$

$$Y - \frac{1}{\rho} (\frac{\partial \tau_{xy}}{\partial x} + \frac{\partial \sigma_y}{\partial y}) = \frac{\partial v_y}{\partial t} + v_x \frac{\partial v_y}{\partial x} + v_y \frac{\partial v_y}{\partial y} \qquad (2.2.6)$$

2.3 Failure Criterion

As stated earlier, slip will occur when the stress components satisfy the relation

9

$$\max \quad \big| \; |\tau_n| - (\sigma_n \tan \varphi + k) \; \big| = 0$$

The points on a Mohr stress diagram which satisfy this relation form an envelope of possible states of stress at failure. One such stress state is shown on the Coulomb-Mohr diagram in Fig. 2.2. The radius of a Mohr circle for a state of stress satisfying the failure criterion is $\frac{1}{2}(\sigma_1 - \sigma_2) = \tau_{max.}$ where σ_1 and σ_2 are the maximum and minimum principal stresses. The principal stresses σ_1 and σ_2, and $\tau_{max.}$ are related to xy-components of stress by

$$\sigma_1 = \frac{1}{2}(\sigma_x + \sigma_y) + \frac{1}{2}\sqrt{(\sigma_x - \sigma_y)^2 + 4\,\tau_{xy}^2} \qquad (2.3.1)$$

$$\sigma_2 = \frac{1}{2}(\sigma_x + \sigma_y) - \frac{1}{2}\sqrt{(\sigma_x - \sigma_y)^2 + 4\,\tau_{xy}^2} \qquad (2.3.2)$$

$$\tau_{max.} = \frac{1}{2}(\sigma_1 - \sigma_2) = \frac{1}{2}\sqrt{(\sigma_x - \sigma_y)^2 + 4\,\tau_{xy}^2} \qquad (2.3.3)$$

Expressions for σ_n and τ_n are obtained from Fig. 2.2 to be

$$\sigma_n = \frac{1}{2}(\sigma_x + \sigma_y) - \frac{1}{2}\sqrt{(\sigma_x - \sigma_y)^2 + 4\,\tau_{xy}^2} \; \sin. \; \varphi \qquad (2.3.4)$$

$$\tau_n = \frac{1}{2}\sqrt{(\sigma_x - \sigma_y)^2 + 4\,\tau_{xy}^2} \; \cos. \; \varphi \qquad (2.3.5)$$

Substituting Eqs. (2.3.4) and (2.3.5) into the Coulomb failure criterion, Eq. (2.1.1), one obtains:

$$(\sigma_x - \sigma_y)^2 + 4\,\tau_{xy}^2 = \sin^2\varphi \, (\sigma_x + \sigma_y + 2k \cot \varphi)^2 \qquad (2.3.6)$$

10

It may be seen from Fig. 2.2 that the two possible slip planes are inclined at angles $\pm \gamma$ to the direction of the maximum principal stress, where the angle γ is given by

$$\gamma = \frac{\pi}{4} - \frac{\Theta}{2} \tag{2.3.7}$$

The angle between the slip planes and the x-axis is determined by introducing the angle β which is the angle between the direction of maximum principal stress and the x-axis. Then the slip planes will form at angles $\beta \pm \gamma$ to the x-axis, as is shown in Fig. 2.3.

2.4 Equation of Continuity

According to the theory of continuous media, the velocity components and the density are related by the principle of conservation of mass in the following way:

$$\frac{\partial \rho}{\partial t} + \frac{\partial(\rho v_x)}{\partial x} + \frac{\partial(\rho v_y)}{\partial y} = C \tag{2.3.8}$$

If the medium is incompressible, the equation of continuity becomes:

$$\frac{\partial v_x}{\partial x} + \frac{\partial v_y}{\partial y} = 0 \tag{2.3.9}$$

2.5 The Kinematic Relations

The kinematic relations are expressions which relate the stresses to the velocity field. The two such relations to be considered here are based on the following assumptions:

1. The shear strain rate is taken to be a maximum along the direction of active slip, (2.5.1).

11

2. Tne velocity vector is restricted to coincide with the directions of active slip, (2.5.2).

The first of these relations considers the soil to be essentially a truly continuous medium while the second attempts to account for the behavior of a medium consisting of a system of particles whose dimensions are small but not insignificant.

The theories resulting from each of these relations will be referred to as the continuum theory and, as Geniev calls it, the macro-structural theory, respectively.

2.5.1 **Kinematic Relation for the Continuum Theory.** Figure 2.4 shows the Mohr circle of the strain rates $\dot{\epsilon}_x$, $\dot{\epsilon}_y$, and $\frac{1}{2}\dot{\gamma}_{xy}$ which are related to the velocity components by

$$\dot{\epsilon}_x = \frac{\partial v_x}{\partial x} \quad , \quad \dot{\epsilon}_y = \frac{\partial v_y}{\partial y}$$

and

$$\frac{1}{2}\dot{\gamma}_{xy} = \frac{1}{2}\left(\frac{\partial v_y}{\partial x} + \frac{\partial v_x}{\partial y}\right)$$

The direction of the maximum shear strain rate with respect to the x-axis is given by the angle χ, which from Fig. 2.4 is

$$\tan 2\chi = \frac{\dot{\epsilon}_y - \dot{\epsilon}_x}{\gamma_{xy}} = \frac{\frac{\partial v_y}{\partial y} - \frac{\partial v_x}{\partial x}}{\frac{\partial v_y}{\partial x} + \frac{\partial v_x}{\partial y}} \qquad (2.5.1)$$

12

Since the maximum shear strain rate occurs along a slip line in this theory, the angle X is:

$$X = (\beta \pm \gamma)$$

In Fig. 2.5, this relationship is shown clearly. Then from Fig. 2.4

$$\tan 2(\beta \pm \gamma) = \frac{\dfrac{\partial v_y}{\partial y} - \dfrac{\partial v_x}{\partial x}}{\dfrac{\partial v_y}{\partial x} \quad \dfrac{\partial v_x}{\partial y}} \tag{2.5.2}$$

From the Mohr circle of stresses shown in Fig. 2.5,

$$\tan 2\beta = \frac{2\,\tau_{xy}}{\sigma_x - \sigma_y} \tag{2.5.3}$$

Combining Eqs. (2.5.2) and (2.5.3), the kinematic relation between the stress and velocity fields is obtained for the continuum theory.

$$\frac{2\,\tau_{xy}}{\sigma_x - \sigma_y} = \frac{\left(\dfrac{\partial v_y}{\partial y} - \dfrac{\partial v_x}{\partial x}\right)\tan\varphi \mp \left(\dfrac{\partial v_y}{\partial x} + \dfrac{\partial v_x}{\partial y}\right)}{\left(\dfrac{\partial v_y}{\partial x} + \dfrac{\partial v_x}{\partial y}\right)\tan\varphi \pm \left(\dfrac{\partial v_y}{\partial y} - \dfrac{\partial v_x}{\partial x}\right)} \tag{2.5.4}$$

This may also be written as follows:

$$\frac{2\,\tau_{xy}}{\sigma_x - \sigma_y} = \frac{\dfrac{1}{2}\left[\dfrac{\dfrac{\partial v_y}{\partial x} + \dfrac{\partial v_x}{\partial y}}{\dfrac{\partial v_x}{\partial x}}\right] \pm \tan\varphi}{1 \mp \dfrac{1}{2}\left[\dfrac{\dfrac{\partial v_y}{\partial x} + \dfrac{\partial v_x}{\partial y}}{\dfrac{\partial v_x}{\partial x}}\right]\tan\varphi} \tag{2.5.5}$$

13

2.5.2 <u>Kinematic Relation for the Macro-Structural Theory</u>. The second kinematic relation is based on the assumption that the velocity vector coincides with the direction of active slip. This assumption follows by considering a state of motion in which the soil grains are moving in tubes or layers of flow formed by adjacent stream lines as shown in Fig. 2.7. The smallest spacing of two stream lines is given by the dimensions of a single particle, and the velocity of flow in any layer varies with the width of that layer. If relative motion occurs in the soil medium, slip will take place along the boundaries of the layers of flow, that is, along the stream lines. Since the tangent to a stream line represents the direction of the velocity vector, the velocity vector may be assumed to coincide with the direction of lines of active slip.

In Fig. 2.7 a field of active slip lines and the direction of the velocity vector at a typical point is shown.

If α is the angle between the direction of the velocity and the x-axis, Fig. 2.7 gives

$$\tan \alpha = \frac{v_y}{v_x} \qquad (2.5.6)$$

Here, the direction of the slip line at the point is also given by the angle α,

$$\alpha = \beta \pm \gamma \qquad (2.5.7)$$

Then

$$\tan (\beta \pm \gamma) = \frac{v_y}{v_x} \qquad (2.5.8)$$

In Eq. (2.5.3), the stress components are related to the angle 2β from the Mohr circle.

14

$$\tan 2\theta = \frac{2\tau_{xy}}{\sigma_x - \sigma_y}$$

Since

$$\tan 2(\beta \pm \gamma) = \frac{2 \tan (\beta \pm \gamma)}{1 - \tan^2 (\beta \pm \gamma)} = \frac{2 \frac{v_y}{v_x}}{1 - (\frac{v_y}{v_x})^2} \qquad (2.5.9)$$

and

$$\tan 2(\beta \pm \gamma) = \frac{\tan 2\beta \pm \tan 2\gamma}{1 \mp \tan 2\beta \tan 2\gamma} \qquad (2.5.10)$$

an expression for $\tan 2\beta$ may be obtained.

$$\tan 2\beta = \frac{\frac{1}{2} (\frac{v_y}{v_x} - \frac{v_x}{v_y}) \pm \frac{1}{\tan 2\gamma}}{1 \pm \frac{1}{2} (\frac{v_y}{v_x} - \frac{v_x}{v_y}) \frac{1}{\tan 2\gamma}} \qquad (2.5.11)$$

Combining Eqs. (2.5.11) and (2.5.3), and noting that one obtains an equation which relates the stress and velocity fields

$$\frac{2\tau_{xy}}{\sigma_x - \sigma_y} = \frac{\frac{1}{2} (\frac{v_y}{v_x} - \frac{v_x}{v_y}) \pm \tan \phi}{1 \pm \frac{1}{2} (\frac{v_y}{v_x} - \frac{v_x}{v_y}) \tan \phi} \qquad (2.5.12)$$

15

Thus, the five unknown functions σ_x, σ_y, τ_{xy}, v_x and v_y are given by the five equations, (2.2.5), (2.2.6), (2.3.6), (2.3.8) or (2.3.9), and (2.5.5) or (2.5.12).

It may be shown that the kinematic relations coincide in any region where the streamlines are parallel and the flow is steady. In this case the velocity vector does not vary with time or position, that is,

$$dv = \frac{\partial v}{\partial t} \, dt + \frac{\partial v}{\partial x} \, dx + \frac{\partial v}{\partial y} \, dy = 0,$$

where dx and dy refer to a segment of streamline.

Since the flow is steady, $\frac{\partial v}{\partial t} = 0$. Dividing the above equation by dt, one obtains the following expression:

$$\frac{\partial v}{\partial x} v_x + \frac{\partial v}{\partial y} v_y = 0 \qquad (2.5.13)$$

The velocity v may be expressed in terms of v_x and v_y by:

$$v^2 = v_x^2 + v_y^2 \qquad (2.5.14)$$

Differentiating Eq. (2.5.14) with respect to x, an expression for $\frac{\partial v}{\partial x}$ is obtained. Similarly $\frac{\partial v}{\partial y}$ is found.

$$\frac{\partial v}{\partial x} = \frac{1}{v} \left(v_x \frac{\partial v_x}{\partial x} + v_y \frac{\partial v_y}{\partial x} \right)$$

$$\frac{\partial v}{\partial y} = \frac{1}{v} \left(v_x \frac{\partial v_x}{\partial y} + v_y \frac{\partial v_y}{\partial y} \right) \qquad (2.5.15)$$

16

Substituting Eqs. (2.5.15) into (2.5.13) and solving the resulting quadratic expressions for $\dfrac{v_y}{v_x}$ and $\dfrac{v_x}{v_y}$, it turns out that:

$$\frac{v_y}{v_x} - \frac{v_x}{v_y} = \frac{\dfrac{\partial v_y}{\partial x} + \dfrac{\partial v_x}{\partial y}}{\dfrac{\partial v_x}{\partial x}} \qquad (2.5.16)$$

Thus, it may be seen that the two kinematic relations given by Eqs. (2.5.5) and (2.5.12) coincide in any region of steady flow with parallel stream lines.

17

3. TRANSFORMATION OF EQUATIONS BY THE METHOD OF CHARACTERISTICS

3.1 Method of Solution

Since the five equations relating the five unknowns form a system
of first order, quasi-linear partial differential equations of the hyperbolic
type, it is possible to formulate a procedure for the solution of these
equations by the method of characteristics[11,12,13]. In this formulation, the
system of five equations in five unknowns is replaced by the differential
equations of the characteristics and the differential equations called
"characteristic equations," to be satisfied along the characteristics. The
solution obtained by integrating the characteristic equations along the
characteristics is equivalent to the solution of the original system, but is
generally more convenient to obtain since the characteristic differential
equations and the differential equations of the characteristics are ordinary
rather than partial as in the original problem.

The method will be developed for the quasi-static case of an
incompressible soil medium. In this case the terms $\partial v_x/\partial t$ and $\partial v_y/\partial t$ are
neglected, and ρ is taken as constant, which results in the five equations:

$$Y - \frac{1}{\rho}\left(\frac{\partial \sigma_x}{\partial x} + \frac{\partial \tau_{xy}}{\partial y}\right) = v_x \frac{\partial v_x}{\partial x} + v_y \frac{\partial v_x}{\partial y} \qquad (3.1.1)$$

$$Y - \frac{1}{\rho}\left(\frac{\partial \tau_{xy}}{\partial x} + \frac{\partial \sigma_y}{\partial y}\right) = v_x \frac{\partial v_y}{\partial x} + v_y \frac{\partial v_y}{\partial y} \qquad (3.1.2)$$

$$(\sigma_x - \sigma_y)^2 + 4\tau_{xy}^2 = \sin^2\varphi\,(\sigma_x + \sigma_y + 2k\cot\varphi)^2 \qquad (3.1.3)$$

$$\frac{\partial v_x}{\partial x} + \frac{\partial v_y}{\partial y} = 0 \qquad (3.1.4)$$

18

$$\frac{2\,\tau_{xy}}{\sigma_x - \sigma_y} = \frac{\frac{1}{2}(\frac{\partial v_y}{\partial x} + \frac{\partial v_x}{\partial y}) \pm \frac{\partial v_x}{\partial x}\,\tan\varphi}{\frac{\partial v_x}{\partial x} \mp \frac{1}{2}(\frac{\partial v_y}{\partial x} + \frac{\partial v_x}{\partial y})\,\tan\varphi} \qquad (3.1.5)$$

or

$$\frac{2\,\tau_{xy}}{\sigma_x - \sigma_y} = \frac{\frac{1}{2}(\frac{v_y}{v_x} - \frac{v_x}{v_y}) \pm \tan\varphi}{1 \mp \frac{1}{2}(\frac{v_y}{v_x} - \frac{v_x}{v_y})\tan\varphi} \qquad (3.1.6)$$

The last equation, (3.1.5) or (3.1.6), is taken depending on which kinematic relation is used.

3.2 Transformation of Variables

It is convenient to define four new unknowns in terms of the original five, so that the algebraic equation of the failure criterion (3.1.3), is automatically satisfied. This will reduce the original system of five equations to four equations in the four new unknowns.

The principal stresses σ_1 and σ_2 may be expressed in terms of the stress components σ_x, σ_y, and τ_{xy}. From the Mohr circle of stresses, Fig. 2.5:

$$\sigma_1 = \frac{1}{2}(\sigma_x + \sigma_y) + \frac{1}{2}\sqrt{(\sigma_x - \sigma_y)^2 + 4\,\tau_{xy}^2}$$

$$\sigma_2 = \frac{1}{2}(\sigma_x + \sigma_y) - \frac{1}{2}\sqrt{(\sigma_x - \sigma_y)^2 + 4\,\tau_{xy}^2}$$

so that

$$\sqrt{(\sigma_x - \sigma_y)^2 + 4\,\tau_{xy}^2} = \sigma_1 - \sigma_2 \qquad (3.2.1)$$

19

and

$$\sigma_x + \sigma_y = \sigma_1 + \sigma_2 \qquad (3.2.2)$$

Taking the square root of both sides of Eq. (3.1.3) and using Eqs. (3.2.1) and (3.2.2), one obtains the equation of the failure criterion in terms of the principal stresses:

$$\sigma_1 + \sigma_2 = \frac{\sigma_1 - \sigma_2}{\sin \varphi} - 2k \cot \varphi \qquad (3.2.3)$$

The stress components σ_x, σ_y, and τ_{xy} are given by:

$$\sigma_x = \frac{1}{2} (\sigma_1 + \sigma_2) + \frac{1}{2} (\sigma_1 - \sigma_2) \cos 2\beta$$

$$\sigma_y = \frac{1}{2} (\sigma_1 + \sigma_2) - \frac{1}{2} (\sigma_1 - \sigma_2) \cos 2\beta$$

$$\tau_{xy} = \frac{1}{2} (\sigma_1 - \sigma_2) \sin 2\beta$$

Using Eq. (3.2.3), these equations become:

$$\sigma_x = \rho\sigma \ (1 + \sin \varphi \cos 2\beta) - k \cot \varphi \qquad (3.2.4)$$

$$\sigma_y = \rho\sigma \ (1 - \sin \varphi \cos 2\beta) - k \cot \varphi \qquad (3.2.5)$$

$$\tau_{xy} = \rho\sigma \ (\sin \varphi \sin 2\beta) \qquad (3.2.6)$$

where

$$\sigma = \frac{\sigma_1 - \sigma_2}{2 \rho \sin \varphi}$$

20

On the Coulomb-Mohr diagram, $\rho\sigma$ represents the distance from the intercept of
the failure envelope and the normal stress axis to the center of the Mohr
circle as shown in Fig. 2.2.

The velocity components v_x and v_y may be expressed as:

$$v_x = v \cos \alpha \qquad (3.2.7)$$

$$v_y = v \sin \alpha \qquad (3.2.8)$$

where

α = angle between the x-axis and the velocity vector v (Fig. 2.6).

3.3 Characteristics of the Continuum Theory

Using Eqs. (3.2.4), (3.2.5), (3.2.6), (3.2.7) and (3.2.8), the
original equations with the kinematic relation of the continuum theory may
be expressed in terms of the new unknowns σ, β, α, and v.

$$\frac{\partial \sigma}{\partial x} \cos (\beta + \gamma) + \frac{\partial \sigma}{\partial y} \sin (\beta + \gamma) + 2\sigma \tan \phi \left[\frac{\partial \beta}{\partial x} \cos (\beta + \gamma) + \frac{\partial \beta}{\partial y} \sin (\beta + \gamma) \right] +$$

$$+ \frac{v^2}{\cos \phi} \left[\frac{\partial \alpha}{\partial x} \cos (\beta - \gamma) + \frac{\partial \alpha}{\partial y} \sin (\beta - \gamma) \right] + \frac{A}{\cos \phi} = 0 \qquad (3.3.1)$$

$$\frac{\partial \sigma}{\partial x} \cos (\beta - \gamma) + \frac{\partial \sigma}{\partial y} \sin (\beta - \gamma) - 2\sigma \tan \phi \left[\frac{\partial \beta}{\partial x} \cos (\beta - \gamma) + \frac{\partial \beta}{\partial y} \sin (\beta - \gamma) \right] -$$

$$- \frac{v^2}{\cos \phi} \left[\frac{\partial \alpha}{\partial x} \cos (\beta + \gamma) + \frac{\partial \alpha}{\partial y} \sin (\beta + \gamma) \right] + \frac{B}{\cos \phi} = 0 \qquad (3.3.2)$$

21

$$v \tan \left[\alpha - (\beta \pm \gamma) \right] \left[\frac{\partial \alpha}{\partial x} \cos (\beta \pm \gamma) + \frac{\partial \alpha}{\partial y} \sin (\beta \pm \gamma) \right] -$$

$$\left[\frac{\partial v}{\partial x} \cos (\beta \pm \gamma) + \frac{\partial v}{\partial y} \sin (\beta \pm \gamma) \right] = 0 \qquad (3.3.3)$$

$$v \cot \left[\alpha - (\beta \pm \gamma) \right] \left[\frac{\partial \alpha}{\partial x} \sin (\beta \pm \gamma) - \frac{\partial \alpha}{\partial y} \cos (\beta \pm \gamma) \right] +$$

$$\left[\frac{\partial v}{\partial x} \sin (\beta \pm \gamma) - \frac{\partial v}{\partial y} \cos (\beta \pm \gamma) \right] = 0 \qquad (3.3.4)$$

where $\quad A = X \sin (\beta - \gamma) - Y \cos (\beta - \gamma)$

$B = -X \sin (\beta + \gamma) + Y \cos (\beta + \gamma)$

The first two equations of this set represent the equations of equilibrium in the directions perpendicular to the slip lines. Eqs. (3.3.3) and (3.3.4) express the conditions that the normal strain rates vanish in the directions along and perpendicular to the slip lines. It is now easy to see that the set (3.3.1), (3.3.2) is equivalent to the set (3.1.1), (3.1.2). Moreover, (3.3.4) and (3.3.5) taken together guarantee that the volumetric strain rate is zero (the center of the circle in Fig. (24) is at the origin). In addition, the normal strain rate of zero on a slip line then implies a maximum shear strain rate on this line. The equivalence with the original set for the first kinematic condition is now apparent.

The characteristics of Eqs. (3.3.1) to (3.3.4) may be defined as those curves $y = y(x)$ across which it is possible for the derivatives of the unknown functions σ, β, α, and v to exhibit finite discontinuities while the functions themselves remain continuous[13,15].

22

Along the curve $y = y(x)$, the unknowns satisfy the following differential relations:

$$d\sigma = \frac{\partial\sigma}{\partial x} dx + \frac{\partial\sigma}{\partial y} dy \quad ; \quad d\beta = \frac{\partial\beta}{\partial x} dx + \frac{\partial\beta}{\partial y} dy \quad ;$$

$$d\alpha = \frac{\partial\alpha}{\partial x} dx + \frac{\partial\alpha}{\partial y} dy \quad ; \quad dv = \frac{\partial v}{\partial x} dx + \frac{\partial v}{\partial y} dy$$

(3.3.5)

Equations (3.3.1) to (3.3.4) and (3.3.5) are a system of eight algebraic equations in the eight unknown derivatives of σ, β, α, and v with respect to x and y. Eliminating all derivatives with respect to x from these equations, the following equations are obtained involving only derivatives with respect to y:

$$\begin{bmatrix} a_1 & b_1 & c_1 & 0 \\ a_2 & b_2 & c_2 & 0 \\ 0 & 0 & c_3 & d_3 \\ 0 & 0 & c_4 & d_4 \end{bmatrix} \cdot \begin{bmatrix} \frac{\partial\sigma}{\partial y} \\ \frac{\partial\beta}{\partial y} \\ \frac{\partial\alpha}{\partial y} \\ \frac{\partial v}{\partial y} \end{bmatrix} = \begin{bmatrix} K_1 \\ K_2 \\ K_3 \\ K_4 \end{bmatrix}$$

(3.3.6)

where

$$a_1 = dx \sin(\beta + \gamma) - dy \cos(\beta + \gamma)$$

$$a_2 = dx \sin(\beta - \gamma) - dy \cos(\beta - \gamma)$$

$$b_1 = 2\sigma \tan\varphi \, a_1$$

$$b_2 = -2\sigma \tan\varphi \, a_2$$

$$c_1 = \frac{v^2}{c \cdot \varphi} a_2$$

$$c_2 = \frac{-v^2}{\cos \varphi} \, a_1$$

$$c_3 = v \tan \left[\alpha - (\beta \pm \gamma) \right] \left[dx \sin (\beta \pm \gamma) - dy \cos (\beta \pm \gamma) \right]$$

$$c_4 = v \cot \left[\alpha - (\beta \pm \gamma) \right] \left[dx \cos (\beta \pm \gamma) + dy \sin (\beta \pm \gamma) \right]$$

$$d_3 = - \left[dx \sin (\beta \pm \gamma) - dy \cos (\beta \pm \gamma) \right]$$

$$d_4 = \left[dx \cos (\beta \pm \gamma) + dy \sin (\beta \pm \gamma) \right] \tag{3.3.7}$$

$$-K_1 = \cos (\beta + \gamma) \, d\sigma + 2\sigma \tan \varphi \cos (\beta + \gamma) \, d\beta + \frac{v^2}{\cos \varphi} \cos (\beta - \gamma) \, d\alpha$$
$$+ \frac{A}{\cos \varphi} \, dx$$

$$-K_2 = \cos (\beta - \gamma) \, d\sigma - 2\sigma \tan \varphi \cos (\beta - \gamma) \, d\beta - \frac{v^2}{\cos \varphi} \cos (\beta + \gamma) \, d\alpha$$
$$+ \frac{B}{\cos \varphi} \, dx$$

$$-K_3 = \cos (\beta \pm \gamma) \left\{ v \tan \left[\alpha - (\beta \pm \gamma) \right] d\alpha - dv \right\}$$

$$K_4 = \sin (\beta \pm \gamma) \left\{ v \cot \left[\alpha - (\beta \pm \gamma) \right] d\alpha + dv \right\}$$

If the determinant of the matrix of coefficients in Eq. (3.3.6) is not zero, the derivatives of the unknowns may be determined uniquely along the curve $y = y(x)$. However, if the slope $\frac{dy}{dx}$ of the curve $y = y(x)$ is such that this determinant does vanish, then the derivatives of the unknown functions along the curve are not uniquely determined, and the curve is called a "characteristic."

The characteristics may be obtained by setting the determinant D of the coefficients in Eq. (3.3.6) equal to zero.

24

$$D = \begin{vmatrix} a_1 & b_1 & c_1 & 0 \\ a_2 & b_2 & c_2 & 0 \\ 0 & 0 & c_3 & d_3 \\ 0 & 0 & c_4 & d_4 \end{vmatrix} = 0 \qquad (3.3.8)$$

This determinant is equal to:

$$D = \begin{vmatrix} a_1 & b_1 \\ a_2 & b_2 \end{vmatrix} \cdot \begin{vmatrix} c_3 & d_3 \\ c_4 & d_4 \end{vmatrix} \qquad (3.3.9)$$

Equating the first of these determinants to zero, leads to the first system of characteristics.

$$\begin{vmatrix} a_1 & b_1 \\ a_2 & b_2 \end{vmatrix} = 0 \text{ or } 4\sigma \tan \varphi \cdot a_1 a_2 = 0$$

This gives

$$\frac{dy}{dx} = \tan (\beta + \gamma) \qquad (3.3.10)$$

and

$$\frac{dy}{dx} = \tan (\beta - \gamma) \qquad (3.3.11)$$

where γ is the angle between the slip planes and the direction of greatest principal stress, see Figs. (2.2) and (2.3).

These are the characteristics of the stress field, since they are a consequence of the stress equation only. Since a system of two real characteristic directions is obtained, the original equations have been shown to be hyperbolic. The stress field characteristics are inclined to the x-axis at angles $(\beta \pm \gamma)$, that is, at the same angles as the lines of slip. Hence, the lines of slip will coincide with the stress field characteristics on the xy-plane.

25

Equating the second of the determinants in Eq. (3.3.9) to zero leads to the second system of characteristics:

$$\begin{vmatrix} c_3 & d_3 \\ c_4 & d_4 \end{vmatrix} = 0$$

or

$$\frac{dy}{dx} = \tan (\beta \pm \gamma) \qquad\qquad (3.3.12)$$

$$\frac{dy}{dx} = -\cot (\beta \pm \gamma) \qquad\qquad (3.3.13)$$

These are the characteristics of the velocity field. The angle $(\beta + \gamma)$ or $(\beta - \gamma)$ is used according to whether the active slip line makes an angle of $(\beta + \gamma)$ or $(\beta - \gamma)$ to the x-axis. Thus, one of the velocity field characteristics coincides with the active slip line and the other is orthogonal to it as is shown in Fig. 3.1.

The characteristics, or lines along which the derivatives of the unknown functions may be discontinuous, have been obtained by setting the determinant of the coefficients in Eq. (3.3.6) equal to zero. However, for any solution to exist at all for the derivatives, the equations must not be inconsistent, that is, the determinant obtained by replacing any column of the matrix of coefficients on the left-hand side by the nonhomogeneous part of the equations must also vanish.

Replacing a column of coefficients on the left-hand side by the column on the right-hand side of Eq. (3.3.6) and setting this determinant equal to zero, yields the relation which must be satisfied along the characteristics. As before the relations decouple into stress field and velocity field equations.

26

Replacing the third column on the left of Eq. (3.3.6) by the column on the right and setting the determinant equal to zero leads to:

$$\begin{vmatrix} K_3 & d_3 \\ K_4 & d_4 \end{vmatrix} = 0 \qquad (3.3.14)$$

for the velocity field.

Evaluating this determinant yields:

along $\frac{dy}{dx} = \tan (\beta \pm \gamma)$;

$$v \tan \left[\alpha - (\beta \pm \gamma) \right] d\alpha - dv = 0 \qquad (3.3.15)$$

along $\frac{dy}{dx} = -\cot (\beta \pm \gamma)$

$$v \cot \left[\alpha - (\beta \pm \gamma) \right] d\alpha + dv = 0 \qquad (3.3.16)$$

The characteristic equations of the stress field are obtained from the following determinant:

$$\begin{vmatrix} a_1 & K_1 & c_1 & 0 \\ a_2 & K_2 & c_2 & 0 \\ 0 & K_3 & c_3 & d_3 \\ 0 & K_4 & c_4 & d_4 \end{vmatrix} = 0 \qquad (3.3.17)$$

Since the function α has been determined from the velocity field, the coefficients c_1 and c_2 times the derivatives of α may be treated as known quantities.

$$\begin{vmatrix} a_1 & K_1 - c_1 \frac{\partial \alpha}{\partial \gamma} \\ a_2 & K_2 - c_2 \frac{\partial \alpha}{\partial \gamma} \end{vmatrix} = 0 \qquad (3.3.18)$$

27

This yields:

along

$$\frac{dy}{dx} = \tan(\beta + \gamma); \qquad K_1 - c_1 \frac{\partial \alpha}{\partial y} = 0$$

$$(3.3.19)$$

along

$$\frac{dy}{dx} = \tan(\beta - \gamma); \qquad K_2 - c_2 \frac{\partial \alpha}{\partial y} = 0$$

Using Eqs. (3.3.7) and simplifying:

$$\frac{dx}{\cos(\beta + \gamma)} = \frac{d\sigma + 2\sigma \tan\varphi\, d\beta + \dfrac{v^2}{\cos\varphi} \dfrac{\cos(\beta - \gamma)}{\cos(\beta + \gamma)}\, d\alpha}{-\dfrac{A}{\cos\varphi} + \dfrac{v^2}{\cos(\beta + \gamma)} \left(\dfrac{\partial \alpha}{\partial y}\right)_1} \qquad (3.3.20)$$

and

$$\frac{dx}{\cos(\beta - \gamma)} = \frac{d\sigma - 2\sigma \tan\varphi\, d\beta - \dfrac{v^2}{\cos\varphi} \dfrac{\cos(\beta + \gamma)}{\cos(\beta - \gamma)}\, d\alpha}{-\dfrac{B}{\cos\varphi} + \dfrac{v^2}{\cos(\beta - \gamma)} \left(\dfrac{\partial \alpha}{\partial y}\right)_2} \qquad (3.3.21)$$

where $\left(\dfrac{\partial \alpha}{\partial y}\right)_1$ and $\left(\dfrac{\partial \alpha}{\partial y}\right)_2$ are evaluated by substituting either $\dfrac{dy}{dx} = \tan(\beta + \gamma)$

or $\dfrac{dy}{dx} = \tan(\beta - \gamma)$ into the last two equations of the system (3.3.6).

The basic equations of the soil medium with the first kinematic assumption have been transformed into a set of characteristics and a set of ordinary differential equations to be integrated along each of the characteristics.

3.4 Characteristics of the Macro-Structural Theory

According to the second kinematic relation, the velocity vector is directed along the active slip line (see Eq. 2.5.7). From Eqs. (3.2.7) and (3.2.8) the velocity components v_x and v_y are given as functions of β and v:

$$v_x = v \cos(\beta \pm \gamma)$$

$$(3.4.1)$$

$$v_y = v \sin(\beta \pm \gamma)$$

28

Using these relations in Eq. (3.1.6) satisfies the kinematic relation of the macro-structural theory identically. As pointed out earlier, the transformation of variables (3.2.4), (3.2.5), and (3.2.6) will satisfy Eq. (3.1.3), the failure criterion, identically as well. Substituting Eq. (3.4.1) into the equation of continuity, (3.1.4) provides the equation relating v and β. Using this, along with Eqs. (3.1.1) and (3.1.2) transformed to the new variables σ and β, one obtains the basic equations of the macro-structural theory.

$$\frac{\partial \sigma}{\partial x} \cos (\beta + \gamma) + \frac{\partial \sigma}{\partial y} \sin (\beta + \gamma) +$$

$$+ 2\sigma \tan \varphi \left\{ \frac{\partial \beta}{\partial x} \left[\cos (\beta + \gamma) + \xi^2 \cos (\beta - \gamma) \right] + \frac{\partial \beta}{\partial y} \left[\sin (\beta + \gamma) + \xi^2 \sin (\beta - \gamma) \right] \right\} +$$

$$+ \frac{A}{\cos \varphi} = 0 \qquad\qquad (3.4.2)$$

$$\frac{\partial \sigma}{\partial x} \cos (\beta - \gamma) + \frac{\partial \sigma}{\partial y} \sin (\beta - \gamma) -$$

$$- 2\sigma \tan \varphi \left\{ \frac{\partial \beta}{\partial x} \left[\cos (\beta - \gamma) + \xi^2 \cos (\beta + \gamma) \right] + \frac{\partial \beta}{\partial y} \left[\sin (\beta - \gamma) + \xi^2 \sin (\beta + \gamma) \right] \right\} +$$

$$+ \frac{B}{\cos \varphi} = 0 \qquad\qquad (3.4.3)$$

$$v \left[\frac{\partial \beta}{\partial x} \sin (\beta \pm \gamma) - \frac{\partial \beta}{\partial y} \cos (\beta \pm \gamma) \right] - \left[\frac{\partial v}{\partial x} \cos (\beta \pm \gamma) + \frac{\partial v}{\partial y} \sin (\beta \pm \gamma) \right] = 0 \qquad (3.4.4)$$

where
$$\xi = \frac{v}{\sqrt{2\sigma} \sin \varphi}$$

29

The characteristics of these equations are found in the same way as in the continuum theory.

Consider the differential relations along a curve $y = y(x)$ in the xy-plane,

$$d\sigma = \frac{\partial \sigma}{\partial x} dx + \frac{\partial \sigma}{\partial y} dy$$

$$d\beta = \frac{\partial \beta}{\partial x} dx + \frac{\partial \beta}{\partial y} dy \qquad (3.4.5)$$

$$dv = \frac{\partial v}{\partial x} dx + \frac{\partial v}{\partial y} dy$$

Using these relations to eliminate the derivatives with respect to x in Eqs. (3.4.2), (3.4.3) and (3.4.4), one obtains the following equations:

$$\begin{bmatrix} a_1 & b_1 & 0 \\ a_2 & b_2 & 0 \\ 0 & b_3 & c_3 \end{bmatrix} \begin{bmatrix} \frac{\partial \sigma}{\partial y} \\ \frac{\partial \beta}{\partial y} \\ \frac{\partial v}{\partial y} \end{bmatrix} = \begin{bmatrix} K_1 \\ K_2 \\ K_3 \end{bmatrix} \qquad (3.4.6)$$

where

$$a_1 = dx \sin(\beta + \gamma) - dy \cos(\beta + \gamma)$$

$$a_2 = dx \sin(\beta - \gamma) - dy \cos(\beta - \gamma)$$

$$b_1 = 2\sigma \tan\varphi (a_1 + \zeta^2 a_2)$$

$$b_2 = -2\sigma \tan\varphi (a_2 + \zeta^2 a_1)$$

$$b_3 = v \left[dx \cos(\beta \pm \gamma) + dy \sin(\beta \pm \gamma) \right]$$

$$c_3 = dx \sin(\beta \pm \gamma) - dy \cos(\beta \pm \gamma) \qquad (3.4.7)$$

$$-K_1 = \cos(\beta + \gamma) d\sigma + 2\sigma \tan\varphi \left[\cos(\beta + \gamma) + \zeta^2 \cos(\beta - \gamma) \right] d\beta + $$
$$+ \frac{A \, dx}{\cos\varphi}$$

30

$$-K_2 = \cos(\beta - \gamma)\, d\sigma - 2\sigma \tan\varphi \left[\cos(\beta - \gamma) + \xi^2 \cos(\beta + \gamma)\right] d\beta + \frac{\beta\, dx}{\cos\varphi}$$

$$K_3 = v \sin(\beta \pm \gamma)\, d\beta + \cos(\beta \pm \gamma)\, dv$$

From Eq (3.4.6),

$$\frac{\partial\sigma}{\partial y} = \frac{\begin{vmatrix} K_1 & b_1 \\ K_2 & b_2 \end{vmatrix}}{\begin{vmatrix} a_1 & b_1 \\ a_2 & b_2 \end{vmatrix}} \quad ; \qquad \frac{\partial\beta}{\partial y} = \frac{\begin{vmatrix} a_1 & K_1 \\ a_2 & K_2 \end{vmatrix}}{\begin{vmatrix} a_1 & b_1 \\ a_2 & b_2 \end{vmatrix}} \qquad (3.4.8)$$

and

$$\frac{\partial v}{\partial y} = \frac{K_3 - b_3 \frac{\partial\beta}{\partial y}}{c_3} \qquad (3.4.9)$$

To obtain the characteristics of the stress field, the determinant in the denominator of Eqs. (3.4.8) is set equal to zero. This gives:

$$2\sigma \tan\varphi \left[2\, a_1\, a_2 + \xi^2 (a_1^2 + a_2^2)\right] = 0$$

Using Eqs. (3.4.7), this simplifies to:

$$\frac{dy}{dx} = \frac{(1 + \xi^2 \sin\varphi)\, \sin 2\beta \pm \cos\varphi \sqrt{1 - \xi^4}}{(1 + \xi^2 \sin\varphi)\, \cos 2\beta + (\xi^2 + \sin\varphi)} \qquad (3.4.10)$$

This equation gives the slope of the characteristic curve. If X is the angle between the x-axis and the characteristic curve at any point, then

$$\tan X = \frac{dy}{dx}$$

31

Let $\bar{\gamma}$ be the angle between the maximum principal stress direction and the tangent to the characteristic curve. Then,

$$\tan \bar{\gamma} = \tan (X - \beta) = \frac{\tan X - \tan \beta}{1 + \tan X \tan \beta} \qquad (3.4.11)$$

Substituting Eq. (3.4.10) into (3.4.11) yields:

$$\tan \bar{\gamma} = \pm \sqrt{\frac{1 - \xi^2}{1 + \xi^2}} \tan \gamma \qquad (3.4.12)$$

or

$$\bar{\gamma} = \pm \tan^{-1} \left[\sqrt{\frac{1 - \xi^2}{1 + \xi^2}} \tan \left(\frac{\pi}{4} - \frac{\varphi}{2}\right) \right] \qquad (3.4.13)$$

The relation between the slip line direction and the characteristics is shown in Fig. 3.2. Equation (3.4.10) may also be written in the form

$$\frac{dy}{dx} = \tan (\beta \pm \bar{\gamma}) \qquad (3.4.14)$$

It is of interest to consider the effect of the factor $\xi = \dfrac{v}{\sqrt{2\sigma \sin \varphi}}$ in Eqs. (3.4.2) to (3.4.4) for various values of ξ. If $\xi = 0$, this implies that $v = 0$. This is the static case for which

$$\tan \bar{\gamma} = \pm \tan \gamma, \quad \text{or} \quad \bar{\gamma} = \pm \gamma$$

and the stress field coincides with the one from the continuum theory.

If, in a dynamic case $\xi = 1$,

$$v = \sqrt{2\sigma \sin \varphi}$$

and

$$\tan \alpha = 0, \quad \text{or} \quad \bar{\gamma} = 0$$

32

for this case the characteristic curves coincide with the direction of maximum principal stress. When the velocity exceeds the critical speed $\sqrt{2\sigma \overline{\sin \varphi}}$ the equations become elliptic, and the method of characteristics does not apply. The existence of a critical speed is an unexpected consequence of the theory, since hyperbolic equations are expected in dynamic problems. However, for the quasi-static case, the difficulty of a critical speed does not arise.

The differential relations to be satisfied along the characteristics of the stress field are obtained by setting the following determinant equal to zero:

$$\begin{vmatrix} a_1 & K_1 \\ a_2 & K_2 \end{vmatrix} = 0 \tag{3.4.15}$$

Expanding this determinant and using Eqs. (3.4.7) and (3.4.14), one obtains the characteristic equations of the stress field.

Along $\quad \dfrac{dy}{dx} = \tan (\beta + \bar{\gamma})$

$$\frac{dx}{\cos (\beta + \bar{\gamma})} = \frac{(c_w + S_\ell\, c_{-w})\,d\sigma + 2\sigma \tan \varphi \left[c_w - S_\ell\, c_{-w} + \ell^2 (c_{-w} - S_\ell\, c_w) \right] d\beta}{-\dfrac{A + S_\ell\, B}{\cos \varphi}} \tag{3.4.16}$$

Along $\quad \dfrac{dy}{dx} = \tan (\beta - \bar{\gamma})$

$$\frac{dx}{\cos (\beta - \bar{\gamma})} = \frac{(c_{-v} + S_\ell\, c_v)\,d\sigma - 2\sigma \tan \varphi \left[c_{-v} - S_\ell\, c_v + \ell^2 (c_v - S_\ell\, c_{-v}) \right] d\beta}{\dfrac{S_\ell\, A + B}{\cos \varphi}} \tag{3.4.17}$$

where

$$c_w = \frac{\cos (\beta + \gamma)}{\cos (\beta + \gamma)} \quad ; \qquad c_{-w} = \frac{\cos (\beta - \gamma)}{\cos (\beta + \gamma)}$$

$$c_v = \frac{\cos (\beta + \gamma)}{\cos (\beta - \gamma)} \quad ; \qquad c_{-v} = \frac{\cos (\beta - \gamma)}{\cos (\beta - \gamma)} \tag{3.4.18}$$

$$S_\ell = \frac{\sin (\gamma - \bar{\gamma})}{\sin (\gamma + \bar{\gamma})}$$

33

The characteristics of the velocity field are obtained by setting c_3 of Eq. (3.4.9) equal to zero. This gives:

$$\frac{dy}{dx} = \tan (\beta \pm \gamma) \qquad (3.4.19)$$

Here the + or - sign is used depending on which slip line family from the stress field is active.

Equation (3.4.19) shows that the characteristics of the velocity field coincide with the families of slip lines. This is to be expected from the basic assumption of the macro-structural theory which required that the velocity vector at any point coincides with the direction of the slip line at that point.

The differential equations to be satisfied along the velocity characteristics are obtained by setting the numerator of Eq. (3.4.9) to zero.

$$K_3 - b_3 \frac{\partial \beta}{\partial y} = 0 \qquad (3.4.20)$$

Using Eqs. (3.4.7), this becomes:

Along $\quad \frac{dy}{dx} = \tan (\beta + \gamma)$

$$\frac{dx}{\cos (\beta + \gamma)} = \frac{d\sigma + 2\sigma \tan \varphi \left[1 + \xi^2 (c_{\mu 1} - S_{\mu 1} \cos \varphi) \right] d\beta + v\, dv}{B/\cos \varphi} \qquad (3.4.21)$$

Along $\quad \frac{dy}{dx} = \tan (\beta - \gamma)$

$$\frac{dx}{\cos (\beta - \gamma)} = \frac{d\sigma - 2\sigma \tan \varphi \left[1 + \xi^2 (c_{\mu 2} + S_{\mu 2} \cos \varphi) \right] d\beta + v\, dv}{A/\cos \varphi} \qquad (3.4.22)$$

34

where

$$c_{u1} = \frac{\cos (\beta - \gamma)}{\cos (\beta + \gamma)} \quad ; \qquad S_{u1} = \frac{\sin (\beta + \gamma)}{\cos (\beta + \gamma)}$$

$$\text{(3.4.23)}$$

$$c_{u2} = \frac{\cos (\beta + \gamma)}{\cos (\beta - \gamma)} \qquad S_{u2} = \frac{\sin (\beta - \gamma)}{\cos (\beta - \gamma)}$$

3.5 Characteristics in the Static Theory

It will be useful to present the development of the method of characteristics for the equations governing the statics of soil media[13,15]. These equations are:

$$X - \frac{1}{\rho} \left(\frac{\partial \sigma_x}{\partial x} + \frac{\partial \tau_{xy}}{\partial y} \right) = 0$$

$$Y - \frac{1}{\rho} \left(\frac{\partial \tau_{xy}}{\partial x} + \frac{\partial \sigma_y}{\partial y} \right) = 0 \qquad \text{(3.5.1)}$$

$$(\sigma_x - \sigma_y)^2 + 4 \tau_{xy}^2 = \sin^2 \varphi \, (\sigma_x + \sigma_y + 2k \cot \varphi)^2$$

Transforming to the new variables σ and β, the last of Eqs. (3.5.1) is satisfied identically and the following two equations are obtained:

$$\frac{\partial \sigma}{\partial x} \cos (\beta + \gamma) + \frac{\partial \sigma}{\partial y} \sin (\beta + \gamma) +$$

$$\text{(3.5.2)}$$

$$+ 2\sigma \tan \varphi \left[\frac{\partial \beta}{\partial x} \cos (\beta + \gamma) + \frac{\partial \beta}{\partial y} \sin (\beta + \gamma) \right] + \frac{A}{\cos \varphi} = 0$$

$$\frac{\partial \sigma}{\partial x} \cos (\beta - \gamma) + \frac{\partial \sigma}{\partial y} \sin (\beta - \gamma) -$$

$$- 2\sigma \tan \varphi \left[\frac{\partial \beta}{\partial x} \cos (\beta - \gamma) + \frac{\partial \beta}{\partial y} \sin (\beta - \gamma) \right] + \frac{B}{\cos \varphi} = 0 \qquad \text{(3.5.3)}$$

35

where

$$A = X \sin (\beta - \gamma) - Y \cos (\beta - \gamma)$$

$$B = -X \sin (\beta + \gamma) + Y \cos (\beta + \gamma)$$

Using the same procedure as in Section 3.3, the characteristics
of these equations are:

$$\frac{dy}{dx} = \tan (\beta + \gamma); \qquad \frac{dy}{dx} = \tan (\beta - \gamma) \qquad (3.5.4)$$

and the differential equations to be satisfied along the characteristics are:

$$d\sigma + 2\sigma \tan \varphi \, d\beta = 0$$
$$d\sigma - 2\sigma \tan \varphi \, d\beta = 0 \qquad (3.5.5)$$

Equations (3.5.5) may be integrated to yield:

$$\frac{\cot \varphi}{2} \ln \sigma - \beta = const = \xi(u)$$

$$(3.5.6)$$

$$\frac{\cot \varphi}{2} \ln \sigma + \beta = const = \eta(z)$$

Here, a function of σ, minus β is a constant on members of one family of
characteristics, and a function of σ, plus β is a constant on members of
the other family. Equations (3.5.6) may be solved for β and the function of
σ.

$$\frac{\cot \varphi}{2} \ln \sigma = \frac{1}{2} [\xi(u) + \eta(z)]$$

$$(3.5.7)$$

$$\beta = \frac{1}{2} [-\xi(u) + \eta(z)]$$

As in the theory of plasticity, special cases arise when, in a particular
region aeing considered, ξ and η are constants, ξ along is a constant, and
η alone is a constant.[15,16,17]

36

When both ξ and η are constant functions in a region, Eqs. (3.5.7) show that both σ and ξ are also constants throughout the region. When this is the case, both families of characteristics are straight lines and the region is called a "region of constant state"[16,17].

When either ξ alone or η along is a constant, one of the characteristics (3.5.4) will form a fan of straight lines. If the fan is centered, that is, if the straight line characteristics intersect at a point, the region is called a "region of radial shear"[1].

3.6 Transformation of Characteristics to Polar Coordinates

For later work in polar coordinates it will be convenient to replace α and β by similar angles $\bar{\alpha}$ and $\bar{\beta}$ measured from the positive direction of the radius vector r and the directions of the velocity vector and of the maximum principal stress, respectively. The angle θ is defined as the counterclockwise angle from the y-axis to the radius vector, as shown in Fig. (3.3). The following relations may be easily obtained from Fig. (3.3):

$$\bar{\beta} = \beta - \theta - \frac{\pi}{2}$$

$$\bar{\alpha} = \beta - \theta + \frac{3\pi}{2}$$

(3.6.1)

Polar coordinates will be used later when in a particular problem the inactive[*] family of slip lines consists of a centered fan of straight line characteristics. In this case the angle $\bar{\beta}$ in polar coordinates has a constant value equal to:

[*] That is to say, slip actually occurs along the other set of slip lines.

37

$$\bar{\beta} = + \gamma \quad \text{for} \quad \frac{dy}{dx} = \tan (\beta + \gamma) \quad \text{active}$$

or   (3.6.2)

$$\bar{\beta} = - \gamma \quad \text{for} \quad \frac{dy}{dx} = \tan (\beta - \gamma) \quad \text{active}$$

In polar coordinates the velocity field characteristics given by
(3.3.12) and (3.3.12) become:

$$\frac{d\theta}{dr} = \pm \frac{\cot \varphi}{r}$$

(3.6.3)

$$\frac{d\theta}{dr} = \mp \frac{\tan \varphi}{r}$$

In transforming the equations to be satisfied along the characteristics, β,
α, $d\alpha$ and dv in Eqs. (3.3.15) and (3.3.16) must be determined from the
expressions (3.6.1) and (3.6.2). These give:

$$\beta = \frac{\pi}{2} + \theta \pm \gamma$$
$$\alpha = \bar{\alpha} + \theta - \frac{3\pi}{2}$$
$$d\alpha = d\bar{\alpha} + d\theta$$
$$dv = dv$$

(3.6.4)

where $d\theta$ may be obtained from (3.6.3).

Using (3.6.4) n (3.3.15) and (3.3.16) yields:

$$\tan (\bar{\alpha} \mp 2\gamma) \left[d\bar{\alpha} - \frac{\cot \varphi}{r} dr \right] - \frac{dv}{v} = 0$$

(3.6.5)

$$\cot (\bar{\alpha} \mp 2\gamma) \left[d\bar{\alpha} + \frac{\tan \varphi}{r} dr \right] + \frac{dv}{v} = 0$$

where the - or + sign is taken depending whether the active slip lines are
inclined at an angle $(\beta + \gamma)$ or $(\beta - \gamma)$ to the x-axis.

38

The characteristics in polar coordinates for the second kinematic assumption may be easily obtained by transforming the basic velocity Eq. (3.4.4) to polar coordinates and then finding the characteristics from the transformed equation.

Transforming (3.4.4) to the polar coordinates of Fig. 3.2 yields:

$$\frac{\partial v}{\partial r} \sin \varphi \pm \frac{\partial v}{\partial \theta} \frac{\cos \varphi}{r} + \frac{v}{r} \sin \varphi = 0 \qquad (3.6.6)$$

Again, the sign in the second term is selected according to whether the active slip lines are inclined at $(\beta + \gamma)$ or $(\beta - \gamma)$ to the x-axis.

Since characteristics are lines along which $\frac{\partial v}{\partial r}$ or $\frac{\partial v}{\partial \theta}$ may be discontinuous, and along which the relation

$$dv = \frac{\partial v}{\partial r} dr + \frac{\partial v}{\partial \theta} d\theta \qquad (3.6.7)$$

holds, the system (3.6.6) and (3.6.7) may be solved in the usual way to yield the differential equations of the characteristics.

$$\frac{d\theta}{dr} = \pm \frac{\cot \varphi}{r} \qquad (3.6.8)$$

Integrating (3.6.8) gives the equation of the velocity field characteristics and active family of slip lines.

$$r = r_{\bullet} e^{\pm \theta \tan \varphi} \qquad (3.6.9)$$

The differential equation to be satisfied along the characteristics (3.6.9) is:

$$\frac{dv}{v} = \mp \tan \varphi \, d\theta \qquad (3.6.10)$$

or upon integration:

$$v = v_{\bullet} e^{\mp \theta \tan \varphi} \qquad (3.6.11)$$

39

4. NUMERICAL SOLUTION OF EQUATIONS

4.1 Finite Difference Method of Solution

In general, the solution of the differential equations to be satisfied along the characteristics can not be obtained analytically. However, a solution can be obtained numerically by transforming the equations to characteristic coordinates, and then converting the differential equations into difference equations along the characteristics.

The region in which the solution is to be obtained is divided into a network by the uz- characteristic coordinates as shown in Fig. 4.1. The solution proceeds in a step-by-step fashion by obtaining the values of the unknowns at the point $\delta_{k,l}$ after the values of the preceding points, $\delta_{k,l-1}$ and $\delta_{k-1,l}$ have been obtained. At the start of the computations, points $\delta_{k,l-1}$ and $\delta_{k-1,l}$ correspond to points on the initial curve for which initial values are prescribed.

Let $u(x,y)$ be the coordinate measured along one family of characteristics and $z(x,y)$ the coordinate along the other family. In the ux-plane

$$du = \frac{\partial u}{\partial x}\, dx + \frac{\partial u}{\partial y}\, dy$$

and   (4.1.1)

$$dz = \frac{\partial z}{\partial x}\, dx + \frac{\partial z}{\partial y}\, dy$$

Solving for dx and dy

$$dx = \frac{1}{D}\left[du\left(\frac{\partial z}{\partial y}\right) - dz\left(\frac{\partial u}{\partial y}\right) \right]$$

$$dy = \frac{1}{D}\left[-du\left(\frac{\partial z}{\partial x}\right) + dz\left(\frac{\partial u}{\partial x}\right) \right]$$ (4.1.2)

40

where

$$D = \frac{\partial u}{\partial x} \frac{\partial z}{\partial y} - \frac{\partial u}{\partial y} \frac{\partial z}{\partial x}$$

Since $x = x(u,z)$ and $y = y(u,z)$

$$dx = \frac{\partial x}{\partial u} du + \frac{\partial x}{\partial z} dz \qquad (4.1.3)$$

and

$$dy = \frac{\partial y}{\partial u} du + \frac{\partial y}{\partial z} dz$$

Equations (4.1.2) and (4.1.3) yield the following transformation relations.

$$\frac{\partial u}{\partial x} = D \frac{\partial y}{\partial z} \quad ; \quad \frac{\partial z}{\partial x} = - D \frac{\partial y}{\partial u}$$

$$(4.1.4)$$

$$\frac{\partial u}{\partial y} = - D \frac{\partial x}{\partial z} \quad ; \quad \frac{\partial z}{\partial y} = D \frac{\partial x}{\partial u}$$

If for any function f, $f = f(u,z)$, then:

$$\frac{\partial f}{\partial x} = D \left[\frac{\partial f}{\partial u} \frac{\partial y}{\partial z} - \frac{\partial f}{\partial z} \frac{\partial y}{\partial u} \right]$$

$$(4.1.5)$$

$$\frac{\partial f}{\partial y} = D \left[\frac{\partial f}{\partial z} \frac{\partial x}{\partial u} - \frac{\partial f}{\partial u} \frac{\partial x}{\partial z} \right]$$

Derivatives with respect to the characteristic coordinates u,z are approximated by the following finite-difference expressions:

41

$$\frac{\partial x}{\partial u} \approx \frac{x_{k,\ell} - x_{k-1,\ell}}{\Delta u} \qquad\qquad \frac{\partial x}{\partial z} \approx \frac{x_{k,\ell} - x_{k,\ell-1}}{\Delta z}$$

$$\frac{\partial y}{\partial u} \approx \frac{y_{k,\ell} - y_{k-1,\ell}}{\Delta u} \qquad\qquad \frac{\partial y}{\partial z} \approx \frac{y_{k,\ell} - y_{\ell,k-1}}{\Delta z} \qquad (4.1.6)$$

$$\frac{\partial f}{\partial u} \approx \frac{f_{k,\ell} - f_{k-1,\ell}}{\Delta u} \qquad\qquad \frac{\partial f}{\partial z} \approx \frac{f_{k,\ell} - f_{k,\ell-1}}{\Delta z}$$

4.2 Equations in Finite-Difference Form

Along the characteristic $u = u(x,y) = \text{const.}$,

$$du = \frac{\partial u}{\partial x} \, dx + \frac{\partial u}{\partial y} \, dy = 0 \qquad (4.2.1)$$

If the velocity field characteristic given by (3.3.12) is named the one along which $u = u(x,y) = \text{const.}$, Eq. (4.2.1) becomes

$$du = \frac{\partial u}{\partial x} \cos (\beta \pm \gamma) + \frac{\partial u}{\partial y} \sin (\beta \pm \gamma) = 0 \qquad (4.2.2)$$

Similarly, along $z = z(x,y) = \text{const.}$, using Eq. (3.3.13)

$$dz = \frac{\partial z}{\partial x} \sin (\beta \pm \gamma) - \frac{\partial z}{\partial y} \cos (\beta \pm \gamma) = 0 \qquad (4.2.3)$$

Using (4.1.4) in Eqs. (4.2.2) and (4.2.3) yields

$$du = \frac{\partial u}{\partial z} \cos (\beta \pm \gamma) - \frac{\partial u}{\partial z} \sin (\beta \pm \gamma) = 0$$

$$\qquad (4.2.4)$$

$$dz = \frac{\partial z}{\partial u} \sin (\beta \pm \gamma) + \frac{\partial z}{\partial u} \cos (\beta \pm \gamma) = 0$$

42

These are the characteristics of the velocity field in the uz-plane.

In a like manner, using (4.1.4), (4.1.5) and (4.2.4) in Eqs. (3.3.15) and (3.3.16), one obtains the equations to be satisfied along the characteristics in the form

$$v \tan \left[\alpha - (\beta \pm \gamma) \right] \frac{\partial u}{\partial z} - \frac{\partial v}{\partial z} = 0$$

$$(4.2.5)$$

$$v \cot \left[\alpha - (\beta \pm \gamma) \right] \frac{\partial u}{\partial u} + \frac{\partial v}{\partial u} = 0$$

Equations (4.2.4) and (4.2.5) may be expressed in finite-difference form by making use of the difference quotients (4.1.6).

$$\left[v_{k,\ell} - v_{k,\ell-1} \right] \cos \left(\beta_{k,\ell-1} \pm \gamma \right) + \left[x_{k,\ell} - x_{k,\ell-1} \right] \sin \left(\beta_{k,\ell-1} \pm \gamma \right) = 0$$

$$(4.2.6)$$

$$\left[v_{k,\ell} - v_{k-1,\ell} \right] \sin \left(\beta_{k-1,\ell} \pm \gamma \right) + \left[x_{k,\ell} - x_{k-1,\ell} \right] \cos \left(\beta_{k-1,\ell} \pm \gamma \right) = 0$$

and

$$\tan \left[\alpha_{k,\ell-1} - \left(\beta_{k,\ell-1} \pm \gamma \right) \right] \left(\alpha_{k,\ell} - \alpha_{k,\ell-1} \right) - \left[\frac{v_{k,\ell} - v_{k,\ell-1}}{v_{k,\ell-1}} \right] = 0$$

$$(1.2.7)$$

$$\cot \left[\alpha_{k-1,\ell} - \left(\beta_{k-1,\ell} \pm \gamma \right) \right] \left(\alpha_{k,\ell} - \alpha_{k-1,\ell} \right) + \left[\frac{v_{k,\ell} - v_{k-1,\ell}}{v_{k-1,\ell}} \right] = 0$$

The finite-difference form of the equations of the velocity field characteristics, Eqs. (3.6.3), in polar coordinates is

49

$$\left(\theta_{k,\ell} - \theta_{k,\ell-1}\right) \; + \; \cot \; \varphi \; \left(\frac{r_{k,\ell} - r_{k,\ell-1}}{r_{k,\ell-1}}\right) = 0$$

$$(4.2.8)$$

$$\left(\theta_{k,\ell} - \theta_{k-1,\ell}\right) \; - \; \tan \varphi \; \left(\frac{r_{k,\ell} - r_{k-1,\ell}}{r_{k-1,\ell}}\right) = 0$$

The equations along the characteristics take the finite-difference form

$$\tan \left(\bar{\alpha}_{k,\ell-1} \mp 2\gamma\right) \; \left[\bar{\alpha}_{k,\ell} - \bar{\alpha}_{k,\ell-1} - \cot \varphi \left(\frac{r_{k,\ell} - r_{k,\ell-1}}{r_{k,\ell-1}}\right)\right] - \left(\frac{v_{k,\ell} - v_{k,\ell-1}}{v_{k,\ell-1}}\right) = 0$$

$$(4.2.9)$$

$$\cot \left(\bar{\alpha}_{k-1,\ell} \pm 2\gamma\right) \left[\bar{\alpha}_{k,\ell} - \bar{\alpha}_{k-1,\ell} + \tan \varphi \left(\frac{r_{k,\ell} - r_{k-1,\ell}}{r_{k-1,\ell}}\right)\right] + \left(\frac{v_{k,\ell} - v_{k-1,\ell}}{v_{k-1,\ell}}\right) = 0$$

44

5. PRESSURE LOADING ON BURIED STRUCTURES

5.1 Stress Field Solution

The theory presented in the previous chapters will be applied to the problem of determining the intensity of pressure ac..ing on a structure buried in a granular soil when the ground surface is subjected to an air-induced over-pressure and the structure is on the verge of collapse. For this case, the pressure applied to the structure corresponds to a measure of its ultimate strength.

The structure considered is a plate having one side much longer than the other so that the two-dimensional state of plane strain will prevail at regions away from the ends of the long side. Taking the xy-plane perpendicular to the long axis of the plate, the slip planes will form as slip lines on the xy-plane.

The intensity of pressure, p_o, applied to the ground surface is assumed to be uniformly distributed over a large area, and directed vertically. Since there is no shearing stress at the ground surface, the vertical stress in the soil at the surface is a principal stress equal to p_o. The structure is assumed symmetrical, so by virtue of symmetry the vertical stress along the axis of symmetry AB in Fig. 5.1 is also a principal stress.

In general, as in the Theory of Plasticity, the stress field equations can not be applied directly to a specific problem to obtain the required failure pressure. However, a solution is obtained by finding a proper stress field for which there exists a compatible velocity field satisfying all velocity boundary conditions [18].

The families of stress characteristics or slip lines have certain geometric properties which facilitate the construction of a stress field

45

from given conditions at the boundary. These properties were first presented by Hencky [18] and Prandtl [19] for the Mises Theory of unrestricted plastic flow. One of the most important of these geometric properties is that the angle formed by the tangents of two slip lines of one family at the points of intersection with a slip line of the other family is a constant no matter what member of the other family is taken.

From Eq. (3.3.9), it is seen that the stress and velocity fields may be considered separately. Additional properties of the slip lines are given by the relations derived for the static theory of Section 3.5 when the quasi-static problem is considered in which inertia forces are not considered.

Since the intensity of applied over-pressure is a constant, a region of constant state consisting of two families of straight slip lines forms at the ground surface. Similarly, assuming a uniform pressure applied to the structure, we have a region of constant state adjacent to the structure.

The horizontal principal stress in the soil at the ground surface is taken to be the maximum principal stress as a result of arching in the soil. Terzaghi [7] has verified this behavior experimentally. With the x-axis vertical, the value of β in the constant state region at the surface is either $\pm\pi/2$. The direction of maximum principal stress at the structure is vertical so that the angle β undergoes a total change of $\pi/2$ and is equal to zero in the constant state region adjacent to the structure.

Figure 5.2 shows the network of characteristics for the stress field solution of the quasi-static probelm. The stress field is divided into four regions, the two constant state regions, COC' and OOD' and the centered fans OCD and OC'D'. In symmetrical problems both families of slip lines will be active [11], so that along the limiting active slip line CD, $dy/dx = \tan(\beta-\gamma)$

46

and along C'D', $dy/dx = \tan(\beta+\gamma)$. The u and z families of characteristics are given in region DOD' by the differential equations $dy/dx = \tan(\beta\pm\gamma)$. In this region the angle $\beta = \text{const.} = 0$, since the direction of the maximum principal stress coincides with the direction of the x-axis. Then the equations of the slip lines are given by

$$y = - x \tan \gamma + c_1 \qquad \text{(u-family)}$$
$$y = x \tan \gamma + c_2 \qquad \text{(z-family)} \qquad (5.1.1)$$

where c_1 and c_2 are arbitrary constants and the u-family is active.

The characteristic for region COC' $(\beta = \text{const.} = \pi/2)$ are obtained in a similar way to be

$$y = x \cot \gamma + c_3 \qquad \text{(u-family)}$$
$$y = - x \cot \gamma + c_4 \qquad \text{(z-family)} \qquad (5.1.2)$$

In region OCD it is convenient to express the characteristic net by a system of plane polar coordinates with θ measured counterclockwise as shown in Fig. 5.2. Here, the direction of the maximum principal stress is given by the angle $\bar{\beta}$ which is measured with respect to the radius vector from point O taking counterclockwise positive. Since the radii from point O are members of the inactive family of slip lines in region OCD, the angle $\bar{\beta}$ is constant in this region (cf. Eqs. 3.8.2). In polar coordinates the differential equations of the stress field characteristics in region OCD are

$$\frac{d\theta}{dr} = - \frac{\cot \varphi}{r} \qquad \text{(u-family)}$$

$$\frac{d\theta}{dr} = 0 \qquad \text{(z-family)} \qquad (5.1.3)$$

47

They yield

$$r = r_1 e^{-(\theta-\gamma)\tan\varphi} \qquad \text{(u-family)}$$

$$\text{(5.1.4)}$$

$$\theta = \theta_1 \qquad \text{(z-family)}$$

The u-family of active slip lines form a family of logarithmic spirals given by the first of Eqs. (5.1.4).

The relations to be satisfied along the characteristics given in Section 3.5 are

$$\bar{\sigma} - \beta = \xi = \text{const. on u-family}$$

$$\text{(5.1.5)}$$

$$\bar{\sigma} + \beta = \eta = \text{const. on z-family}$$

where

$$\bar{\sigma} = \frac{\cot\varphi}{2} \ln\left[\frac{\sigma_x + k\cot\varphi}{1 + \sin\varphi\cos 2\beta}\right]$$

In the constant state region DOD', both ξ and η are constants. Thus, this region transforms into a single point on the line $\xi = \eta$ on the $\xi\eta$-characteristic plane shown in Fig. 5.3.

On the right-hand side of the axis of symmetry AB, the maximum principal stress direction changes from 0 to 90 degrees with respect to the x-axis by a counterclockwise (positive) rotation, so the angle β in region ACC is $+ \pi/2$. On the left-hand side of AB, the maximum principal stress direction changes by a clockwise (negative) rotation of 90 degrees, so the value of β in region AOC' is $- \pi/2$. In general, the proper sign of the angle β must be used in determining the correct values of the stress components.

Regions AOC and AOC' are shown in Fig. 5.3 as points on the $\xi\eta$-plane. The centered fans OCD and OC'D' transform into the lines $\xi = $ const. and $\eta = $ const. connecting the constant state regions. Although the region COC' is transformed into two points on the characteristic plane, only one need be considered since each point yields the same values of stress components.

The applied pressure p_o required to develop the assumed stress field may now be determined. Using the first of Eqs. (5.1.5) to determine the value of ξ in regions AOC and BOD in terms of the pressures p_o and q, it may be seen from Fig. 5.2 and Fig. 5.3 that these values must be equal. By equating the values of ξ_{AOC} and ξ_{BOD} the pressure p_o is obtained as a function of the ultimate plate resistance q.

In region AOC, $\sigma_x = p_o$ and $\beta = \pi/2$. From the first of Eqs. (5.1.5)

$$\xi_{AOC} = \bar{\sigma}_{AOC} - \beta_{AOC} = \frac{\cot\varphi}{2} \ln\left[\frac{p_o + k\cot\varphi}{1 - \sin\varphi}\right] - \frac{\pi}{2} \qquad (5.1.6)$$

In region BOC, $\sigma_x = q$ and $\beta = 0$. Then

$$\xi_{BOC} = \bar{\sigma}_{BOC} - \beta_{BOC} = \frac{\cot\varphi}{2} \ln\left[\frac{q + k\cot\varphi}{1 + \sin\varphi}\right] - 0 \qquad (5.1.7)$$

Since $\xi_{AOC} = \xi_{BOC}$

$$\frac{\cot\varphi}{2} \ln\left[\frac{p_o + k\cot\varphi}{1 - \sin\varphi}\right] - \frac{\pi}{2} = \frac{\cot\varphi}{2} \ln\left[\frac{q + k\cot\varphi}{1 + \sin\varphi}\right] \qquad (5.1.8)$$

or

$$\ln\left[\frac{p_o + k\cot\varphi}{q + k\cot\varphi} \cdot \frac{1 + \sin\varphi}{1 - \sin\varphi}\right] = \pi\tan\varphi \qquad (5.1.9)$$

Then

$$p_o = (q + k \cot \varphi) \left[\frac{1 - \sin \varphi}{1 + \sin \varphi} \right] e^{\pi \tan \varphi} - k \cot \varphi \qquad (5.1.10)$$

For $\varphi = 30°$, $k = 0$ (ideal granular material)

$$p_o = q \left[\frac{1 - \sin \varphi}{1 + \sin \varphi} \right] e^{\pi \tan \varphi}$$

or

$$p_o = 2.03q$$

Expressing the soil cohesion k by the relation

$$k = C_k q$$

Eq. (5.1.10) becomes

$$p_o = q \left[(1 + C_k \cot \varphi) f(\varphi) - C_k \cot \varphi \right] \qquad (5.1.11)$$

where

$$C_k = \frac{k}{q}$$

$$f(\varphi) = \left[\frac{1 - \sin \varphi}{1 + \sin \varphi} \right] e^{\pi \tan \varphi}$$

It should be noted that this solution corresponds to a particular depth of burial depending on the span length L and the angle of internal friction of the soil φ. Evaluating the arbitrary constant r_1 in the first of Eqs. (5.1.4), the equation of the line CD is obtained

$$r = \overline{OD} \, e^{-(\theta - \gamma + \frac{\pi}{2}) \tan \varphi} \qquad (5.1.12)$$

The length OC is found by setting $\theta = + \Upsilon$

$$OC = OD \ e^{-\frac{\pi}{2} \tan \varphi} \tag{5.1.13}$$

From this the length CC' and the depth H may be found in terms of the span L.

$$CC' = L \cot \Upsilon \ e^{-\frac{\pi}{2} \tan \varphi} \tag{5.1.14}$$

$$H = L \left[\frac{1}{2} e^{-\frac{\pi}{2} \tan \varphi} + \frac{1}{2} \cot \Upsilon \right] \tag{5.1.15}$$

for $\varphi = 30°$

$$\Upsilon = \frac{\pi}{4} - \frac{\varphi}{2} = 30°$$

Then

$$CC' = 0.70L$$

and

$$H = 1.07L$$

It should be remembered that the solution obtained here is valid for only one depth if the span of the structure and φ is given.

5.2 Solution for Arbitrary Depths

The solution for the stress field obtained in Section 5.1 is based on the assumption that the entire region bounded by the limiting slip lines CD and C'D' is in a state of plastic equilibrium. Using this assumption and the stress field of Fig. 5.2 leads to a particular ratio of depth to span length for given soil properties. The velocity field corresponding to this stress field will be given later.

When the depth of burial is greater or less than the "critical" depth given by Eq. (5.1.15), the failure region bounded by the limiting slip lines may contain zones which remain essentially in the elastic state. In these elastic regions the distribution of stresses is unknown since the basic equations of the analysis do not apply. However, if an elastic zone forms on a boundary of the failure region, it may be possible to determine the total pressure transmitted by the elastic region to the interior and to obtain a solution without knowing the stress distribution completely. Such an approach was used by Hill, Lee and Tupper [20,21] for the problem of a ductile material compressed between rigid plates.

Solutions for depths less than the "critical" may be obtained by assuming that regions COC' and DOD' are not fully plastic and that the angle β in the plastic regions OCD and OC'D; undergoes a change of less than 90 degrees in going from OD to OC. If β_{OC} and β_{OD} are the values of β along OC and OD and p_o and q are taken to be equal to σ_x on OC and OD, then the failure pressure p_o is given in terms of q by

$$p_o = q \left\{ (1 + C_k \cot \Phi) \left[\frac{1 + \sin \Phi \cos 2\beta_{OC}}{1 + \sin \Phi \cos 2\beta_{OD}} \right] \left[e^{2 \tan \Phi (\beta_{OC} - \beta_{OD})} \right] - C_k \cot \Phi \right\}$$

(5.? !)

where

$$C_k = \frac{k}{q}$$

The depth of burial H will now be found in terms of β_{OC} and β_{OD}. The equation of the curve CD is given by

52

$$r_{CD} = OD \ e^{-(\theta + \frac{\pi}{2} - \gamma - \beta_{OD}) \tan \varphi} \tag{5.2.2}$$

Since $\theta_{OC} = \gamma - \pi/2 + \beta_{OC}$, Eq. (5.2.2) becomes

$$OC = OD \ e^{-(\beta_{OC} - \beta_{OD}) \tan \varphi} \tag{5.2.3}$$

Since

$$OD = \frac{L}{2} \cdot \frac{1}{\sin(\gamma + \beta_{OD})}$$

and

$$OA = OC \ \sin(\gamma + \beta_{OC} - \frac{\pi}{2})$$

the depth H and the length CC' are given by

$$H = \frac{L}{2} \left[\cot(\gamma + \beta_{OD}) + \frac{\sin(\gamma + \beta_{OC} - \frac{\pi}{2})}{\sin(\gamma + \beta_{OD})} \ e^{-(\beta_{OC} - \beta_{OD}) \tan \varphi} \right] \tag{5.2.4}$$

and

$$CC' = L \left[\frac{\sin(\gamma + \beta_{OC})}{\sin(\gamma + \beta_{OD})} \ e^{-(\beta_{OC} - \beta_{OD}) \tan \varphi} \right] \tag{5.2.5}$$

when $\beta_{OC} = \pi/2$ and $\beta_{OD} = 0$, Eqs. (5.2.4) and (5.2.5) reduce to

$$H = \frac{L}{2} \left[\cot \gamma + e^{-\frac{\pi}{2} \tan \varphi} \right] \tag{5.2.6}$$

and

$$CC' = L \cot \gamma \ e^{-\frac{\pi}{2} \tan \varphi} \tag{5.2.7}$$

These are the same as Eqs. (5.1.14) and (5.1.15) given in Section 5.1.

Equations (5.2.1) and (5.2.4) yield a range of failure pressures for any particular depth depending on the values of β_{0C} and β_{0D} used. The proper values of β_{0C} and β_{0D} are the ones which yield the smallest failure pressure at a given depth. Figure 5.4 shows the configuration of the failure region for the critical depth and for three other cases in which the depth is less than critical. These cases are for a cohesionless material with an angle of internal friction Φ equal to 30 degrees.

When the depth of burial is much greater than the critical depth, the state of stress at the ground surface will be affected only slightly by the arching of the soil above the yielding structure. It has been shown experimentally [7] that the pressure of a yielding structure in a granular medium has little or no effect on the state of stress at the ground surface when the depth of burial is on the order of 2 to 3 times the width of the yielding element. If the state of stress at the surface is not affected by the yielding structure, then it may be concluded that failure as defined herein will not occur. The structure will be safe provided that it has sufficient deformation capacity to absorb the energy of the initial impulse applied by the pressure wave.

Solutions for depths greater than the critical may be obtained by considering the stress field at the critical depth to be extended by a region consisting of elastic zones and a centered fan in which the angle β undergoes a change of less than 90°. As the depth increases, the change in β approaches 90° and β at the ground surface approaches 0°, the value corresponding to the state of stress existing in the soil if no yielding structure was present.

A stress field for a depth greater than the critical is shown in Fig. 5.5(a). Considering the regions to the right of the axis of symmetry,

54

the failure region consists of the critical-depth field, regions $\bar{O}AC$ and $\bar{O}\bar{B}\bar{D}$, and the centered fan $\bar{O}C\bar{D}$ in which η = const.

Regions $\bar{O}AC$ and $\bar{O}\bar{B}\bar{D}$ are taken to be in the elastic state, that is, they move as rigid bodies. As in the case of the solutions at depths less than the critical, the velocity field associated with this stress field will develop if the structure moves vertically downward with a uniformly distributed velocity so that the elastic regions may move downward without deforming. The failure pressure obtained on the basis of this assumption should be a minimum since any other motion of the structure requires the elastic regions to become partially or completely plastic and, thus, more work must be done by the external loads in deforming them.

In the centered fan $\bar{O}C\bar{D}$, the angle β changes by an amount varying from $0°$ to $90°$ depending on the depth. When the change in β is less than $90°$, the point on the $\xi\eta$-plane representing region $\bar{O}\bar{B}\bar{D}$ falls between the $\beta = \pi/2$ and $\beta = 0$ lines as shown in Fig. 5.5(b).

Figure 5.6 shows the stress field for the critical depth and three other cases at a greater depth for a cohesionless material with $\vartheta = 30°$. It may be observed from the values of failure pressure given that above the critical depth the pressure required for failure increases very rapidly. This behavior should be expected on the basis of the experimental results mentioned previously.

The effect of angle ϑ on failure pressure at critical depth H is shown in Fig. 5.7. The sensitivity of failure pressure to variations of ϑ is apparent here. A plot of failure pressure versus depth is given in Fig. 5.8 for $\vartheta = 30°$ and $k = 0$. Here the large increase in failure pressure for depths greater than the critical is clearly shown.

55

5.3 Velocity Field Solution for the Continuum Theory

The equations of the velocity characteristics and the differential relations to be satisfied along them for the quasi-static incompressible case are (cf. Section 3.3):

$$u = const. \ family$$

$$\frac{dy}{dx} = \tan(\beta \pm \gamma); \qquad v \tan (\alpha - (\beta \pm \gamma)) \ d\alpha - dv = 0 \qquad (5.3.1)$$

$$z = const. \ family$$

$$\frac{dy}{dx} = - \cot(\beta \pm \gamma); \qquad v \cot (\alpha - (\beta \pm \gamma)) \ d\alpha + dv = 0 \qquad (5.3.2)$$

For the regions to the right of the axis of symmetry AB, the active family of slip lines is given by the equation

$$\frac{dy}{dx} = \tan(\beta \pm \gamma) \qquad (5.3.3)$$

Thus, one family of velocity characteristics is coincident with the active family of slip lines and the other family is orthogonal.

The velocity field characteristics are shown in Fig. 5.9 in the xy-plane and in Fig. 5.10 in the uz-characteristic plane. In region OBD the angle β maintains the constant value determined by the stress solution to be

$$\beta = 0$$

Then, in this region, along the lines u = const.

$$\frac{dy}{dx} = \tan \gamma; \qquad \tan(\alpha + \gamma)d\alpha - \frac{dv}{v} = 0 \qquad (5.3.4)$$

56

and along z = const.

$$\frac{dy}{dx} = -\cot \gamma; \qquad \cot(\alpha + \gamma)d\alpha + \frac{dv}{v} = 0 \qquad (5.3.5)$$

Integrating the equations to be satisfied along the characteristics yields

$$\text{along } u = \text{const.;} \qquad v \cos(\alpha + \gamma) = C_u(u) \qquad (5.3.6)$$

$$\text{along } z = \text{const.;} \qquad v \sin(\alpha + \gamma) = C_z(z) \qquad (5.3.7)$$

The initial velocity distribution will be specified at the boundary formed by the yielding structure.

It is assumed that the soil particles immediately adjacent to the yielding structure will move in a vertical direction, that is, $\alpha = 0$. Also, by virtue of symmetry, the soil particles must move vertically ($\alpha = 0$) along the axis of symmetry AB. These boundary conditions are given by

$$\text{on BD} \qquad v = v_o(\gamma) \qquad (5.3.8)$$
$$\alpha = 0$$

$$\text{on AB} \qquad \alpha = 0 \qquad (5.3.9)$$

Since both α and v are known along the non-characteristic BD, the solution may be obtained in the triangular region formed by BD and the characteristics BB_1 and DB_1 through the points B and D. Next, the solution may be obtained in the region BB_1E since α is known along the non-characteristic BE.

At this stage, conditions in the curvilinear region OCD must be considered.

57

In region OCD it is convenient to express the equations in polar coordinates r,θ with r measured from the origin of the xy-coordinates and θ measured from the positive y-axis, positive counterclockwise. In the new coordinates, $\bar{\beta}$ and $\bar{\alpha}$ represent the angles between the positive direction of the radius vector and the directions of the maximum principal stress and the velocity vector v, respectively, taking counterclockwise positive. By using polar coordinates in region OCD, the angle $\bar{\beta}$ has a constant value equal to

$$\bar{\beta} = \pi - \gamma \qquad (5.3.10)$$

In Section 3.6 it was shown that the angles $\bar{\beta}$ and $\bar{\alpha}$ in polar coordinates are related to β and α by

$$\bar{\beta} = \beta - \theta - \frac{\pi}{2}$$

$$\bar{\alpha} = \alpha - \theta + \frac{3\pi}{2} \qquad (5.3.11)$$

The characteristics in polar coordinates and the relations to be satisfied along them for $dy/dx = \tan(\beta - \gamma)$ active are (cf. Eqs. 3.6.3 and 3.6.5)

along $u = $ const.

$$\frac{d\theta}{dr} = \frac{-\cot\varphi}{r} \qquad (5.3.12)$$

$$\tan(\bar{\alpha} + 2\gamma)\left[d\bar{\alpha} - \frac{\cot\varphi \, dr}{r}\right] - \frac{dv}{v} = 0 \qquad (5.3.13)$$

along $z = $ const.

$$\frac{d\theta}{dr} = \frac{\tan\varphi}{r} \qquad (5.3.14)$$

$$\cot(\bar{\alpha} + 2\gamma)\left[d\bar{\alpha} + \frac{\tan \varphi \ dr}{r}\right] + \frac{dv}{v} = 0 \qquad (5.3.15)$$

The Eqs. (5.3.12) and (5.3.14) may be integrated to yield the characteristics

$u = $ const.

$$r = r_o e^{-(\theta + \frac{\pi}{2} - \gamma)\tan \varphi}$$

$z = $ const.

$$r = r_o e^{(\theta + \frac{\pi}{2} - \gamma)\cot \varphi}$$

where r_o is measured along OD.

Along the limiting slip line CD, the normal component of velocity vanishes[11] so that the velocity vector at any point on CD has a direction given by the tangent to CD at that point.

Then along CD the angle $\bar{\alpha}$ is

$$\bar{\alpha} = 2\pi - 2\gamma \qquad (5.3.16)$$

Substituting this value of $\bar{\alpha}$ into (5.3.13), the equation which holds along the $u = $ const line CD, yields

$$\tan(2\pi)\left[d\bar{\alpha} - \frac{\cot \varphi \ dr}{r}\right] - \frac{dv}{v} = 0$$

Since $\tan(2\pi) = 0$, this equation shows that along CD

$$dv_{CD} = 0$$

or $\qquad (5.3.17)$

$$v_{CD} = \text{const.}$$

The value of α in xy-coordinates at point D is

$$\alpha_D = -\gamma$$

59

Substituting this into (5.3.5), the differential equation to be satisfied along the z = const. line DE, yields

$$d\alpha_{DE} = 0$$

or   (5.3.18)

$$\alpha_{DE} = const. = -\gamma$$

Equation (5.3.18) shows that the angle α undergoes an abrupt change along the characteristic DE. Substituting the value of α given by (5.3.13) into (5.3.7) shows that v_{DE} is arbitrary. The value of v_{DE} to be used along DE in extending the solution is obtained from the condition that the components of the velocity vector normal to DE must be continuous when the direction of the velocity undergoes an abrupt change across DE.

The value of v along CD may now be obtained from the initial velocity at point D

$$v_{CD} = \frac{v_D}{\cos\gamma}$$ (5.3.19)

Both α and v are now known along the characteristics CD and DE and the solution may be extended into the region DEE_5C bounded by the initial characteristics DE and DC and the characteristics EE_5 and CE_5. The solution is next obtained in region EE_2F in the same way as region BB_1E. This method is continued until the solution is obtained in the region $BDCH_5$.

A method of finite-differences is used in obtaining the solution in the curvilinear region OCD since the equations to be satisfied along the characteristics can not be integrated as they could in region OBD. For the finite-difference solution the region is divided into a network of u and z characteristics and the node points are numbered by the coordinates k and ℓ taking ℓ along the u = const. lines and k along the z = const. lines.

Expressed in finite-difference form, the equations along the characteristic become

along u = const.

$$\tan(\bar{\alpha}_{k,\ell-1} + 2\gamma)\left\{\bar{\alpha}_{k,\ell} - \bar{\alpha}_{k,\ell-1} - \cot\varphi\left[\frac{r_{k,\ell} - r_{k,\ell-1}}{r_{k,\ell-1}}\right]\right\} - \left[\frac{v_{k,\ell} - v_{k,\ell-1}}{v_{k,\ell-1}}\right] = 0$$

$$(5.3.20)$$

along z = const.

$$\cot(\bar{\alpha}_{k-1,\ell} + 2\gamma)\left\{\bar{\alpha}_{k,\ell} - \alpha_{k-1,\ell} + \tan\varphi\left[\frac{r_{k,\ell} - r_{k-1,\ell}}{r_{k-1,\ell}}\right]\right\} + \left[\frac{v_{k,\ell} - v_{k-1,\ell}}{v_{k-1,\ell}}\right] = 0$$

$$(5.3.21)$$

Knowing the values of $\bar{\alpha}$ and v at the points $k,\ell-1$ and $k-1,\ell$ the above algebraic equations may be solved to yield $\bar{\alpha}$ and v at the point k,ℓ.

The solution for the values of $\bar{\alpha}$ and v at node points on the line OD are obtained by solving (5.3.6) and (5.3.21) simultaneously. Using (5.3.11), the equations to be solved for points on OD are

$$v_{k,\ell} = \frac{v_{k,\ell-1}\cos(\alpha_{k,\ell-1} + \gamma)}{\cos(\alpha_{k,\ell} + \gamma)}$$

$$(5.3.22)$$

and

$$v_{k,\ell} = -v_{k-1,\ell}\cot(\bar{\alpha}_{k-1,\ell} + 2\gamma)\left\{\bar{\alpha}_{k,\ell} - \bar{\alpha}_{k-1,\ell} + \tan\varphi\left[\frac{r_{k,\ell} - r_{k-1,\ell}}{r_{k-1,\ell}}\right]\right\} + v_{k-1,\ell}$$

$$(5.3.23)$$

where

$$\bar{\alpha}_{k-1,\ell} = \alpha_{k-1,\ell} - \theta_{k-1,\ell} - \frac{\pi}{2}$$

61

The solution for OAC is carried out in essentially the same way.

5 4   Velocity Field for the Macro-Structural Theory

The velocity field solution obtained with the second kinematic
relation will be presented for the corresponding stress field solutions of
Sections 5.1 and 5.2. The velocity of the yielding structure will be assumed
to be uniformly distributed, that is, the structure is assumed to move down
as a rigid body. This behavior corresponds to the stress field solutions
given in Section 5.2 in which a region of the granular medium remains elastic
and moves essentially as a rigid body. Solutions for the case of a non-uniform
motion of the structure are given in Section 5.3.

The velocity equation of the basic system of the second kinematic
relation was given in Section 3.6 in polar coordinates. For $dy/dx = \tan(\theta - \gamma)$
active, this equation becomes

$$\sin \varphi \frac{\partial v}{\partial r} - \frac{\cos \varphi}{r} \frac{\partial v}{\partial \theta} + \frac{v}{r} \sin \varphi = 0 \qquad (5.4.1)$$

The differential equation of the characteristics which correspond to the active
slip lines is

$$\frac{d\theta}{dr} = \frac{-\cot \varphi}{r} \qquad (5.4.2)$$

and the differential relation which must be satisfied along the characteristics
is

$$dv = v \tan \varphi \, d\theta \qquad (5.4.3)$$

Equation (5.4.3) yields

$$v = v_i e^{\theta \tan \varphi} \qquad (5.4.4)$$

62

where v_1 is an arbitrary constant.

In region OCD of Fig. 5.11, the velocity vector at any point is tangent to the slip line given by Eq. (5.4.2); however, in region ODD' the velocity vector is vertical. This requires that a velocity discontinuity forms on the cha.acteristics GD. Similarly, the velocity is discontinuous across the characteristic OC. Across a discontinuity of this type only the tangential components of velocity are discontinuous while the normal components are continuous[16].

The velocity in region OCD just across the discontinuity OD may be obtained in terms of the velocity of the structure v_q, by equating the normal components of the velocity vectors on each side of OD as is shown in Fig. 5.12(a). From Fig. 5.12(a)

$$v_{qn} = v_q \sin(\gamma + \beta_{00}) \tag{5.4.5}$$

Since the normal components of velocity are equal,

$$v_{qn} = v_{00} \cos\left(\frac{\pi}{2} - 2\gamma\right)$$

$$\tag{5.4.6}$$

or

$$v_{00} = \frac{v_q(\sin \gamma + \beta_{00})}{\cos\left(\frac{\pi}{2} - 2\gamma\right)}$$

The arbitrary constant in Eq. (5.4.4) may be evaluated as follows:

$$v_{00} = v_1 e^{\left(\gamma + \beta_{00} - \frac{\pi}{2}\right)\tan\phi}$$

or

$$v_1 = v_{00} e^{\left(-\gamma - \beta_{00} + \frac{\pi}{2}\right)\tan\phi}$$

Equation (5.4.4) now becomes

$$v = v_{OD}e^{(\theta + \frac{\pi}{2} - \gamma - \beta_{OD}) \tan \varphi} \qquad (5.4.7)$$

The velocity on OC is obtained by substituting the value of θ on OC into Eq. (5.4.7).

$$v_{OC} = v_{OD}e^{(\beta_{OC} - \beta_{OD}) \tan \varphi} \qquad (5.4.8)$$

The velocity in region OCC', v_p, is obtained in terms of v_{OC} by equating the normal components of velocity across OC as is shown in Fig. 5.12(b).

$$v_p \cos(\gamma + \beta_{OC} - \tfrac{\pi}{2}) = v_{OC} \cos(\tfrac{\pi}{2} - 2\gamma) \qquad (5.4.9)$$

Substituting Eqs. (5.4.6) and (5.4.8) into Eq. (5.4.9), one obtains the velocity in region OCC', v_p, as a function of v_q, the velocity in region ODD'.

$$v_p = v_q \frac{\sin(\gamma + \beta_{OD})}{\sin(\gamma + \beta_{OC})} e^{(\beta_{OC} - \beta_{OD}) \tan \varphi} \qquad (5.4.10)$$

For the stress field given in Section 5.1, $\beta_{OC} = \pi/2$ and $\beta_{OD} = 0$. Then Eq. (5.4.10) becomes

$$v_p = v_q \tan \gamma \, e^{\frac{\pi}{2} \tan \varphi} \qquad (5.4.11)$$

It may now be shown that overall continuity of the velocity field is satisfied. Multiplying the velocity of OCC' by the length CC' given by Eq. (5.1.14), one obtains

$$v_p \cdot CC' = v_q \left[\frac{\sin(\gamma + \beta_{OD})}{\sin(\gamma + \beta_{OC})} e^{(\beta_{OC} - \beta_{OD}) \tan \varphi} \cdot L \cdot \frac{\sin(\gamma + \beta_{OC})}{\sin(\gamma + \beta_{OD})} e^{-(\beta_{OC} - \beta_{OD}) \tan \varphi} \right]$$

$$(5.4.12)$$

64

or

$$v_p \cdot CC' = v_q \cdot L$$

Thus, a velocity field has been found which is compatible with the corresponding stress field.

6. RESULTS AND CONCLUSIONS BASED ON THE QUASI-STATIC THEORY

6.1 Comparison with Experiments

The results obtained in an analysis using the Geniev theory of motion of a granular media to predict the intensity of air-induced overpressure transmitted to an underground structure are shown in Fig. 6.1 along with experimental data obtained by Selig, McKee and Vey. [10,22] The experimental work was conducted with a dense, cohesionless Ottawa sand ($\varphi = 35^o$) contained in a glass-walled pressure device. The yielding structure was a 4-inch square plate. It may be readily seen from Figure 6.1 that the experimental pressures required for failure are several times greater than those predicted by the Geniev theory. The lack of agreement between these two curves is to be expected because of two major factors. For one, the experiments were not actually performed under conditions of two-dimensional plane-strain as assumed in the Geniev theory, since the glass walls of the pressure box contributed some frictional resistance to slip. Also, and more significantly, the Geniev theory used here assumes that plastic flow takes place at constant volume, that is, the flow is incompressible. In the case of granular materials, this assumption is correct only after initial slip has occurred and the flow field is established. [23] For a dense granular material, initial slip must be accompanied by an increase in volume as the individual particles "unlock" from their positions in the dense state and ride over adjacent grains on the slip-plane. This intuitively apparent behavior has been proved conclusively by experiment [23,24]. As slip first occurs, there is a change in volume of the granular mass, and after a certain strain the deformation settles down to one occurring at constant volume. It is in this constant volume deformation that the Geniev theory is applicable.

66

The volume increase required for slip in dense granular soils and the lateral constraint provided by the soil mass itself have a significant effect on the pressure required to produce first slip. Terzaghi has indicated that the so-called internal friction of the soil is a function of the amount of lateral expansion possible in the soil and that the angle φ may vary between wide limits. [25]

In another paper, Terzaghi states that for granular materials the value of φ, the angle of internal friction, may vary between the limits of 30 and 54 degrees. [26] If in the Geniev analysis the value of φ is allowed to vary in accordance with the degree of lateral constraint provided by the soil mass at various depths, a failure pressure vs. depth of burial curve is obtained which gives much improved agreement with the experimental results as shown in Fig. 6.1. The assumed variation of φ with depth is presented in Fig. 6.2 as the ratio of the value of φ used in determining the failure pressure at a particular depth to φ_0, the value of internal friction determined by the usual laboratory tests. The value of φ/φ_0 is assumed to vary from 1.0 for structures placed near the ground surface where there is a small lateral constraint to 1.5 for a depth of burial equal to the span length. At greater depths the value of φ/φ_0 is assumed to remain constant. Although the angle of internal friction φ is shown to vary with depth in Fig. 6.2, it is not treated as a variable at any one particular depth. Solutions including the effect of lateral constraint may be obtained by using the value of φ_0 to determine the shape of the slip field and then incorporating the effect of lateral constraint by determining the failure pressure based on the value of φ given in Fig. 6.2 for the particular depth associated with the slip field. This approach is

undoubtedly only approximate but it does provide an indication of the pressure required for first slip of the soil.

Since the pressure required to maintain slip in a dense granular material is less than that required to produce slip, it is clear that a question of stability is involved in regard to the safety of the structure after first slip has occurred. Whether or not complete collapse of the structure will take place depends on the intensity and timewise variation of the loading pulse and the ductility of the structure. However, the question of stability does not apply if the failure pressures are determined by the Geniev analysis (without the lateral constraint correction), since the failure pressure is based on that required to maintain flow not start it, and thereby neglects what may be an appreciable, although highly undependable, resistance of the soil.

6.2 Comparison with Previous Theoretical Studies

A theory of plastic flow of granular media developed by Drucker and Prager [27] based on the concepts of the plastic potential [28,29] has been applied by Shield [30] to problems of plastic flow in granular soils. In this theory plastic flow of a granular media is always accompanied by a volume increase (a property Drucker and Prager refer to as dilatancy). However in this theory the volume expansion continues at the same rate for all values of strain; a very unlikely event for continued plastic flow and a behavior which experimental evidence has shown does not occur. [13] Geniev cites experimental work on a particular problem solved analytically by Shield using the Drucker-Prager Theory. The test results indicate that the flow trajectories predicted on the basis of a constant rate of volumetric strain theo y are not realized. Rather, the experimentally determined flow field could be

68

hetter approximated by a constant volume (zero rate of volumetric strain) theory such as Geniev's.

Another solution of the underground structure problem is included in a theory presented by Terzaghi for the design of tunnels at great depths.[1] This theory, modified slightly to correspond to the specific problem considered here, is based on the assumption that the vertical stresses are uniformly distributed on horizontal sections and that the slip-planes form vertically. According to this theory the pressure applied at the ground surface to cause failure is given by

$$p_o = q \exp \left(2 \frac{H}{L} K \tan \varphi \right) \qquad (6.2.1)$$

where K is an empirical coefficient which represents the ratio σ_H/σ_V on the surface of sliding. Terzaghi recommended that the value of K be at least equal to unity. Failure pressure vs. depth curves for Terzaghi's theory with K = 1 and K = 1.5 are shown in Fig. 6.3 along with a curve for the Geniev theory for $\varphi = 35^\circ$ and k = 0. The experimental curve given in Fig. 6.1 is also shown for comparison.

It may be seen from Fig. 6.3 that the general trend of the Terzaghi curves does not follow either the Geniev or the experimental curve except at depth-span ratios greater than about 1.5, where the Terzaghi and Geniev curves predict very nearly the same failure pressure.

Also shown in Fig. 6.3 is a curve for a theory presented by Selig, McKee and Vey, the same group who presented the experimental results shown in Figs. 6.1 and 6.3. Their theory is based on the formation of vertical slip planes and a uniform distribution of vertical stress on horizontal sections. For the quasi-static case of a uniform, slowly varying overpressure, this

theory is essentially the same as Terzaghi's with a linear variation of
failure pressure vs. depth on semi-logarithmic coordinates as shown in Fig

Takagi [31] has presented a theory of granular soils deformation in
which the volume change resulting from the plastic deformation may be taken
into account. Unfortunately, the rate of volume change is considered to be
constant depending on the nature of the deofrmation. As a result, Takagi's
theory does not account for the real behavior of expansion or contraction c
the start of motion and subsequent slip at constant volume.

6.3 Limitations of the Theory

The results of this study indicate that the Geniev theory has several significant limitations when applied to the problem of underground structures in a granular soil subjected to air overpressures. The fact that the deformation is assumed to occur at constant volume does not allow the volume change occurring at initial slip of a dense granular material to be taken into account. This neglect of the volume increase at initial slip is particularly significant in the type of problem considered here, as the tendency for a volume increase brings into play a considerable lateral constraining effect in the soil which serves to greatly increase the resistance of the soil structure system against slip. In contrast to this, a constant volume theory should introduce little error for problems in which the soil is permitted to expand at a free surface such as in the determination of the passive earth pressure of retaining walls and the bearing capacity of footings.

Another weakness of the Geniev theory common to all theories of rigid plastic behavior is the fact that no information is available regarding the formation of failure zones from the previous elastic equilibrium state. In other words, with rigid-plastic theories it is not possible to predict the origin and trace the growth of distressed regions in the medium since the elastic stress distribution prior to flow is not available. On the other hand, with elasto-plastic theories the formation of failure zones may be predicted from the elastic solution by increasing the loads until the flow criterion is satisfied.

An important complication in theories of granular media arises from the fact that the failure criterion is a function of the mean normal

stress at a point and not simply a function of the deviatoric component of
stress as is the case with ideal plasticity. For plasticity problems it has
been shown that upper and lower bounds for the failure load may be obtained
by application of limit theorems [32,33,34,35]. In addition, these theorems
guarantee that any solution which is both statically and geometrically
admissable must give the correct failure load. When the yield criterion
depends on the mean normal stress, the bound theorems of plasticity do not
apply and the failure load cannot easily be bounded. However, a theory such
as Geniev's which neglects a portion of the soil's resistance will give
conservative failure pressures.

Failure pressures obtained with the Geniev theory may be improved
to account approximately for the effect of lateral constraint of the soil at
initial slip by assuming the angle of internal friction ϕ to be a function of
the amount of soil cover over the roof of the structure.

Since large deformations of a granular media occur essentially at
constant volume, the Geniev solutions should provide a good estimate of the
resistance of the soil-structure system to sustained loads if the structure
has sufficient ductility to withstand the initial displacement.

The results of this study indicate that a theory more realistic
than Geniev's is needed for the analysis of the truly dynamic problem of
soil-structure interaction. This more elaborate theory must necessarily
include the effects of expansion or contraction of the granular soil as
motion takes place and the relation between this volume change and the
failure law. In addition, the mode of development of failure zones requires
clarification in future work.

REFERENCES

1. Terzaghi, K., _Theoretical Soil Mechanics_ , Wiley, New York, 1943

2. Terzaghi, K. and Peck, R. B., _Soil Mechanics in Engineering Practice_ , Wiley, New York, 1956.

3. Whipple, C. R., _The Dynamic Response of Shallow Buried Arches Subjected to Blast Loading_ . Ph.D. Thesis, Department of Civil Engineering, University of Illinois, Urbana, Illinois, 1961.

4. Anderson, F. E. Jr., "Blast Phenomena from a Nuclear Burst", _Proceedings of the American Society of Civil Engineers_, Volume 84, No. ST7, November, 1958, pp. 1836-1 to 1836-8.

5. _The Effects of Nuclear Weapons_, U.S. Department of Defense and Atomic Energy Commission, U. S. Government Printing Office, Washington 25, D.C., April, 1962.

6. Smith, R. H., and Newmark, N. M., _Numerical Integration for One-Dimensional Stress Waves_, Report to Office of Naval Research, U.S. Navy, Contract Nonr 1834 (03), University of Illinois Civil Engineering Studies, Structural Research Series No. 162, Urbana, Illinois August, 1958.

7. Terzaghi, K., "Stress Distribution in Dry and in Saturated Sand Above a Yielding Trap Door", _Proceedings of the International Conference on Soil Mechanics and Foundation Engineering_, Cambridge, Massachusetts 1936 V. I, p. 307.

8. McDonough, G. F. Jr., _Dynamic Loads on Buried Structures_ Ph.D. Thesis Department of Civil Engineering, University of Illinois, Urbana, Illinois 1959

9. Walls, W. A., _The Influence of Blast and Earth Pressure Loadings on the Dynamic Response of Flexible Underground Two-Hinged Arches_ , Ph.D. Thesis, Department of Civil Engineering, University of Illinois, Urbana, Illinois, 1960.

10. Selig, E. T., McKee, K. E. and Vey, E., "Underground Structures Subjected to Air Overpressure", _Proceedings of the American Society of Civil Engineers_, V. 86, No. EM4, August 1960, pp. 87-103.

11. Geniev, G. A., _Problems of the Dynamics of Granular Media_ (in Russian) Academy for Structures and Architecture, U.S.S.R., Scientific Communication No. 2, Mosco 1958.

12. Crandall, S. H., _Engineering Analysis_ , McGraw-Hill Book Co., New York, 1956.

REFERENCES (continued)

13. Hansen, J. B., Earth Pressure Calculations , The Danish Technical Press, Copenhagen, 1953.

14. Hill, R. The Mathematical Theory of Plasticity , The Clarendon Press, Oxford, 1950.

15. Sokolovski, V. V., Statics of Soil Media , Butterworth, London, 1960 (Translated from 2nd Edition of Statics of Soil Media (Russian), 1954 by D. H. Jones and A. N. Scholfield).

16. Prager, W. and Hodge, P. G., Theory of Perfectly Plastic Solids , John Wiley and Sons, New York, 1951.

17. Sokolovski, V. V., Theorie der Plastizität , Verlag Technik, Berlin, 1955 (German translation of Russian Text published in Moscow, 1950).

18. Hencky, H., "Über Einige Statisch Bestimmte Fälle des Gleichgewichts in Plastischen Körpern", Zeitschrift für Angewandte Mathematik und Mechanik, Vol. 3, 1923 pp. 241-251.

19. Prandtl, L., "Anwendungsbeispiele zu einem Henckyschen Satz über das plastische Gleichgewicht", Zeitschrift für Angewandte Mathematik und Mechanik, Vol. 3, 1923, pp. 401-406.

20. Hill, R., Lee, E. H. and Tupper, S. J., "A Method of Numerical Analysis of Plastic Flow in Plane Strain and Its Application to the Compression of a Ductile Material Between Rough Plates", Journal of Applied Mechanics Vol. 18, No. 1, March 1951, pp. 46-52.

21. Lee, E. H., "On Stress Discontinuities in Plane Plastic Flow", Symposia in Applied Mathematics, Vol. III, pp. 213-228, McGraw-Hill Book Co., New York, 1950.

22. Selig, E. T., McKee, and Vey, E., discussion of paper "Underground Structures Subjected to Air Overpressures" Proceedings of the American Society of Civil Engineers. V. 87, No. EM3, June, 1961, pp. 55-58.

23. DeJong, G. J., Statics and Kinematics in the Failable Zone of a Granular Material , Uiteverij, Waltman, Delft, 1958.

24. Spangler. M. G., Soil Engineering , 2d. Ed., International Textbook Co., Scranton, Pennsylvania, 1960.

25. Terzaghi, K., discussion of paper by J. Feid, "Lateral Earth Pressure", Transaction of the American Society of Civil Engineers, V. 86, 1923, pp. 1525-1543.

REFERENCES (continued)

26. Terzaghi, K., "Old Earth Pressure Theories and New Test Results",
    Engineering News-Record, V. 85, No. 14, 1920, pp. 632-637.

27. Drucker, D. C. and Prager, W., "Soil Mechanics and Plastic Analysis
    or Limit Design", Quarterly of Applied Mathematics,V. 10, 1952,
    pp. 157-165.

28. von Mises, R., "Mechanik der Plastischen Formänderung von Kristallen",
    Zeitschrift für Angewandte Mathematik und Mechanik,Vol. 8, 1928,
    pp. 161-185.

29. Koiter, W. T., "Stress-Strain Relations, Uniqueness and Variational
    Theorems for Elastic-Plastic Materials with a Singular Yield Surface",
    Quarterly of Applied Mathematics, Vol. 11, 1953, pp. 350-354.

30. Shield, R. T., "Mixed Boundary Value Problems in Soil Mechanics",
    Quarterly of Applied Matnematics, V. 11,1953, pp. 61-75.

31. Takagi, S., "Plane Plastic Deformation of Soils", Proceedings of the
    American Society of Civil Engineers, V. 88, No. EM3, June, 1962,
    pp. 107-151.

32. Greenberg, H. J. and Prager, W., "Limit Design of Beams and Frames",
    Proceedings of the American Society of Civil Engineers, Vol. 77,
    Separate No. 59, February, 1951.

33. Drucker, D. C., Greenberg, H. J. and Prager, W. "The Safety Factor of
    an Elastic-Plastic Body in Plane Strain", Journal of Applied Mechanics,
    Vol. 18, 1951, pp. 371-378.

34. Drucker. D. C., Prager, W. and Greenberg, H. J. "Extended Limit
    Design Theorems for Continuous Media", Quarterly of Applied Mathematics,
    Vol. 9, 1952, pp. 381-389.

35. Prager, W., "The General Theory of Limit Design", Proceedings 8th
    International Congress on Theoretical and Applied Mechanics, Istanbul
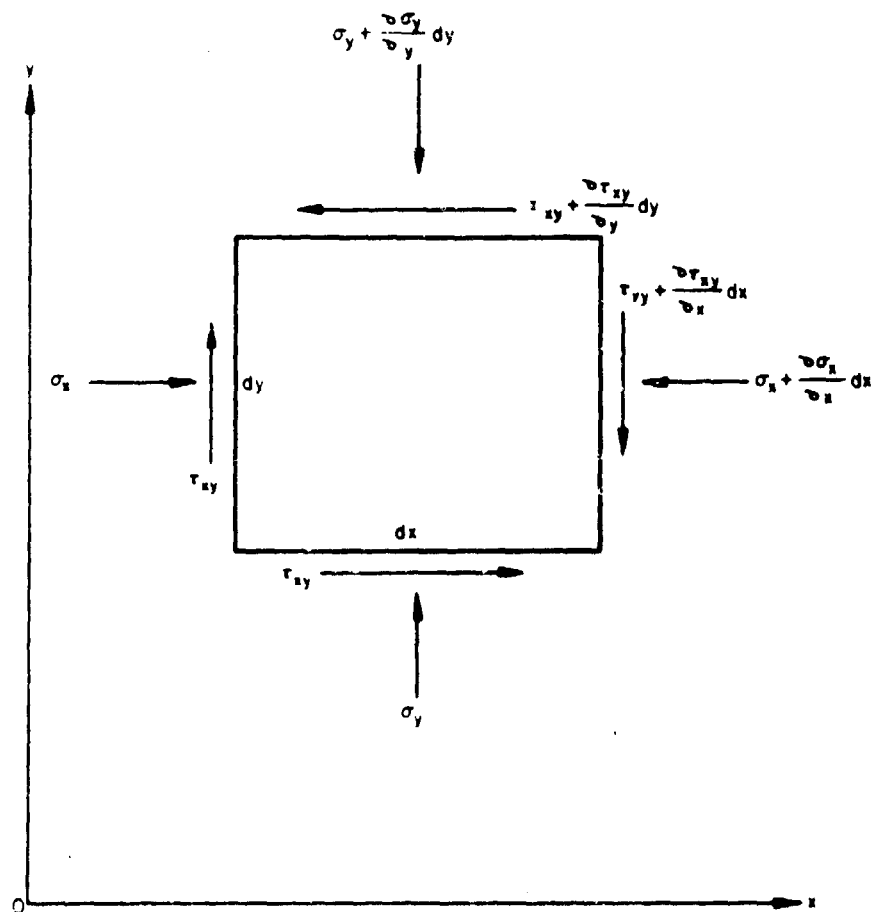   1952, pp. 65-75.

$\sigma_y + \dfrac{\partial \sigma_y}{\partial y} dy$

$\tau_{xy} + \dfrac{\partial \tau_{xy}}{\partial y} dy$

$\tau_{yy} + \dfrac{\partial \tau_{xy}}{\partial x} dx$

σ_x

$\sigma_x + \dfrac{\partial \sigma_x}{\partial x} dx$

dy

τ_{xy}

dx

τ_{xy}

σ_y

FIG. 2.1 INFINITESIMAL ELEMENT OF THE SOIL MEDIUM
WITH POSITIVE STRESS COMPONENTS
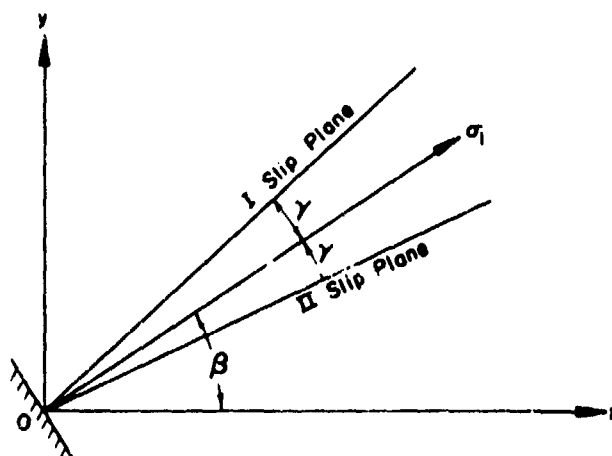
76
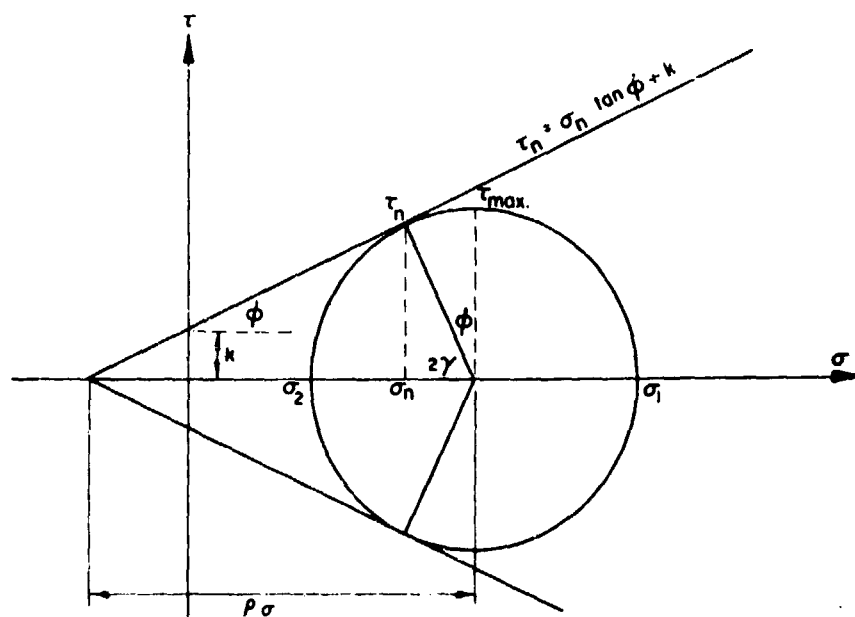
FIG. 2.2   COULOMB-MOHR FAILURE DIAGRAM

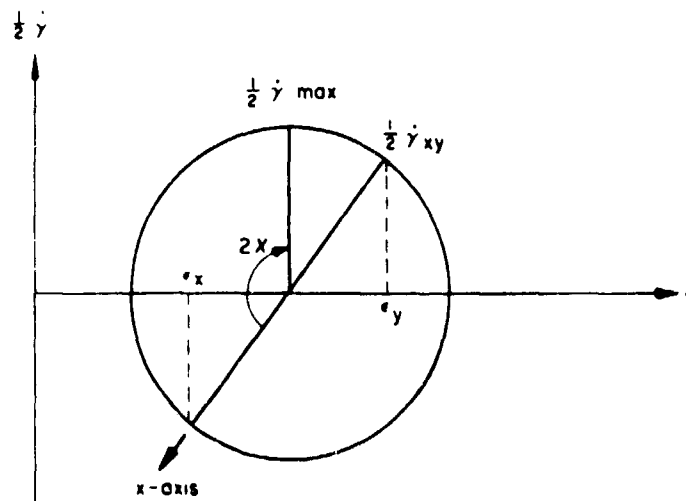FIG. 2.3   ORIENTATION OF THE SLIP PLANES WITH
RESPECT TO THE x-AXIS

77

FIG. 2.4 MOHR'S CIRCLE OF STRAIN RATES
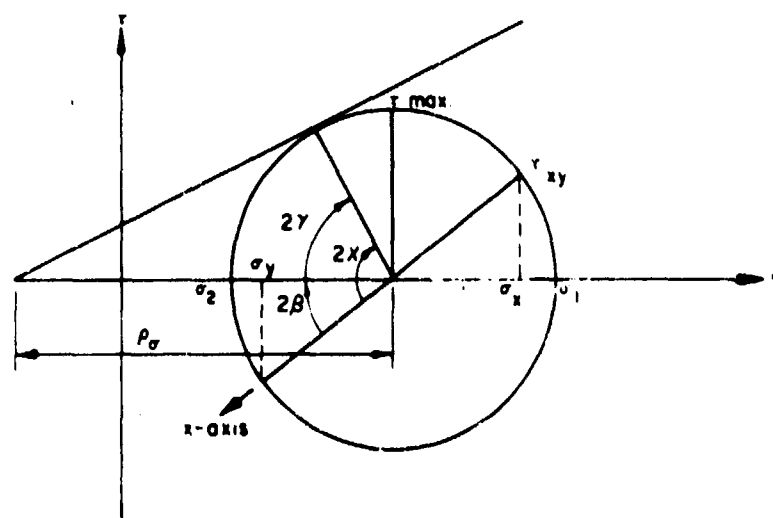
FIG. 2.5 MOHR'S CIRCLE OF STRESSES

78
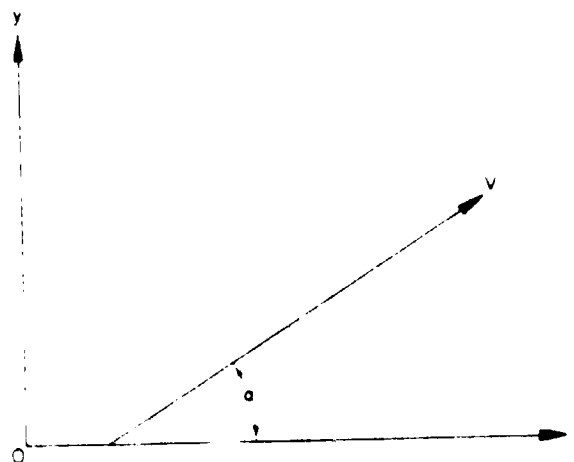
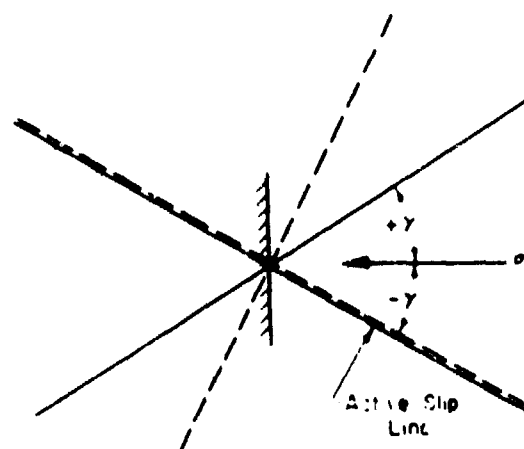FIG. 2.6   VELOCITY VECTOR ON THE xy-PLANE
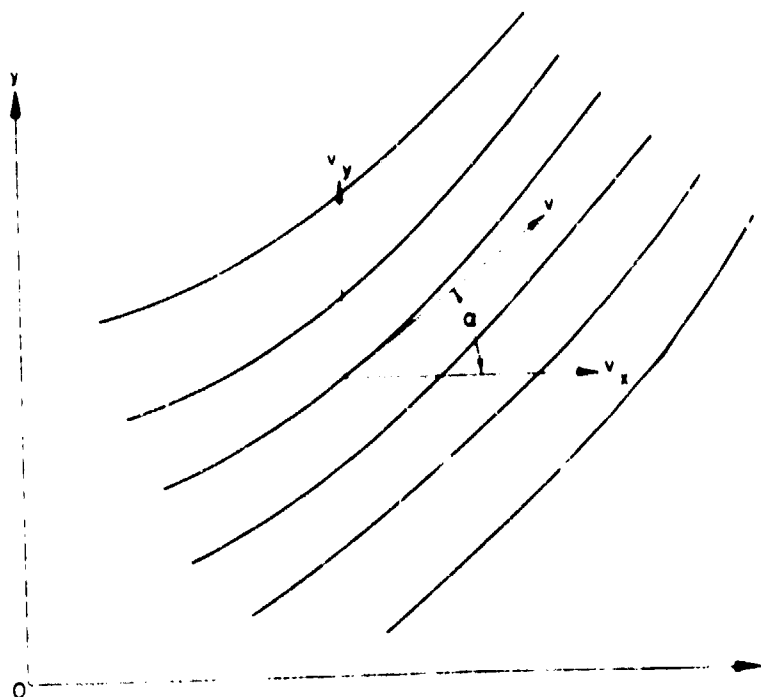
FIG. 2.7   SLIP LINE FIELD FOR THE MACRO-STRUCTURAL THEORY

79
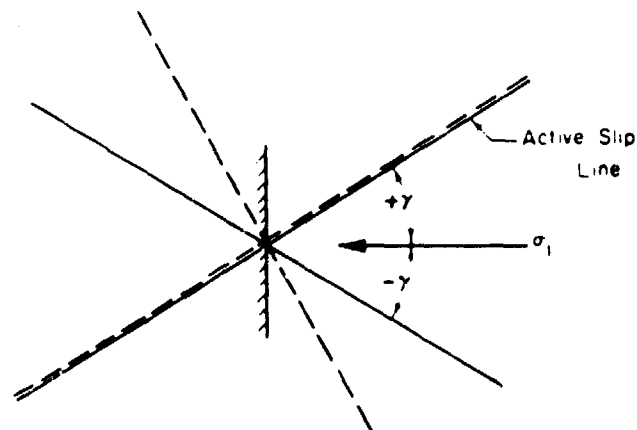
(a) Active Slip Line is $\frac{dy}{dx} = \tan(\beta + \gamma)$

(b) Active Slip Line is $\frac{dy}{dx} = \tan(\beta - \gamma)$

Characteristics of Stress Field ————

Characteristics of Velocity Field -------

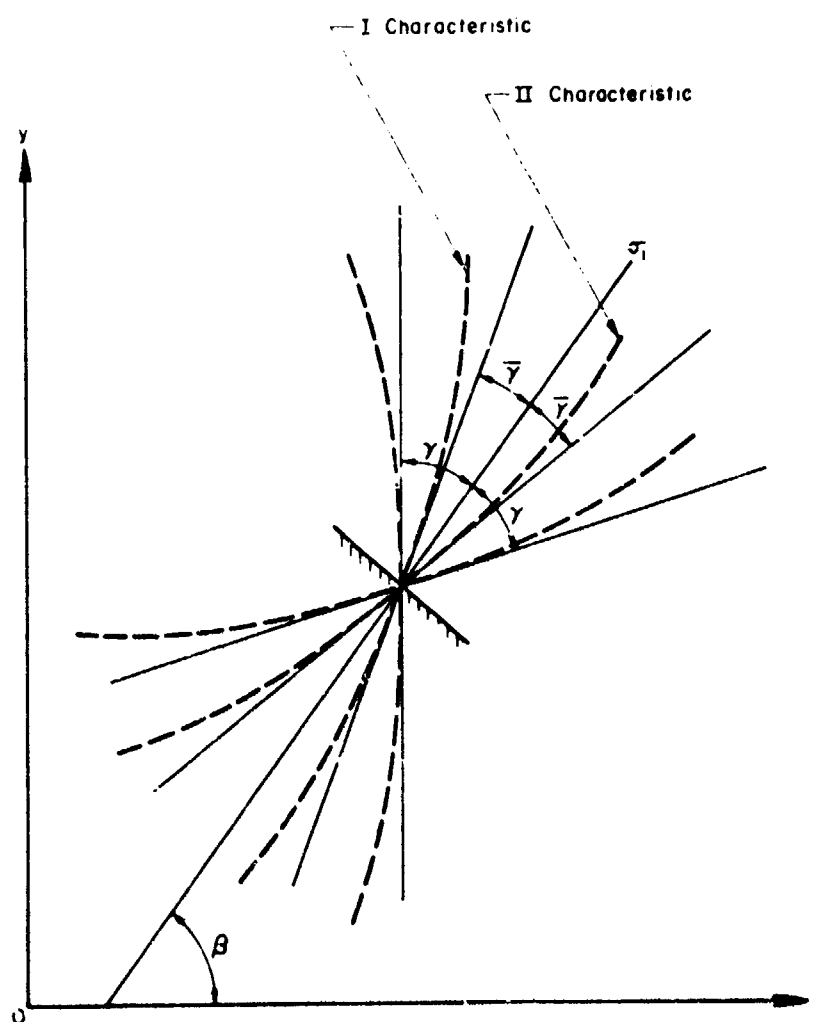FIG. 3.1 STRESS AND VELOCITY FIELD CHARACTERISTICS
          FOR THE CONTINUUM THEORY

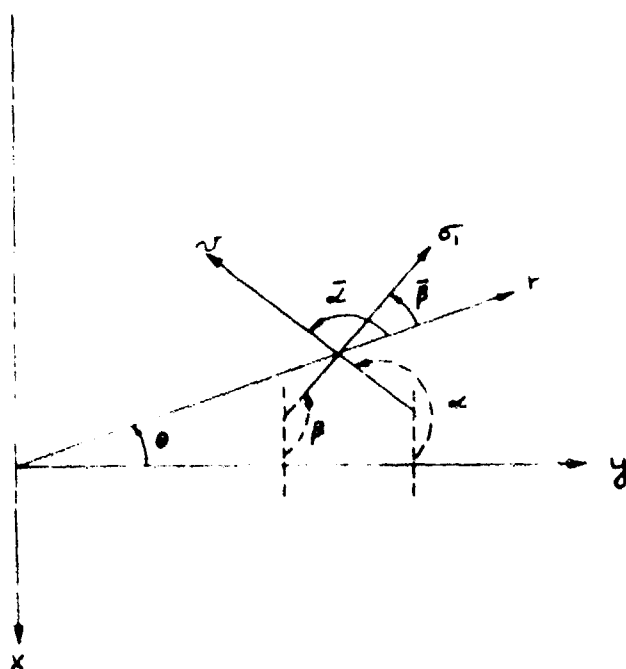FIG. 3.2 SYSTEM OF CHARACTERISTICS FOR THE
MACRO-STRUCTURAL THEORY

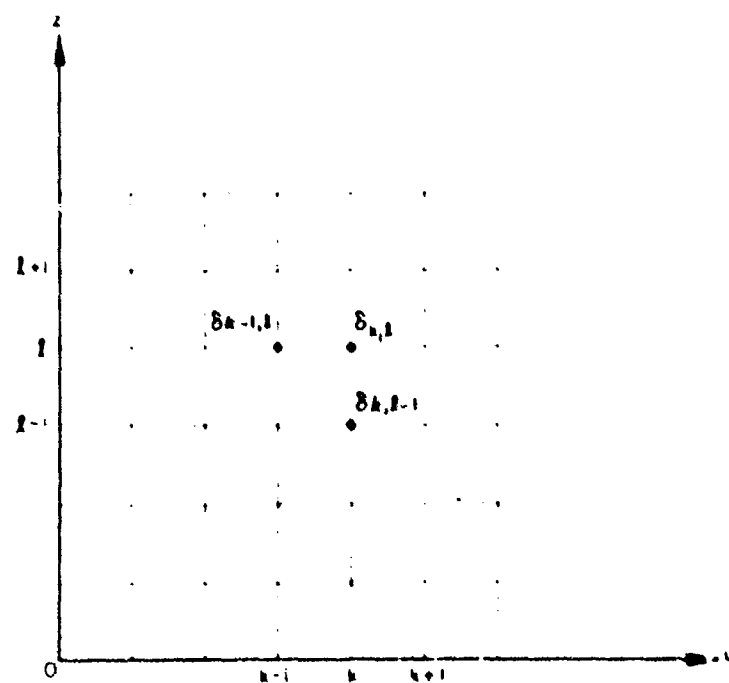**FIG. 3.3 SYSTEM OF PLANE POLAR COORDINATES USED IN THE CURVILINEAR REGION CD**

82

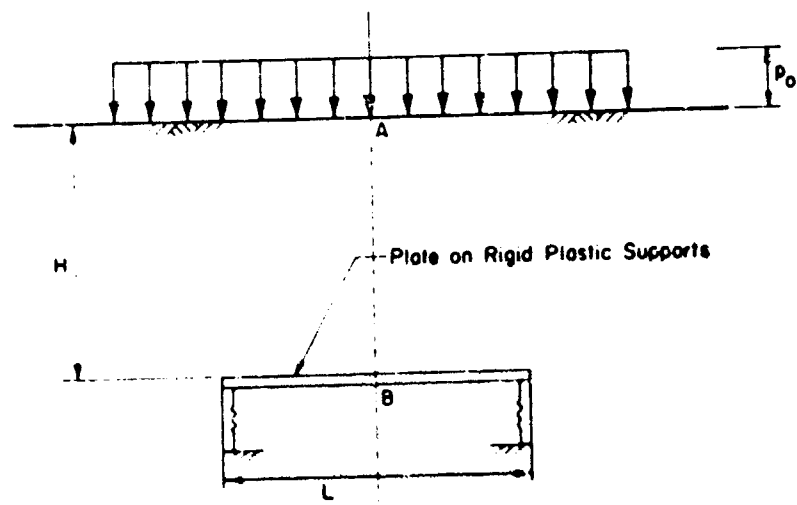FIG. 4.1 FINITE-DIFFERENCE NETWORK ON THE CHARACTERISTIC PLANE
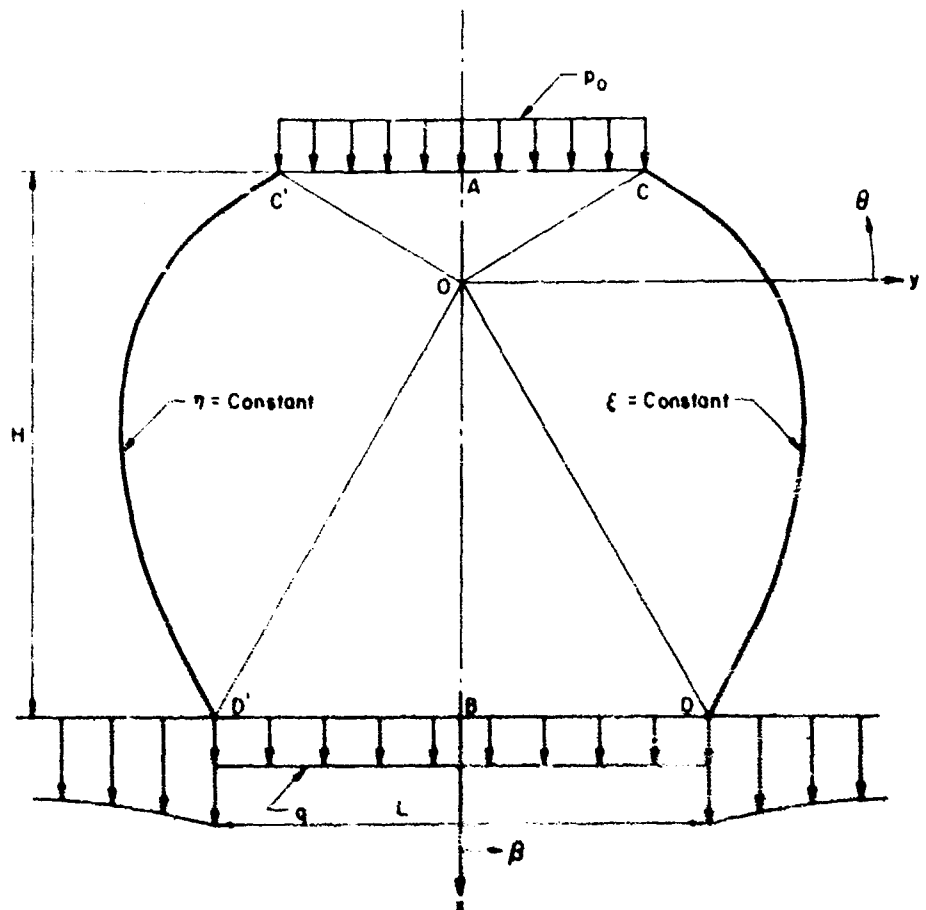
83

FIG. 5.1 UNDERGROUND STRUCTURE IN A GRANULAR MEDIUM

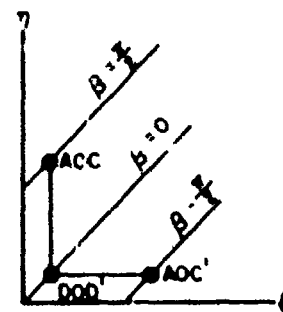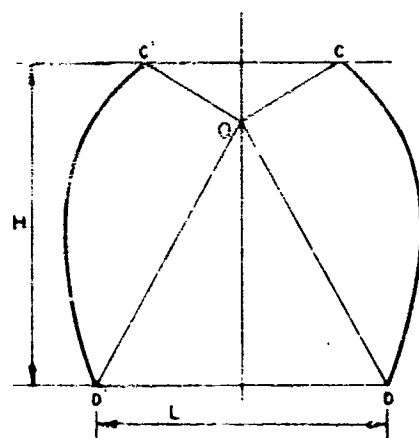FIG. 5.2 CHARACTERISTICS OF THE STRESS FIELD

FIG. 5.3 TRANSFORMATION TO THE ξη-CHARACTERISTIC PLANE
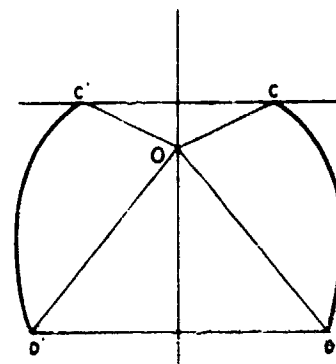
$\beta_{00} = 0°$
$\beta_{0c} = 90°$
$po/q = 2.04$
$H/L = 1.07$
(a)

$\beta_{00} = 10°$
$\beta_{0c} = 80°$
$po/q = 1.46$
$H/L = 0.73$
(b)
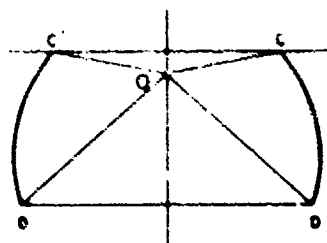
$\beta_{00} = 20°$
$\beta_{0c} = 70°$
$po/q = 1.21$
$H/L = 0.49$
(c)

$\beta_{00} = 30°$
$\beta_{0c} = 60°$
$po/q = 1.10$
$H/L = 0.36$
(d)

FIG. 5.4 STRESS FIELD AT DEPTHS LESS THAN CRITICAL, $k = 0$, $\varphi = 30°$
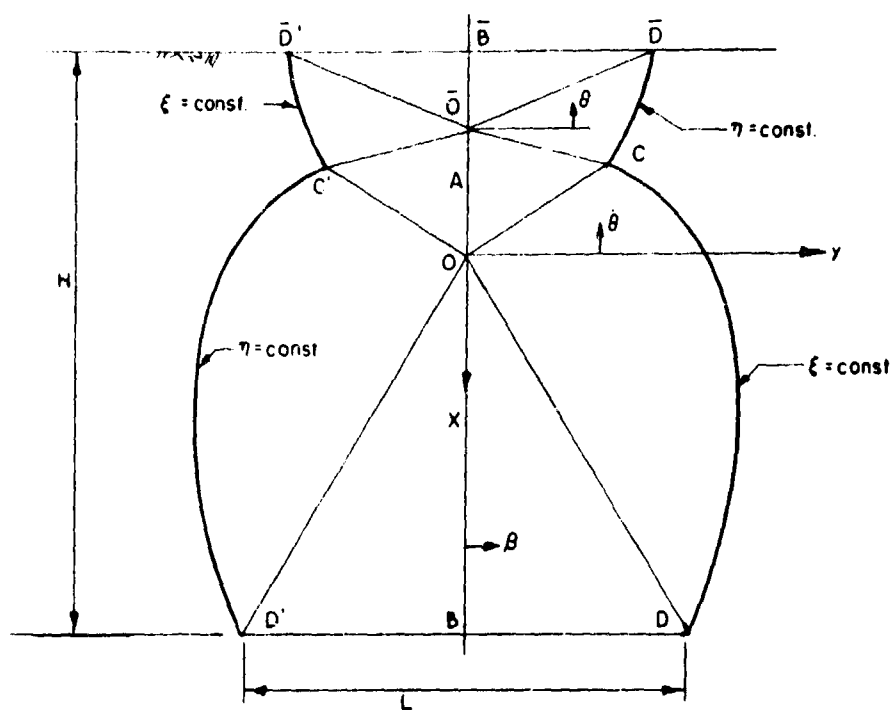
(a)
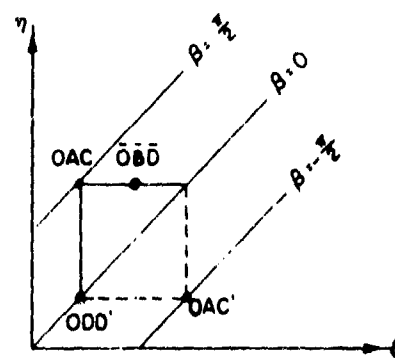
(b)

FIG. 5.5 STRESS FIELD AT A DEPTH GREATER THAN CRITICAL, $k = 0$, $\psi = 30^{\circ}$

$p_o/q = 2.04$

$H/L = 1.07$

$p_o/q = 4.50$

$H/L = 1.25$

$p_o/q = 20.5$

$H/L = 1.75$

$p_o/q = 37.6$

$H/L = 2.14$
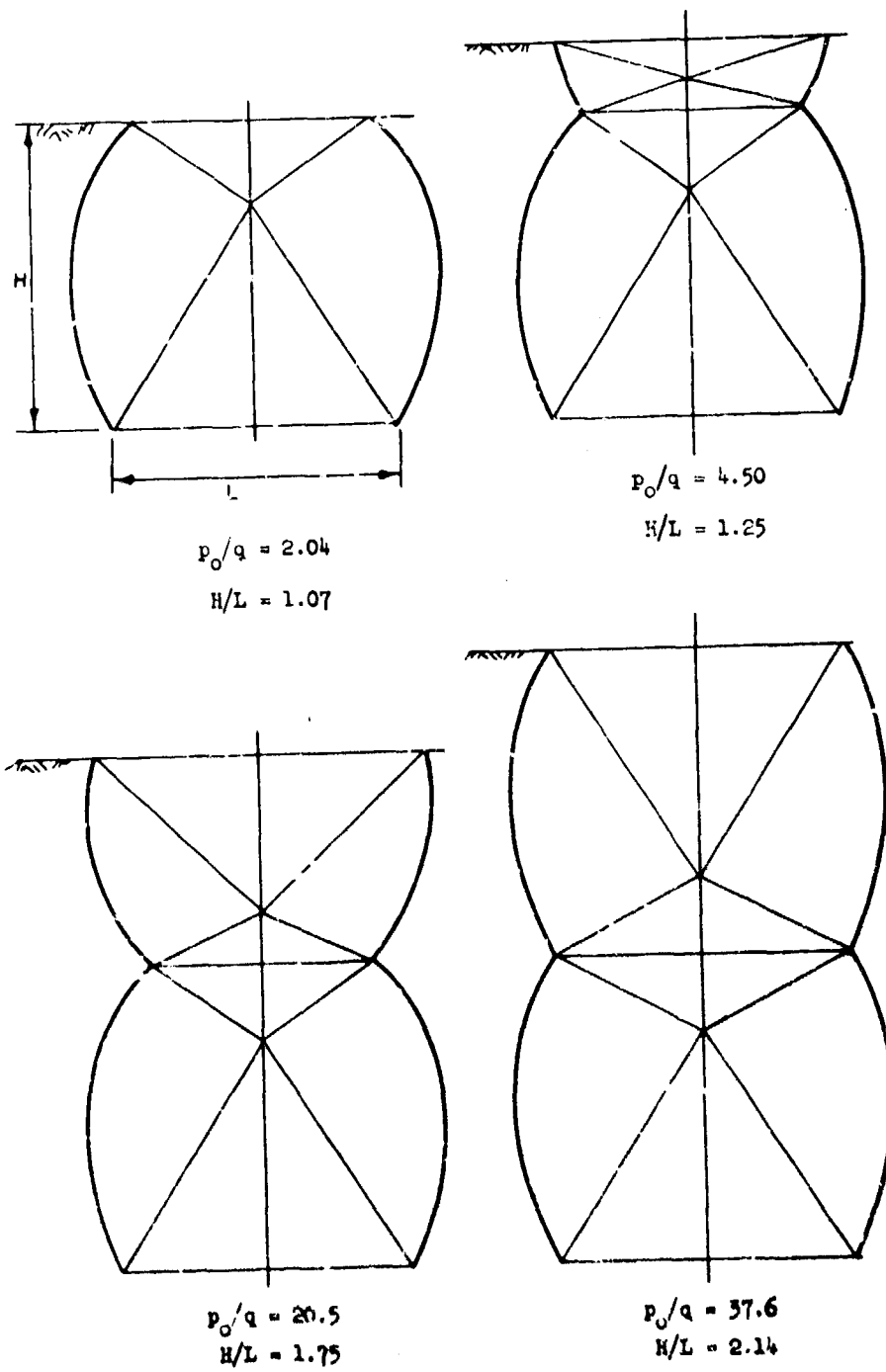
FIG. 5.6 STRESS FIELD AT DEPTHS GREATER THAN CRITICAL, $k = 0$, $\varphi = 30°$
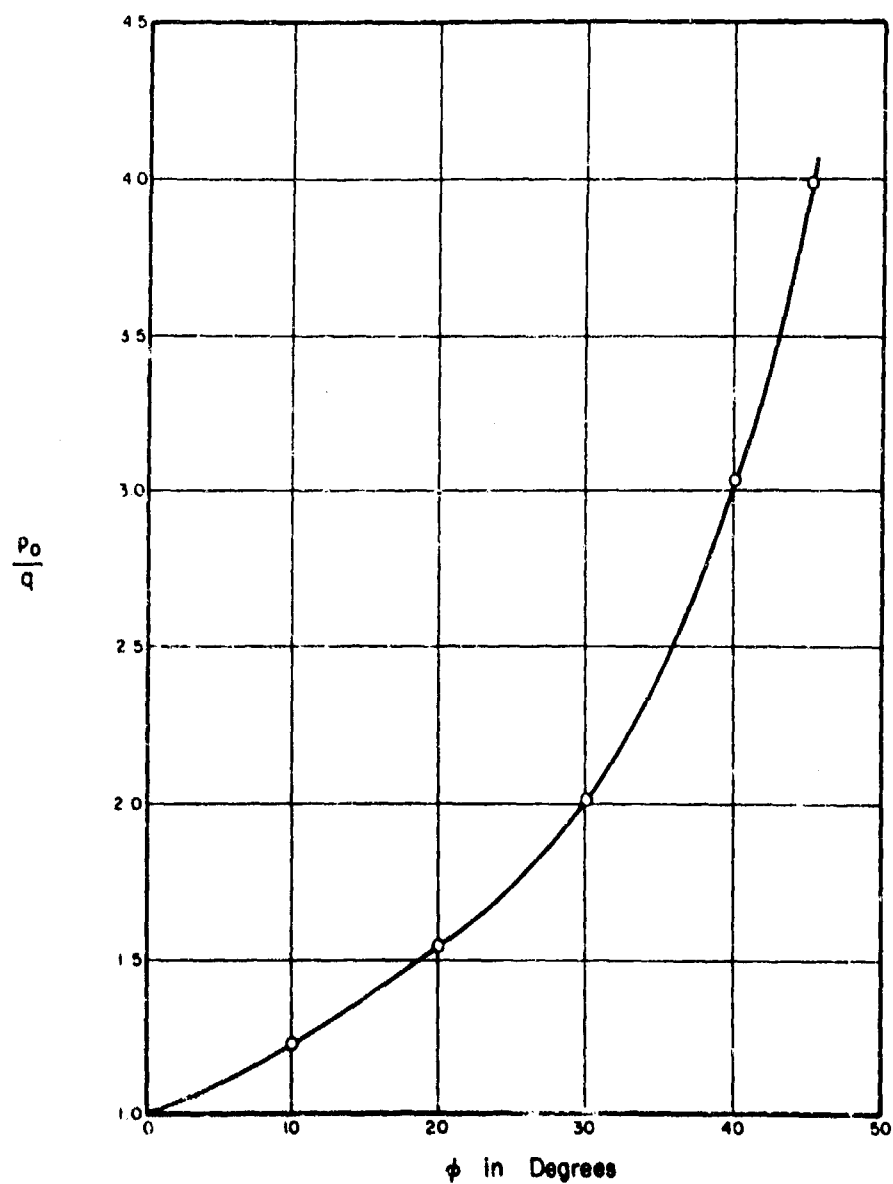
FIG. 5.7 EFFECT OF ANGLE OF INTERNAL FRICTION φ ON
FAILURE PRESSURE AT THE CRITICAL DEPTH IN
A COHESIONLESS MATERIAL

89
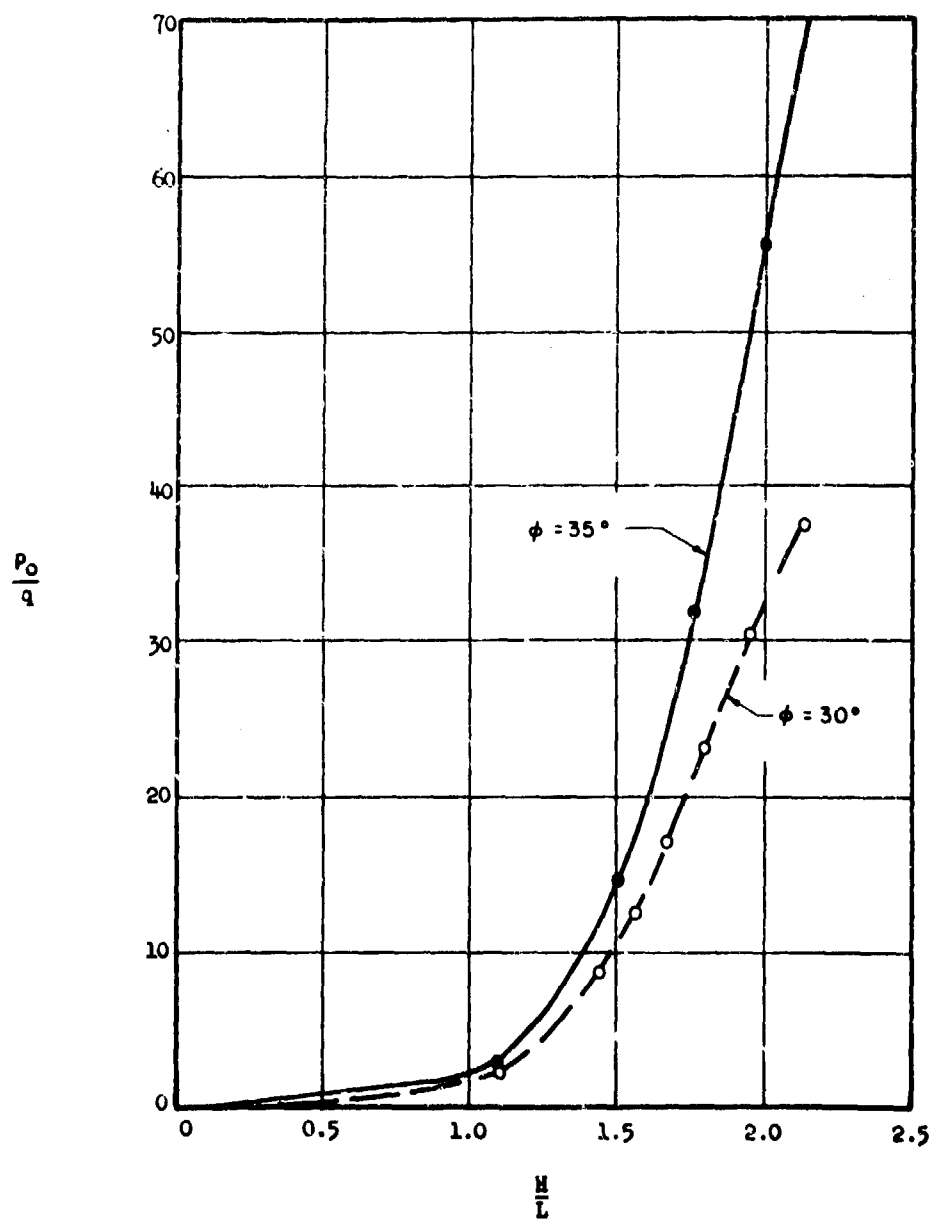
FIG. 5.8 FAILURE PRESSURE VS DEPTH-SPAN RATIO FOR
GENIEV THEORY (COHESIONLESS MATERIAL)

90

(a)

(b) Detail Near Point O

FIG. 5.9 VELOCITY CHARACTERISTICS. (FIRST KINEMATIC ASSUMPTION)
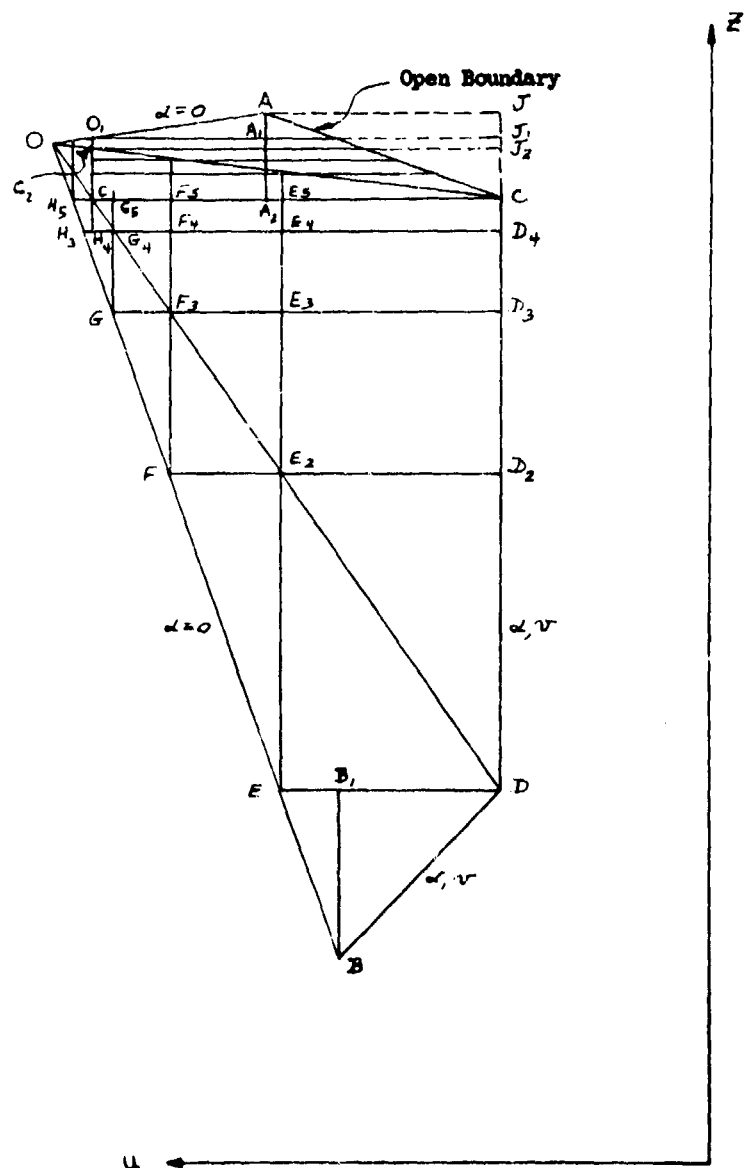
FIG. 5.10 CONFIGURATION OF PROBLEM ON uz-CHARACTERISTIC PLANE.
(FIRST KINEMATIC ASSUMPTION)

92
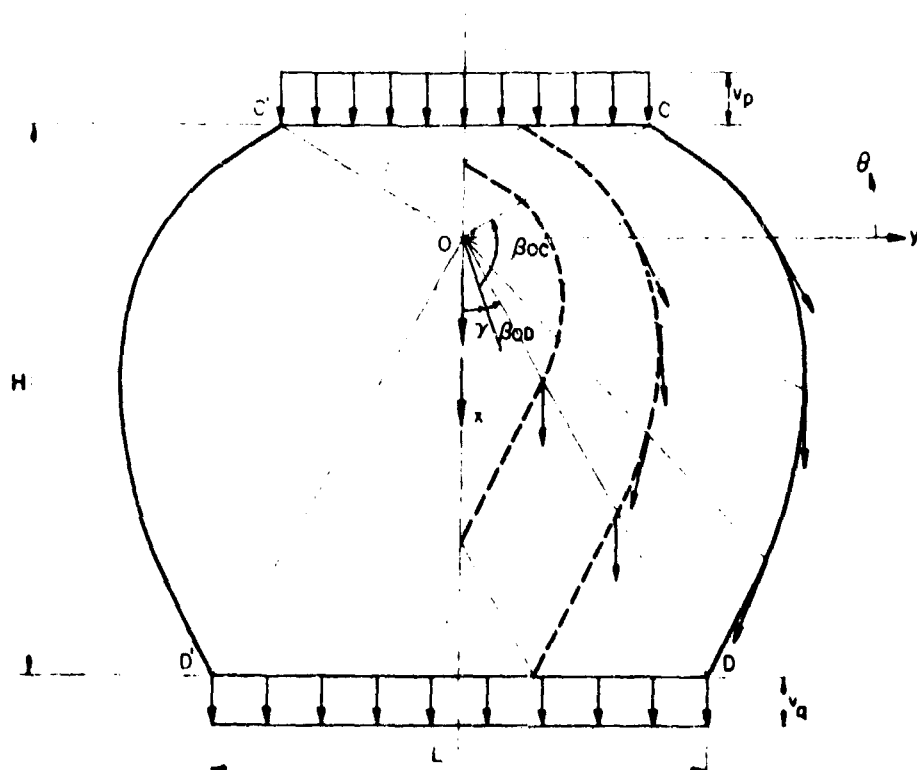
FIG. 5.11 VELOCITY FIELD CHARACTERISTICS. (SECOND KINEMATIC ASSUMPTION)
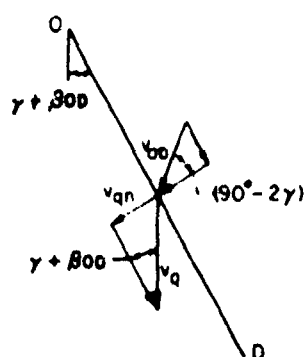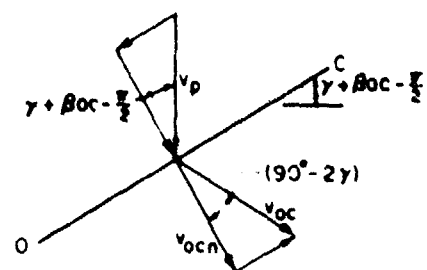
(a)   (b)

FIG. 5.12 VELOCITY DISCONTINUITIES ON OD AND OC

93
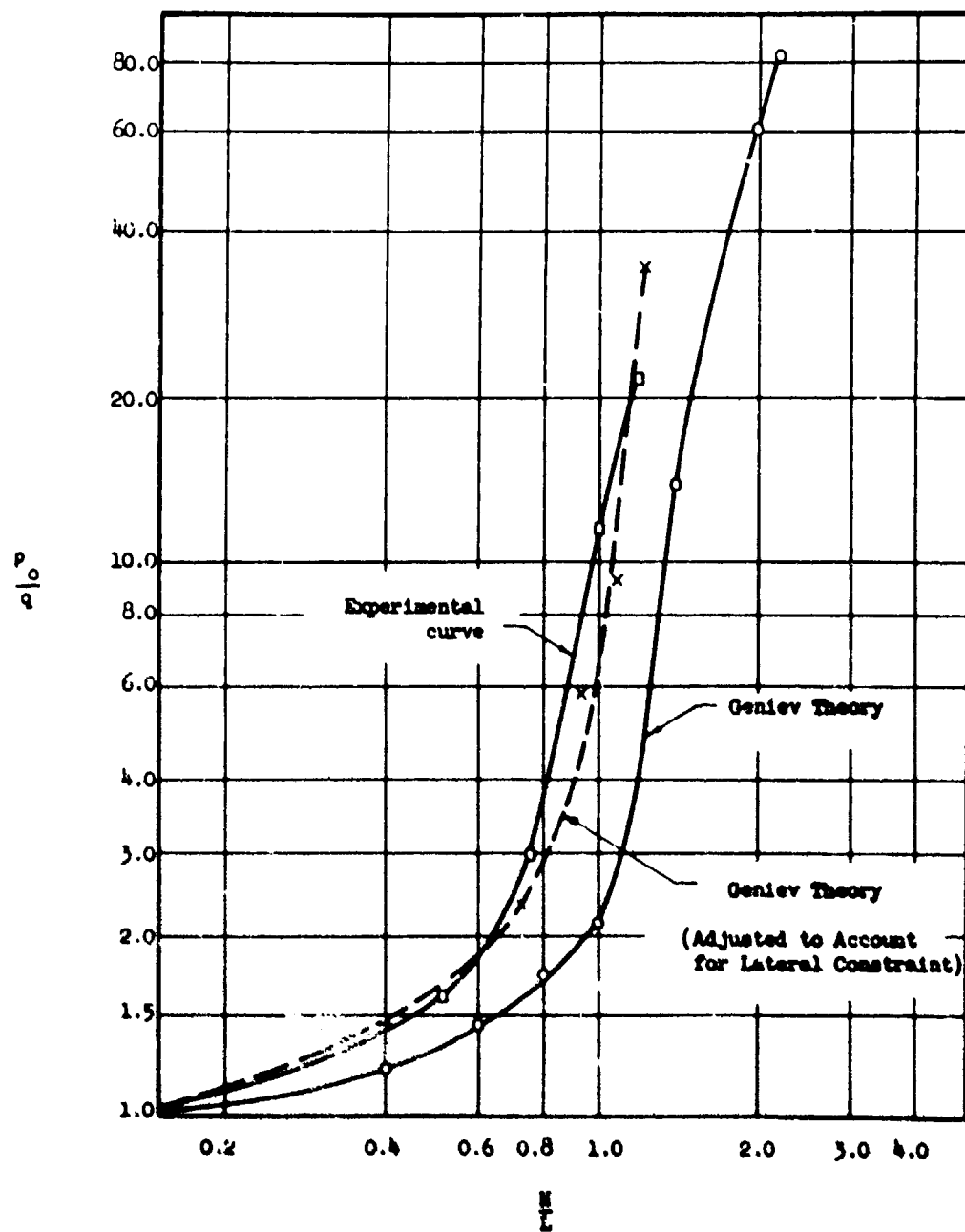
FIG. 6.1 COMPARISON OF GENIEV THEORY WITH

EXPERIMENTAL RESULTS, k = 0, θ = 35°

94
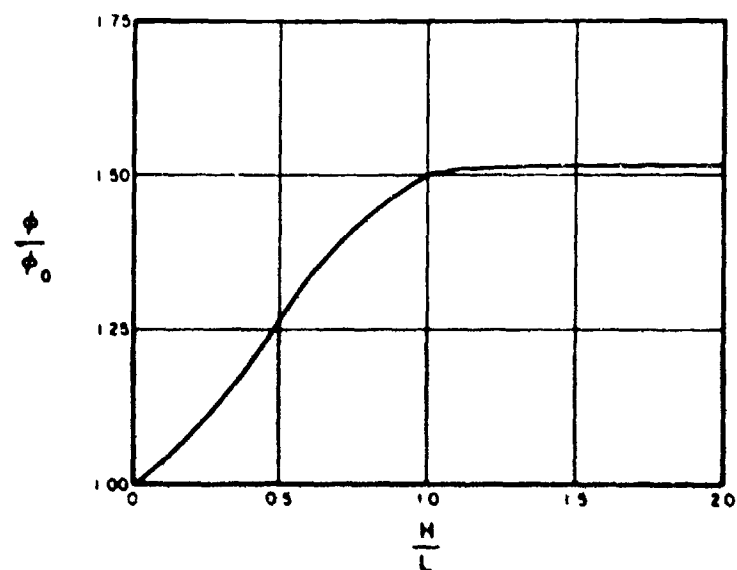
FIG. 6.2 ASSUMED VARIATION OF φ WITH DEPTH TO
ACCOUNT FOR EFFECT OF LATERAL CONSTRAINT
OF THE SOIL
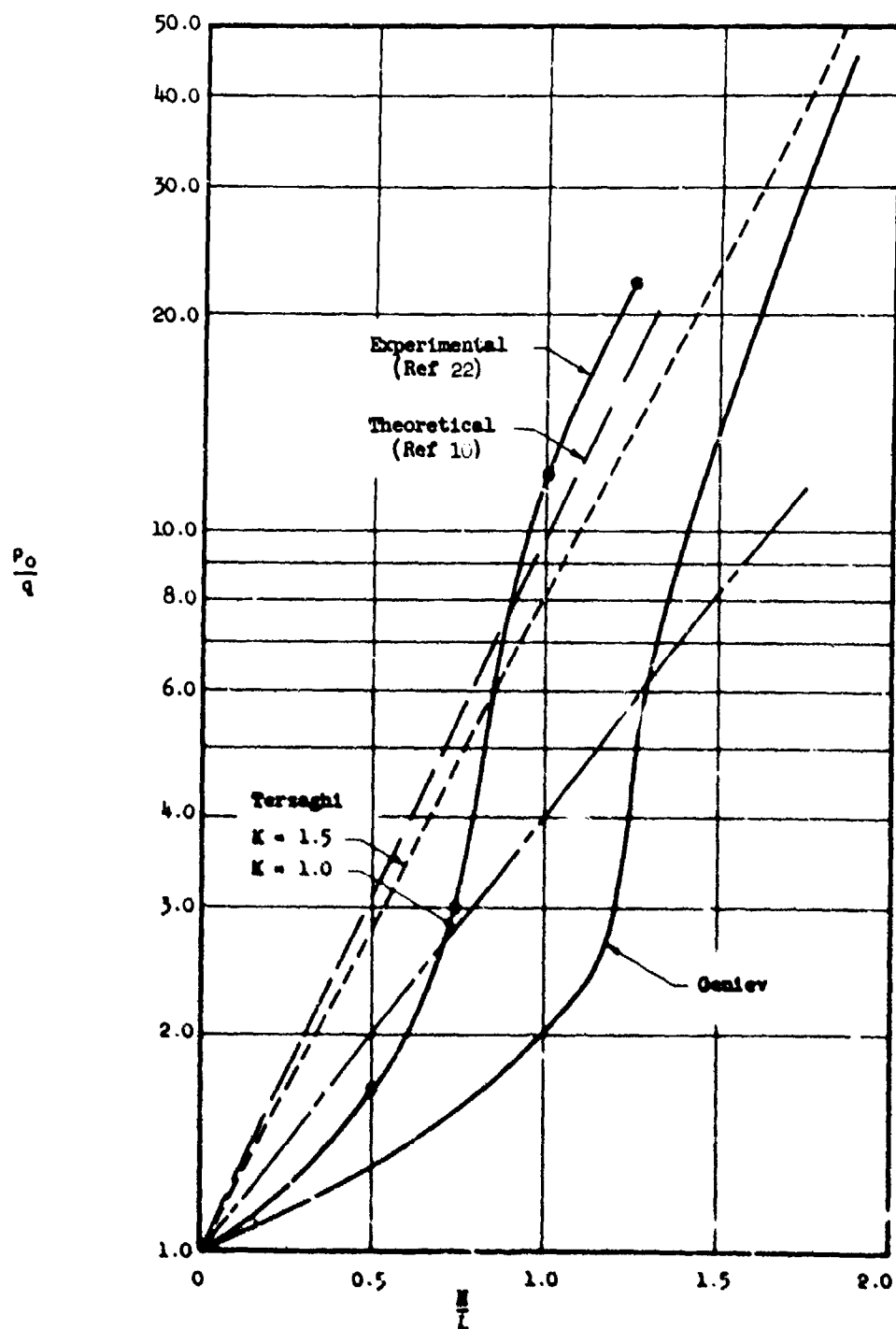
FIG. 6.3 COMPARISON OF FAILURE PRESSURE VS DEPTH CURVES FOR THE
GENIEV, TEMCAMEL, AND SELEG, ET. AL. (REFERENCE 10)
THEORIES, k = 0, θ = 35°

APPENDIX: APPROXIMATE DYNAMIC THEORY FOR SOIL-STRUCTURE INTERACTION

A.1 General

The purpose of this Appendix is to present a simple approximate method of introducing time into the quasi-static solutions obtained in Chapter 5. In developing the approximate method it is assumed that the slip lines found for the quasi-static solution do not change appreciably with time. In this way, a one-dimensional treatment is possible which, for long times, approaches the quasi-static case previously found. For simplicity in this treatment the resistance of the structure was taken as constant.

For extremely short times, of the order of the time for the first effects to reach the structure from the surface above it, it is not easy to give an _a priori_ justification of the present approximate theory. The final evaluation of this approximation will have to await comparison with more exact analytical solutions or with experiments.

We consider here the static problem, treated in Section 5.1, of a long plate below a finite depth of soil layer. The soil layer is supported by a rigid plane except for the part carried by the plate. The static and the quasi-static solutions of this problem with a uniform static load on the top of the soil layer is treated in great detail in the main body of this report. Referring to Fig. A.1, the values of β in the regions OAB and OCD are 0 and $\pm \frac{\pi}{2}$, respectively. In the region OBD, β is given by

$$\beta = \ell - \gamma; \qquad \gamma \leq \ell \leq (\gamma + \frac{\pi}{2})$$

Equation of slip line BD is

$$r = \frac{1}{2} L \, \csc \gamma \; e^{- (\beta - \gamma) \, \tan \varphi}$$

97

The depth of the soil layer as a function of the span of the plate and the angle of internal friction of the soil is given by

$$h = \frac{1}{2} L \left(\cot \gamma + e^{-\frac{\pi}{2} \tan \varphi} \right) \; ; \quad \gamma = \frac{\pi}{4} - \frac{\varphi}{2}$$

$$h_o = \frac{1}{2} L \tan \upsilon \; ; \quad \upsilon = \frac{\pi}{4} + \frac{\varphi}{2}$$

A.2 Basic Equations of Approximate One-Dimensional Problem

The stress components are expressed in the following way:

$$\sigma = \left[\frac{1 + \sin \varphi \, \cos 2\beta}{1 - \sin \varphi \, \cos 2\beta} \right] H(x,t) \qquad \text{(A.2.1a)}$$

$$\sigma_y = H(x,t) \qquad \text{(A.2.1b)}$$

$$\sigma_{xy} = \left[\frac{\sin \varphi \, \sin 2\beta}{1 - \sin \varphi \, \cos 2\beta} \right] H(x,t) \qquad \text{(A.2.1c)}$$

Here $\beta = \beta(x,y)$ is known throughout the region and $H(x,t)$ is unknown. We can isolate a small layer of the soil such as $A_0 \, A_1 \, B_1 \, B_0$ at any height x, and consider the equilibrium of that elemental layer. From Fig. A.2, it can be seen that the layer is acted on by the vertical average stress $\psi(x) \, H(x,t)$ along $A_0 \, B_0$ and the normal and tangential stresses σ_n and τ_n on the inclined faces $A_1 \, A_0$ and $B_1 \, B_0$. The stresses on the inclined faces have to satisfy the boundary condition

$$\tau_n = \sigma_n \tan \varphi$$

To find the normal component σ_n, we refer to Fig. A.3 which shows an elemental soil mass at the inclined boundary with all the stresses acting on its three faces. From Fig. A.3 we have

98

$$\bar{X} = \sigma_x \frac{dy}{ds} + \sigma_{xy} \frac{dx}{ds} = \sigma_x \cos(\beta + \gamma + \varphi) + \sigma_{xy} \sin(\beta + \gamma + \varphi)$$

$$\bar{Y} = \sigma_y \frac{dx}{ds} + \sigma_{xy} \frac{dy}{ds} = \sigma_y \sin(\beta + \gamma + \varphi) + \sigma_{xy} \cos(\beta + \gamma + \varphi)$$

$$\sigma_n = \bar{X} \cos(\beta + \gamma + \varphi) + \bar{Y} \sin(\beta + \gamma + \varphi)$$

$$= \sigma_x \cos^2(\beta + \gamma + \varphi) + \sigma_y \sin^2(\beta + \gamma + \varphi) + \sigma_{xy} \sin 2(\beta + \gamma + \varphi)$$

Using Eqs. (A.2.1) and simplifying, we obtain the normal and tangential stresses to be

$$\sigma_n = \left[\frac{\cos^2 \varphi}{1 - \sin \varphi \cos 2\beta} \right] H(x,t) \qquad (A.2.2a)$$

$$\tau_n = \left[\frac{\sin \varphi \cos \varphi}{1 - \sin \varphi \cos 2\beta} \right] H(x,t) \qquad (A.2.2b)$$

The total vertical component of the normal and tangential stresses is

$$F_x = \sigma_n \cos(\beta + \gamma + \varphi) + \tau_n \sin(\beta + \gamma + \varphi) = \left[\frac{\cos \varphi \cos(\beta + \gamma)}{1 - \sin \varphi \cos 2\beta} \right] H(x,t)$$

The total vertical forces from the two faces $A_0 A_1$ and $B_0 B_1$:

$$2 F_x \, ds = \frac{2 F_x \, dx}{\sin(\beta + \nu)} = 2 f(\beta) \, H(x,t) \, dx$$

where $f(\beta)$ is given by

$$f(\beta) = \left[\frac{\cos \varphi \cos(\beta + \gamma)}{\sin(\beta + \nu) (1 - \sin \varphi \cos 2\beta)} \right]$$

Writing the equation of motion in the vertical direction, we have

$$- \psi H \lambda(x) - \frac{\lambda}{dx} (H \psi) \, dx \, \lambda(x) + H \psi \, \lambda(x) - 2f(\beta) H \, dx + \rho \bar{X} \lambda(x) \, dx =$$

$$= \rho \lambda(x) \, dx \, \varphi_x$$

Here,

$$\psi(x) = \ell(x)^{-1} \int_{-\frac{1}{2}\ell(x)}^{+\frac{1}{2}\ell(x)} \Gamma(\beta) \ dy$$

where

$$\Gamma(\beta) = \left[\frac{1 + \sin \varphi \cos 2\beta}{1 - \sin \varphi \cos 2\beta}\right]$$

$\ell(x)$ = length of the elemental layer at a height x,

X = body force intensity

a_x = acceleration of the layer,

= $\frac{\partial v}{\partial t} + v \frac{\partial v}{\partial x}$, since x is an Eulerian coordinate,

$v(x,t)$ = average velocity of the layer

Simplifying the above expression, we obtain the equation of motion of the layer in the form:

$$X - \frac{1}{\rho}\left[\psi(x)\frac{\partial M}{\partial x} + \zeta(x) M\right] = \frac{\partial v}{\partial t} + \frac{v \partial v}{\partial x} \qquad (A.2.3)$$

where

$$\zeta(x) = \left[\frac{\partial \psi}{\partial x} + 2 \frac{\psi(\beta)}{\ell(x)}\right]$$

the velocity $v(x,t)$ has to satisfy the continuity equation which is of the form.

$$\frac{\partial \rho}{\partial t} + \frac{v \partial \rho}{\partial x} + \frac{\rho \partial v}{\partial x} = 0 \qquad (A.2.4)$$

Here we have two unknowns, $M(x,t)$ and $v(x,t)$, and two equations, (A.2.3) and (A.2.4) to obtain them.

A.3 Expressions for $\beta(x,y)$ and $\ell(x)$

To obtain the function $\psi(x)$, we have to evaluate the integral

$$\psi(x) = \frac{1}{\ell(x)} = \int_{-\frac{1}{2}\ell(x)}^{+\frac{1}{2}\ell(x)} \Gamma(\beta)\ dy$$

This is difficult to do exactly since $\beta(x,y)$ is a complicated function of x and y and, also, the limit $y = \pm\, \ell(x)$ is actually a transcendental function. Instead, we can find an approximate expression for the average value of $\beta(x,y)$ over the range $-h \leq x \leq 0$ as a function of x only. Then,

$$\beta(x,y) = \bar{\beta}(x) \quad \text{and} \quad \Gamma(\beta) = \Gamma(\bar{\beta})$$

We can obtain the function $\psi(x)$ easily as follows:

$$\psi(x) = \frac{\Gamma(\bar{\beta})}{\ell(x)} \int_{-\frac{1}{2}\ell(x)}^{+\frac{1}{2}\ell(x)} dy = \Gamma(\bar{\beta})$$

Now, $\bar{\beta}(x)$ has to satisfy the following conditions:

$$\bar{\beta} = 0, \quad \frac{\partial \bar{\beta}}{\partial x} = 0 \qquad x = 0 \qquad\qquad \text{(A.3.1a)}$$

$$\bar{\beta} = \frac{\pi}{2}, \quad \frac{\partial \bar{\beta}}{\partial x} = 0 \qquad x = -h \qquad\qquad \text{(A.3.1b)}$$

$$\bar{\beta} = v, \qquad\qquad\qquad x = -h \qquad\qquad \text{(A.3.1c)}$$

We can take $\beta(x)$ as a polynomial in x with five constants and obtain the constants to satisfy the conditions (A.3.1). Then we get the following expression for $\bar{\beta}(x)$:

101

$$\bar{\beta}(x) = \pi \frac{x^2}{h^2} \left(\frac{3}{2} + \frac{x}{h}\right) + \pi_\bullet \frac{x^2}{h^2} \left(1 + \frac{x}{h}\right)^2 \qquad (A.3.2)$$

where

$$\pi_\bullet = \left[\frac{v - \pi \frac{h_\bullet^2}{h^2} \left(\frac{3}{2} - \frac{h_\bullet}{h}\right)}{\left(1 - \frac{h_\bullet}{h}\right)^2}\right] \left(\frac{h^2}{h_\bullet^2}\right)$$

Now,

$$\frac{\partial \psi(x)}{\partial x} = \frac{\partial \Gamma(\bar{\beta})}{\partial \bar{\beta}} \cdot \frac{\partial \bar{\beta}}{\partial x}$$

$$= -\left[\frac{4 \sin \varphi \sin 2\bar{\beta}}{(1 - \sin \varphi \sin 2\bar{\beta})^2}\right] \frac{\partial \bar{\beta}}{\partial x}$$

We need this derivative of $\psi(x)$ in evaluating the function $\zeta(x)$.

The function $\mathbf{\mathit{L}}(x)$ which gives the width of the elemental layer at any height x is required to evaluate the function $\zeta(x)$ which is a variable coefficient of Eq. (A.2.3). In cartesian coordinates, if we assign any value for x, we have to compute $\mathbf{\mathit{L}}(x)$ as a solution of a transcendental equation, as the equation of the curve BD in Fig. A.1 is known in polar coordinates. Instead, we can assign values of angle θ in the range γ and $(\gamma + \frac{\pi}{2})$ and then compute the values of $\mathbf{\mathit{L}}(x)$ in a very simple manner from the following equations:

$$\mathbf{\mathit{L}}(x) = \frac{k}{\sin \gamma} \left[\sin \theta \; e^{-(\theta - \gamma) \tan \varphi}\right]$$

$$\theta = \beta + \gamma \qquad (A.3.3)$$

$$\gamma \leq \theta \leq \gamma + \frac{\pi}{2}$$

These equations are useful to compute the functions $\psi(x)$ and $\zeta(x)$ as functions of θ.

A.4 Boundary and Initial Conditions

On the top of the soil layer a uniform load which is a function of time acts vertically down. At the bottom of the soil layer, the component of the stress in the soil normal to the plate at the interface will be the load on the plate so that this is resisted by the inertia of the plate as well as its yield resistance. It is assumed that there is no separation between soil and the plate along the interface so that the velocity of a point of the plate is the same as the adjacent velocity of the soil. Hence, the boundary conditions may be defined as follows:

on the top where $x = -h$

$$\sigma_x = P(t)$$

at the bottom where $x = 0$

$$\sigma_x = \rho_p\, h_p\, \frac{\partial v(0,t)}{\partial t} + K(0,t)$$

where

ρ_p = density of the material of the plate,

h_p = thickness of the plate

K = yield resistance of the plate.

Using Eqs. (A.2.1) the boundary conditions may be written as

$$H\,(-h,t) = \left(\frac{1 + \sin \varphi}{1 - \sin \varphi}\right)\, P(t) \qquad x = -h \qquad (A.4.1a)$$

103

$$H(o,t) = \left(\frac{1 - \sin\varphi}{1 + \sin\varphi}\right)\left(\rho_p\, h_p\, \frac{\partial v(o,t)}{\partial t} + K\right) \qquad x = 0 \qquad (A.4.1b)$$

Tne initial conditions may be

$$H(x,o) = H_o(x) \quad \text{and} \quad v(x,0) = v_o(x) \quad \text{at } t = 0 \qquad (A.4.2)$$

A.5 Method of Solution

Equations (A.2.3) and (A.2.4) are quasilinear with two unknowns $H(x,t)$ and $v(x,t)$ and they can be solved by the method of characteristics. The density of the soil ρ is taken to be a function of pressure, so that

$$\rho = \rho(H)$$

then

$$\frac{\partial \rho}{\partial x} = \frac{d\rho}{dH}\frac{\partial h}{\partial x} = \rho'(H)\frac{\partial H}{\partial x}$$

and

$$\frac{\partial \rho}{\partial t} = \frac{d\rho}{dH}\frac{\partial H}{\partial t} = \rho'(H)\frac{\partial H}{\partial t}$$

where

$$\rho'(H) = \frac{d\rho}{dH}$$

Substituting these expressions into Eq. (A.2.4) we obtain

$$v\frac{\partial H}{\partial x} + \frac{\partial H}{\partial t} + \frac{\rho(H)}{\rho'(H)}\frac{\partial v}{\partial x} = 0 \qquad (A.5.1)$$

Now,

$$\frac{\partial H}{\partial t} = \frac{dH}{dt} - \frac{\partial H}{\partial x}\frac{dx}{dt}$$

$$\frac{\partial v}{\partial t} = \frac{dv}{dt} - \frac{\partial v}{\partial x}\frac{dx}{dt}$$

Substituting these equations into (A.2.3) and (A.5.1) and simplifying, we obtain

104

$$\psi \frac{\partial H}{\partial x} + \rho \left[v - \frac{dx}{dt} \right] \frac{\partial v}{\partial x} = \left[\rho X - \zeta H - \rho \frac{dv}{dt} \right] \qquad \text{(A.5.2a)}$$

$$\left[v - \frac{dx}{dt} \right] \frac{\partial H}{\partial x} + \frac{\rho(H)}{\rho'(H)} \frac{\partial v}{\partial x} = \left[- \frac{dH}{dt} \right] \qquad \text{(A.5.2b)}$$

From Eqs. (A.5.2) we can solve for the partial derivatives of $H(x,t)$ and $v(x,t)$ to get the characteristics and the equations to be integrated along them as follows:

$$\frac{\partial H}{\partial x} = \frac{\begin{vmatrix} (\rho X - \zeta H - \rho \frac{dv}{dt}) & \rho(v - \frac{dx}{dt}) \\ (- \frac{dH}{dt}) & \frac{\rho(H)}{\rho'(H)} \end{vmatrix}}{\begin{vmatrix} \psi(x) & \rho(v - \frac{dx}{dt}) \\ (v - \frac{dx}{dt}) & \frac{\rho(H)}{\rho'(H)} \end{vmatrix}} \qquad \text{(A.5.3)}$$

By setting the denominator equal to zero and simplfying, we find the characteristic equations

$$\frac{dx}{dt} = \left[v \pm \mu(H) \right] \qquad \text{(A.5.4)}$$

where

$$\mu(H) = \sqrt{\psi(x) \frac{dH}{d\rho}}$$

By setting the numerator equal to zero, we find the equations to be integrated along the characteristics:

$$\psi(x) \frac{dH}{dt} \pm \mu(H) \left[\rho \frac{dv}{dt} + \zeta(x) H - \rho X \right] = 0 \qquad \text{(A.5.5)}$$

105

Hence, we have the following set of ordinary differential equations:

$$dx - \left[v + \mu(H) \right] dt = 0$$

$$\frac{\Psi(x)}{\mu(H)} dH + \rho(H)\ dv + \left[\zeta(x)\ H - \rho X \right] dt = 0$$

$$\text{(A.5.6a)}$$

$$dx - \left[v - \mu(H) \right] dt = 0$$

$$\frac{\Psi(x)}{\mu(H)} dH - \rho(H)\ dv - \left[\zeta(x)\ H - \rho X \right] dt = 0$$

$$\text{(A.5.6b)}$$

We have thus reduced the quasilinear partial differential equations, (A.2.3) and (A.2.4) to a set of ordinary differential equations which can be solved numerically by the method of finite differences.

A.6 Method of Finite Differences

Equations (A.5.6) may be written in finite-difference form for the purpose of numerical computation. The first step is to transform Eqs. (A.5.6) to curvilinear coordinates of the characteristics. Let the first and the second characteristics, respectively, be given by

$$U = U(x,t) = \text{constant}$$

$$Z = Z(x,t) = \text{constant}$$

We can take these as curvilinear coordinates and transform Eqs. (A.5.6) from xt-plane to UZ-plane by treating x, t, H and v as functions of U and Z. Along the first system of characteristics we have

$$dx = \frac{\partial x}{\partial Z}\ dZ \qquad ; \qquad dt = \frac{\partial t}{\partial Z}\ dZ$$

$$dH = \frac{\partial H}{\partial Z}\ dZ \qquad ; \qquad dv = \frac{\partial v}{\partial Z}\ dZ$$

106

Similar relations are written for the U-characteristics.

With the help of these relations, Eqs. (A.5.6) may be written in the UZ-plane in the form:

$$\frac{\partial x}{\partial Z} - \left[v + \mu(H) \right] \frac{\partial t}{\partial Z} = 0 \left.\begin{array}{c}\\[2em]\end{array}\right\}$$

$$\frac{\Psi}{\mu(H)} \frac{\partial H}{\partial Z} + \rho \frac{\partial v}{\partial Z} + \left[\zeta H - \rho X \frac{\partial t}{\partial Z} \right] = 0 \left.\begin{array}{c}\\\end{array}\right\} \qquad (A.6.1a)$$

$$\frac{\partial x}{\partial U} - \left[v - \mu(H) \right] \frac{\partial t}{\partial U} = 0 \left.\begin{array}{c}\\[2em]\end{array}\right\}$$

$$\frac{\Psi}{\mu(H)} \frac{\partial H}{\partial U} - \rho \frac{\partial v}{\partial U} - \left[\zeta H - \rho X \right] \frac{\partial t}{\partial U} = 0 \left.\begin{array}{c}\\\end{array}\right\} \qquad (A.6.1b)$$

Now, the derivatives can be written as differences over a finite length as follows:

$$\frac{\partial f}{\partial U} = \frac{f_{k,\ell} - f_{k-1,\ell}}{\Delta U} \quad ; \quad \frac{\partial f}{\partial Z} = \frac{f_{k,\ell} - f_{k,\ell-1}}{\Delta Z}$$

Following this rule, Eqs. (A.5.6) are written as difference equations as shown below:

$$(x_{k,\ell} - x_{k,\ell-1}) - \left[v_{k,\ell-1} + \mu(H_{k,\ell-1}) \right] (t_{k,\ell} - t_{k,\ell-1}) = 0 \qquad (A.6.2a)$$

$$(x_{k,\ell} - x_{k-1,\ell}) - \left[v_{k-1,\ell} - \mu(H_{k-1,\ell}) \right] (t_{k,\ell} - t_{k-1,\ell}) = 0 \qquad (A.6.2b)$$

$$\frac{\Psi_{k,\ell-1}}{\mu(H_{k,\ell-1})} (H_{k,\ell} - H_{k,\ell-1}) + \rho_{k,\ell-1} (v_{k,\ell} - v_{k,\ell-1}) + \qquad (A.6.2c)$$

$$+ \left[\zeta_{k,\ell-1} H_{k,\ell-1} - \rho_{k,\ell-1} X_{k,\ell-1} \right] \Delta t_1 = 0$$

107

$$\frac{v_{k-1,\ell}}{\mu(H_{k-1,\ell})} (H_{k,\ell} - H_{k-1,\ell}) - \rho_{k-1,\ell} (v_{k,\ell} - v_{k-1,\ell}) - \tag{A.6.2d}$$

$$- \left[\zeta_{k-1,\ell} H_{k-1,\ell} - \rho_{k-1,\ell} x_{k-1,\ell} \right] \Delta t_2 = 0$$

Equations (A.6.2a) and (A.6.2b) give the values of x and t at any point (k,ℓ) in the UZ-plane with the known values of x, t, H and v at the previous points $(k-1,\ell)$ and $(k,\ell-1)$. Similarly, Eqs. (A.6.2c) and (A.6.2d) give the values of H and v at the point (k,ℓ) with the known values at the previous points $(k-1,\ell)$ and $(k,\ell-1)$. Using these relations a computational scheme may be easily arrived at.

The network on the UZ-plane is shown in Fig. A.4. AB represents the initial conditions. In the region ABC, along the line AB, we know the values of x, t, H and v, the given initial conditions. At points along $t = 0$, we have the following data:

Points	(6,1)	(5,2)	(4,3)	(3,4)	(2,5)	(1,6)
t	0	0	0	0	0	0
x/h	0	-0.2	-0.4	-0.6	-0.8	-1.0
H	H_{61}	H_{52}	H_{43}	H_{34}	H_{25}	H_{16}
v	v_{61}	v_{52}	v_{43}	v_{34}	v_{25}	v_{16}

We may compute x, t, H and v at various points in the region ABC in the following manner:

$$(6,2) \qquad (5,3) \qquad (4,4) \qquad (3,5) \qquad (2,6)$$

$$(6,3) \qquad (5,4) \qquad (4,5) \qquad (3,6)$$

$$(6,4) \qquad (5,5) \qquad (4,6)$$

$$(6,5) \qquad (5,6)$$

$$(6,6)$$

At each of these points we have the following four equations:

$$(x_{66} - x_{65}) - \left[v_{65} + \mu(H_{65}) \right] (t_{66} - t_{65}) = 0 \qquad \text{(A.6.3a)}$$

$$(x_{66} - x_{56}) - \left[v_{56} - \mu(H_{56}) \right] (t_{66} - t_{56}) = 0 \qquad \text{(A.6.3b)}$$

$$\frac{v_{65}}{\mu(H_{65})} (H_{66} - H_{65}) + \rho_{65} (v_{66} - v_{65}) +$$
$$(\zeta_{65} H_{65} - \rho_{65} X_{65}) \cdot \Delta t_1 = 0 \qquad \text{(A.6.3c)}$$

$$\frac{v_{56}}{\mu(H_{56})} (H_{66} - H_{56}) - \rho_{56} (v_{66} - v_{56}) -$$
$$(\zeta_{56} H_{56} - \rho_{56} X_{56}) \cdot \Delta t_2 = 0 \qquad \text{(A.6.3d)}$$

where

$$\Delta t_1 = (t_{66} - t_{65})$$

$$\Delta t_2 = (t_{66} - t_{56})$$

in the region ACD, we may proceed along the points shown below:

$$(2,7) \qquad (3,7) \qquad (4,7) \qquad (5,7) \qquad (5,7)$$
$$(3,8) \qquad (4,8) \qquad (5,8) \qquad (6,8)$$
$$(4,9) \qquad (5,9) \qquad (6,9)$$
$$(5,10) \qquad (6,10)$$
$$(5,11)$$

To compute the values at the point $(2,7)$:

$$(x_{27} - x_{26}) - \left[v_{26} + \mu(H_{26}) \right] (t_{27} - t_{26}) = 0 \qquad (A.6.4a)$$

$$x_{27} = -h \qquad (A.6.4b)$$

$$\frac{v_{26}}{\mu(H_{26})} (H_{27} - H_{26}) + \rho_{26} (v_{27} - v_{26}) + \qquad (A.6.4c)$$

$$+ (\zeta_{26} H_{26} - \rho_{26} x_{26}) (t_{27} - t_{26}) = 0$$

$$H_{27} = \left(\frac{1 + \sin \varphi}{1 - \sin \varphi} \right) \rho(t_{27}) \qquad (A.6.4d)$$

These equations are to be used at points $(2,7)$, (3.8), $(4,9)$, $(5,10)$ and $(6,11)$, which are the boundary points. At the other points, the same equations as in the region ABC are to be used.

In the region BCE, the values at points are computed in the following manner:

$$(7,2) \qquad (7,3) \qquad (7,4) \qquad (7,5) \qquad (7,6)$$
$$(8,3) \qquad (8,4) \qquad (8,5) \qquad (8,6)$$
$$(9,4) \qquad (9,5) \qquad (9,6)$$
$$(10,5) \qquad (10,6)$$
$$(11,6)$$

To compute the values at the point (7,2) we use the following
equations:

$$(x_{72} - x_{62}) - \left[v_{62} - \mu(H_{62}) \right] (t_{72} - t_{62}) = 0 \qquad \text{(A.6.4a)}$$

$$x_{72} = 0 \qquad \text{(A.6.4b)}$$

$$\frac{v_{62}}{\mu(H_{62})} (H_{72} - H_{62}) - \rho_{62} (v_{72} - v_{62}) \qquad \text{(A.6.4c)}$$

$$- (\zeta_{62} H_{62} - \rho_{62} X_{62}) (t_{72} - t_{62}) = 0$$

$$H_{72} = (\frac{1 - \sin \varphi}{1 + \sin \varphi}) \left[\rho_P h_P \left\{ \frac{v_{72} - v_{62}}{t_{72} - t_{62}} \right\} + K \right] \qquad \text{(A.6.4d)}$$

These equations should be used at points (7,2), (8,3), (9,4),
(10,5) and (11,6) as the boundary points. At other points, the same equations
as in region ABC are used.

In the region DCEF, the unknowns at various points are computed as
follows:

(7,7)	(8,7)	(9,7)	(10,7)	(11,7)
(7,8)	(8,8)	(9,8)	(10,8)	(11,8)
(7,9)	(8,9)	(9,9)	(10,9)	(11,9)
(7,10)	(8,10)	(9,10)	(10,10)	(11,10)
(7,11)	(8,11)	(9,11)	(10,11)	(11,11)

At all these points, same equations as in the region ABC are used.

The region DFG is similar to the region ACD and the region EFI is
similar to the region BCE and so on.

111
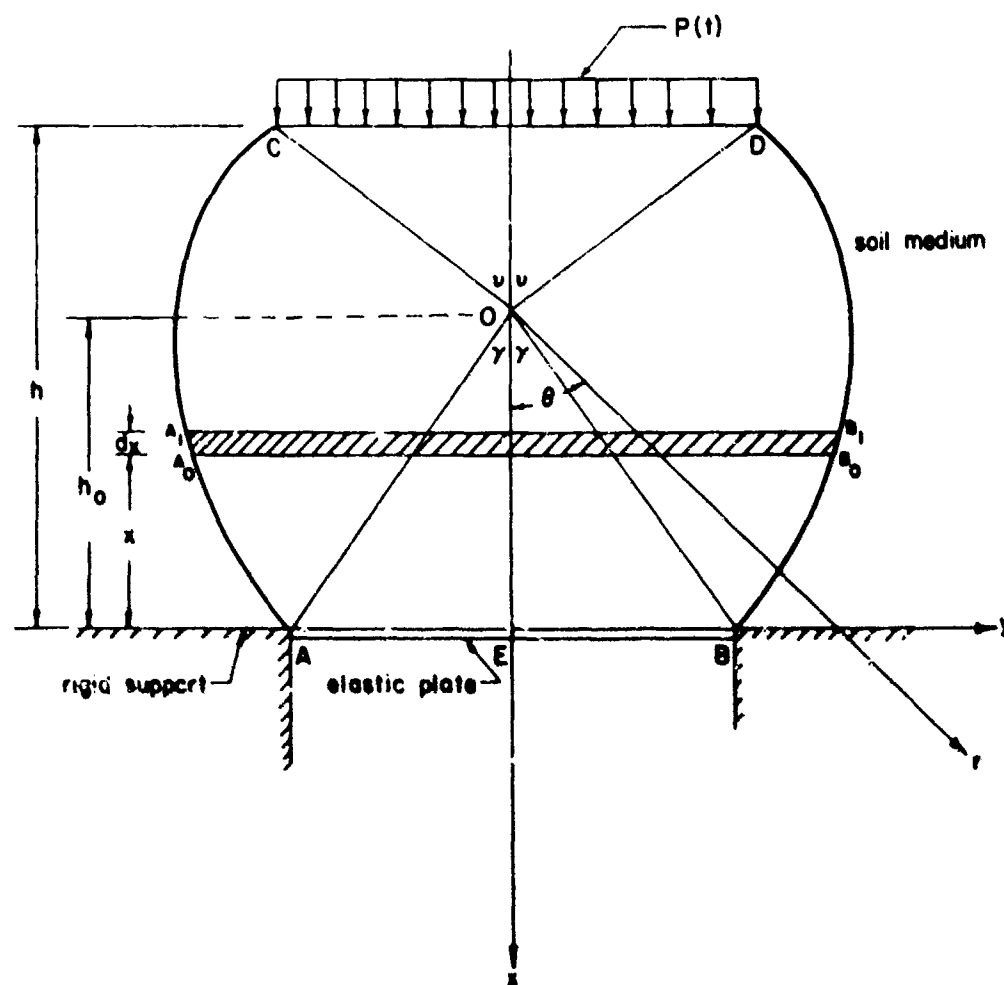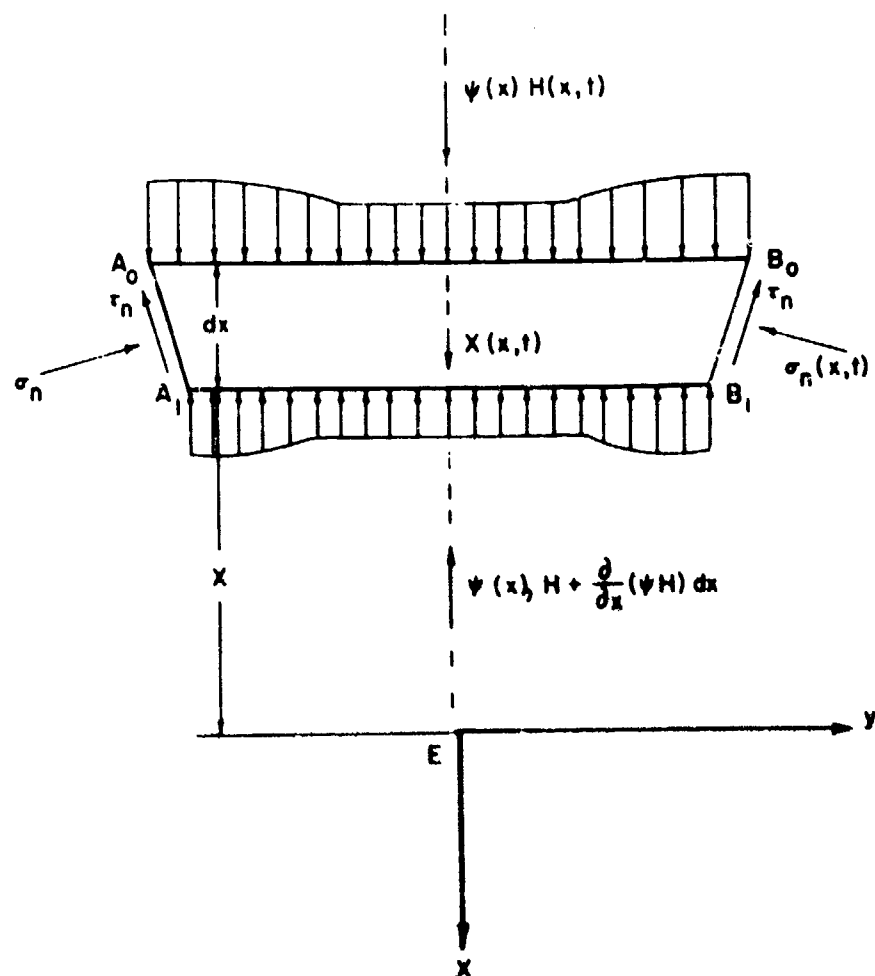
FIG. A.1 SOIL MASS IN CRITICAL EQUILIBRIUM
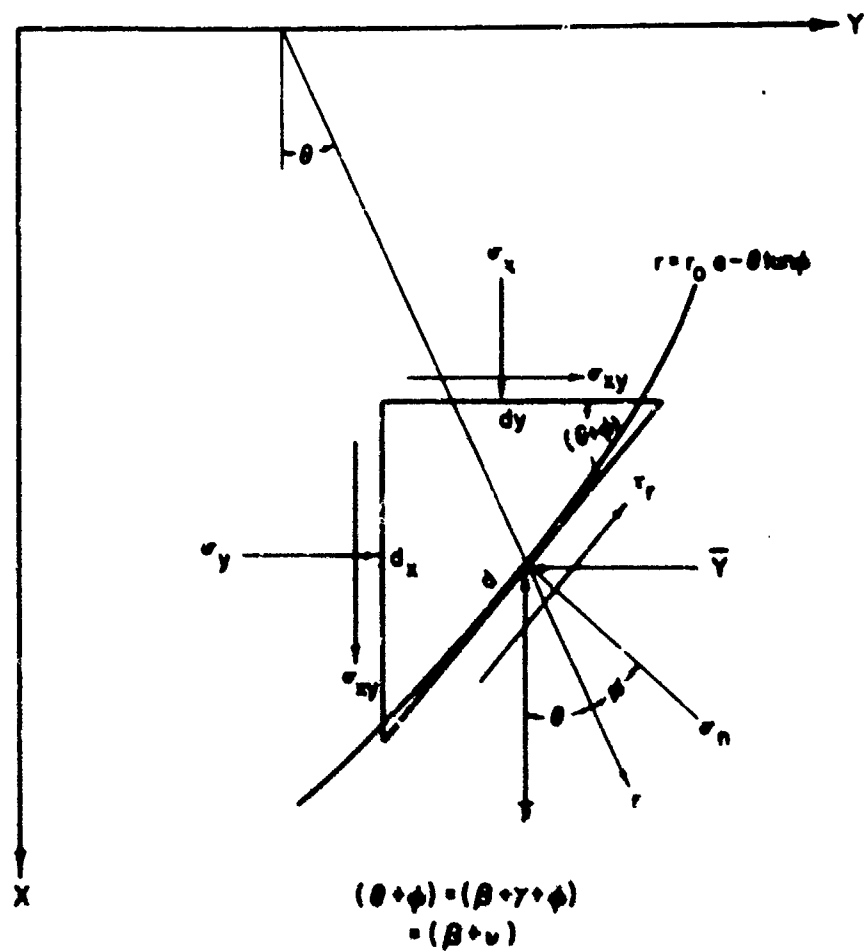
112

FIG. A.2 EQUILIBRIUM OF A SOIL LAYER

113

$$(\theta + \phi) = (\beta + \gamma + \phi)$$
$$= (\beta + \nu)$$

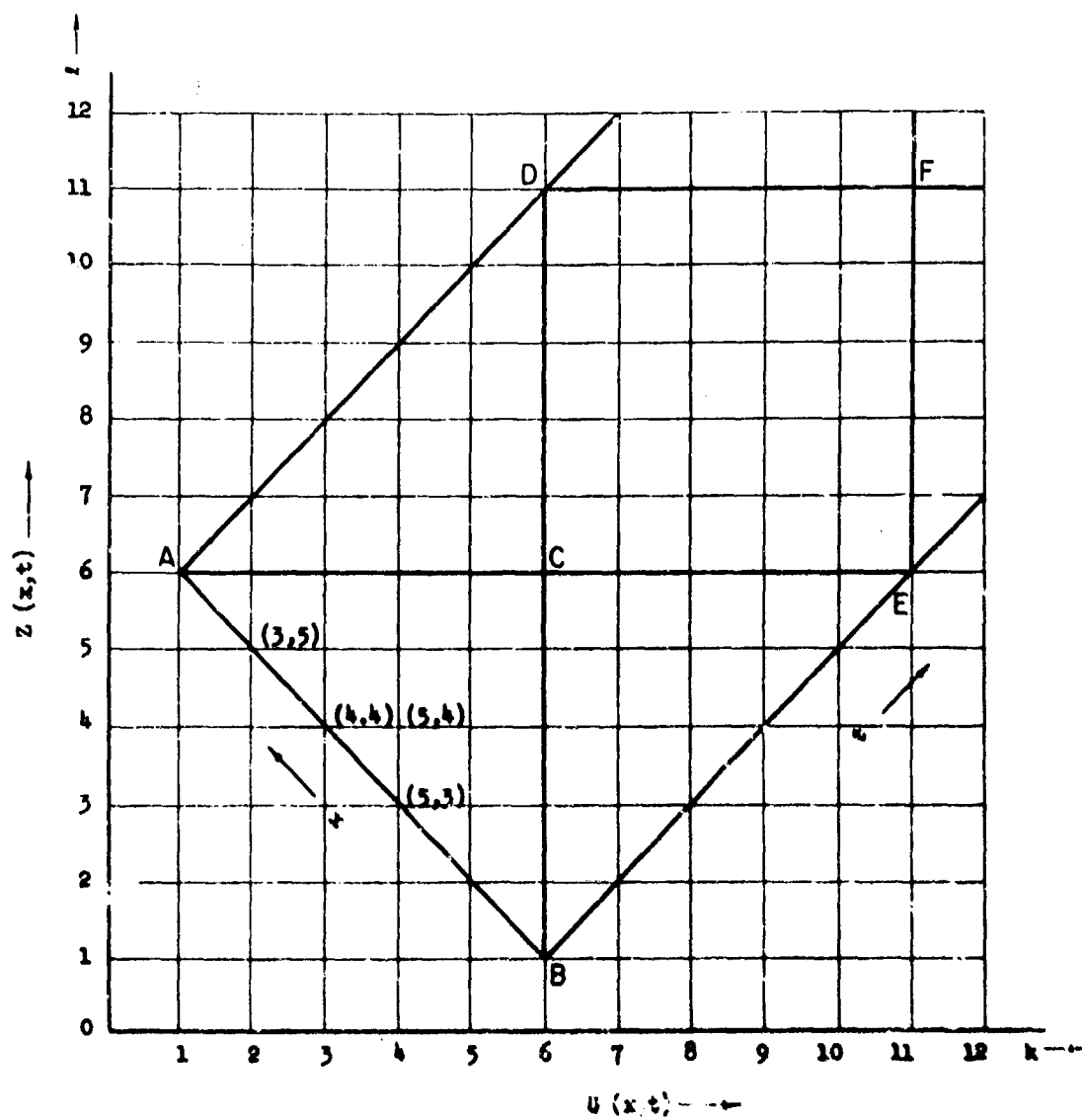FIG. A.3 COMPRESSION AT THE END OF A COIL LAYER

FIG. A.4 NETWORK ON THE UZ-PLANE

115

DISTRIBUTION

No. cys

HEADQUARTERS USAF

1   Hq USAF (AFOCE), Wash, DC 20330

1   Hq USAF (AFRNE-A, Maj Griesmer), Wash, DC 20330

1   USAF Dep, The Inspector General (AFIDI), Norton AFB, Calif 92409

1   USAF Directorate of Nuclear Safety (AFINS), Kirtland AFB, NM 87117

MAJOR AIR COMMANDS

1   AFSC (SCMC), Andrews AFB, Wash, DC 20331

1   AUL, Maxwell AFB, Ala 36112

1   USAFIT, Wright-Patterson AFB, Ohio 45433

AFSC ORGANIZATIONS

1   RTD, Bolling AFB, Wash, DC 20332

1   BSD (BSSF), Norton AFB, Calif 92409

KIRTLAND AFB ORGANIZATIONS

1   AFSWC (SWEH), Kirtland AFB, NM 87117

   AFWL, Kirtland AFB, NM 87117

8   (WLIL)

1   (WLR)

10   (WLRC)

OTHER AIR FORCE AGENCIES

1   Director, USAF Project RAND, via: Air Force Liaison Office, The RAND Corporation, 1700 Main Street, Santa Monica, Calif 90406

ARMY ACTIVITIES

1   Chief of Research and Development, Department of the Army (Special Weapons and Air Defense Division), Wash, DC 20301

1   Director, Ballistic Research Laboratories (Library), Aberdeen Proving Ground, Md 21005

1   Chief of Engineers (ENGMC-EM), Department of the Army, Wash, DC 20315

1   Director, US Army Waterways Experiment Sta (WESWL), P. O. Box 631, Vicksburg, Miss 39181

1   Director, US Army Engineer Research and Development Laboratories, ATTN: STINFO Branch, Ft Belvoir, Va

NAVY ACTIVITIES

1   Bureau of Yards and Docks, Department of the Navy, Code 22.102, (Branch Manager, Code 42.330), Wash 25, DC

DISTRIBUTION (cont'd)

No. cys

1 Commanding Officer, Naval Research Laboratory, Wash, DC 20390

1 Commanding Officer and Director, Naval Civil Engineering Laboratory, Port Hueneme, Calif

1 Commander, Naval Ordnance Laboratory, ATTN: Dr. Rudlin, White Oak, Silver Spring, Md 20390

1 Office of Naval Research, Wash, DC 20360

OTHER DOD ACTIVITIES

1 Director, Defense Atomic Support Agency (Document Library Branch), Wash, DC 20301

1 Commander, Field Command, Defense Atomic Support Agency (FCAG3, Special Weapons Publication Distribution), Dandia Base, NM 87115

1 Director, Advanced Research Projects Agency, Department of Defense, The Pentagon, Wash, DC 20301

1 Office of Director of Defense Research and Engineering, ATTN: John E. Jackson, Office of Atomic Programs, Room 3E 1071, The Pentagon, Wash, DC 20330

20 Hq Defense Documentation Center for Scientific and Technical Information (DDC), Bldg 5, Cameron Sta, Alexandria, Va 22314

AEC ACTIVITIES

1 Director, Los Alamos Scientific Laboratory (Helen Redman, Report Library), P. O. Box 1663, Los Alamos, NM 87554

OTHER

1 Grumman Aircraft Engineering Corp, Research Dept, Special Projects Section, ATTN: Dr. Hyman R. Garnet, Bethpage, NY

1 Cornell University, Applied Mechanics Dept, ATTN: Dr. Y. H. Pao, Thurston Hall, Ithaca, NY

1 Paul Weidlinger Associates, Consulting Engineers, ATTN: Dr. M. L. Baron, 777 Third Avenue, New York, NY 10017

1 Illinois Institute of Technology, Research Institute, Mechanics Research Division, ATTN: Mr. M. Salmon, 33 West 34 Street, Chicago 16, Ill

1 General American Transportation Corp, MRD Division, 7501 N. Natchez Avenue, Niles 48, Ill

1 Stanford Research Institute, ATTN: Dr. Roy Alverson, 333 Ravens Wood, Menlo Park, Calif

 University of Illinois, Urbana, Ill

5 (Dr. Art Robinson, Dept of Civil Engineering)

1 (Dr. N. M. Newmark, Dept of Civil Engineering)

1 (Prof A. P. Boresi, Dept of Theoretical and Applied Mechanics)

DISTRIBUTION (cont'd)

No. cys

1	Northrop-Ventura, ATTN: Dr. R. P. Branaugh, 1515 Rancho Conejo Blvd, Newbury Park, Calif
1	The MITRE Corp, P. O. Box 208, Bedford, Mass
1	Massachusetts Institute of Technology, ATTN: Dr. Robert V. Whitman, Dept of Civil and Sanitary Engineering, 77 Massachusetts Avenue, Cambridge 39, Mass
1	North Carolina State College, School of Engineering, ATTN: Dean Ralph Fadum, Raleigh, NC
1	Portland Cement Association, Research and Development Laboratories, ATTN: Mr. Eivind Hognestad, Manager, Structural Development Section, 5420 Old Orchard Road, Skokie, Ill
1	Agbabian-Jacobsen and Associates, ATTN: Dr. Lydik S. Jacobsen, 8939 S. Sepulveda Blvd, Los Angeles 45, Calif
	Michigan College of Mining and Technology, Houghton, Mich
1	(Prof Frank Kerekes, Dean of the Faculty)
1	(Dr. George A. Young, Head, Dept of Civil Engineering)
1	St Louis University, Institute of Technology, Dept of Geophysics and Geophysical Engineering, ATTN: Prof Carl Kisslinger, 3621 Olive Street, St Louis 8, Mo
1	University of Michigan, School of Civil Engineering, ATTN: Prof Frank E. Richart, Jr., Ann Arbor, Mich
1	OTS, Department of Commerce, Wash 25, DC
1	Official Record Copy (Lt J. E. Johnson, WLRC)

DOCUMENT CONTROL DATA - R&D

(Security classification of title, body of abstract and indexing annotation must be entered when the overall report is classified)

1. ORIGINATING ACTIVITY (Corporate author)	2a. REPORT SECURITY CLASSIFICATION
University of Illinois, Dept of Civil Engineering Urbana, Illinois	Unclassified
	2b. GROUP

3. REPORT TITLE

A QUASI-STATIC THEORY OF SOIL-STRUCTURE INTERACTION

4. DESCRIPTIVE NOTES (Type of report and inclusive dates)

5. AUTHOR(S) (Last name, first name, initial)

Bedesem, W. B., Das, Y. C., Robinson, A. R.

6. REPORT DATE	7a. TOTAL NO. OF PAGES	7b. NO. OF REFS
September 1964	125	35

8a. CONTRACT OR GRANT NO.	9a. ORIGINATOR'S REPORT NUMBER(S)
AF 29(601)-4508	
b. PROJECT NO. 1080	WL TDR-64-91
c. TASK: 108003	9b. OTHER REPORT NO(S) (Any other numbers that may be assigned this report)
d. DASA WEB No. 13.078	

10. AVAILABILITY/LIMITATION NOTICES

Qualified requesters may obtain copies of this report from DDC.

11. SUPPLEMENTARY NOTES	12. SPONSORING MILITARY ACTIVITY
	AFWL (WLRC) Kirtland AFB, NMex 87117

13. ABSTRACT

This study treats the effect of the interaction between underground structures and the surrounding soil in reducing the loads transmitted to the structure, the so-called "arching" phenomenon. A continuum theory of soils proposed by G. A. Geniev is applied to a quasi-static, plane-strain problem of arching. The basic partial differential equations are shown to form a hyperbolic set and are solved by the method of characteristics. Consistent stress and velocity fields are obtained. Comparison with available experimental results shows that the Geniev theory underestimates the surface pressure required for failure of an underground structure in relatively dense granular soils. The source of this difficulty is explained and an approximate method of overcoming it is presented. A simplified extension to a theory taking account of inertia of the soil and unsteady motions is treated in an appendix.

DD FORM 1473

14.		LINK A		LINK B		LINK C	
KEY WORDS		ROLE	WT	ROLE	WT	ROLE	WT
"Arching" phenomenon							
Continuum theory of soils							
Quasi-static							
Plane-strain							
Differential equations							
Hyperbolic set							
Stress and velocity fields							
Geniev theory							
Surface pressure							
Underground structure							
Inertia of soil							
Unsteady motions							

INSTRUCTIONS

1. ORIGINATING ACTIVITY: Enter the name and address of the contractor, subcontractor, grantee, Department of Defense activity or other organization (corporate author) issuing the report.

2a. REPORT SECURITY CLASSIFICATION: Enter the overall security classification of the report. Indicate whether "Restricted Data" is included. Marking is to be in accordance with appropriate security regulations.

2b. GROUP: Automatic downgrading is specified in DoD Directive 5200.10 and Armed Forces Industrial Manual. Enter the group number. Also, when applicable, show that optional markings have been used for Group 3 and Group 4 as authorized.

3. REPORT TITLE: Enter the complete report title in all capital letters. Titles in all cases should be unclassified. If a meaningful title cannot be selected without classification, show title classification in all capitals in parenthesis immediately following the title.

4. DESCRIPTIVE NOTES: If appropriate, enter the type of report, e.g., interim, progress, summary, annual, or final. Give the inclusive dates when a specific reporting period is covered.

5. AUTHOR(S): Enter the name(s) of author(s) as shown on or in the report. Enter last name, first name, middle initial. If military, show rank and branch of service. The name of the principal author is an absolute minimum requirement.

6. REPORT DATE: Enter the date of the report as day, month, year; or month, year. If more than one date appears on the report, use date of publication.

7a. TOTAL NUMBER OF PAGES: The total page count should follow normal pagination procedures, i.e., enter the number of pages containing information.

7b. NUMBER OF REFERENCES: Enter the total number of references cited in the report.

8a. CONTRACT OR GRANT NUMBER: If appropriate, enter the applicable number of the contract or grant under which the report was written.

8b, 8c, & 8d. PROJECT NUMBER: Enter the appropriate military department identification, such as project number, subproject number, system numbers, task number, etc.

9a. ORIGINATOR'S REPORT NUMBER(S): Enter the official report number by which the document will be identified and controlled by the originating activity. This number must be unique to this report.

9b. OTHER REPORT NUMBER(S): If the report has been assigned any other report numbers (either by the originator or by the sponsor), also enter this number(s).

10. AVAILABILITY/LIMITATION NOTICES: Enter any limitations on further dissemination of the report, other than those

imposed by security classification, using standard statements such as:

(1) "Qualified requesters may obtain copies of this report from DDC."

(2) "Foreign announcement and dissemination of this report by DDC is not authorized."

(3) "U. S. Government agencies may obtain copies of this report directly from DDC. Other qualified DDC users shall request through

                                                            ."

(4) "U. S. military agencies may obtain copies of this report directly from DDC. Other qualified users shall request through

                                                            ."

(5) "All distribution of this report is controlled. Qualified DDC users shall request through

                                                            ."

If the report has been furnished to the Office of Technical Services, Department of Commerce, for sale to the public, indicate this fact and enter the price, if known.

11. SUPPLEMENTARY NOTES: Use for additional explanatory notes.

12. SPONSORING MILITARY ACTIVITY: Enter the name of the departmental project office or laboratory sponsoring (paying for) the research and development. Include address.

13. ABSTRACT: Enter an abstract giving a brief and factual summary of the document indicative of the report, even though it may also appear elsewhere in the body of the technical report. If additional space is required, a continuation sheet shall be attached.

It is highly desirable that the abstract of classified reports be unclassified. Each paragraph of the abstract shall end with an indication of the military security classification of the information in the paragraph, represented as (TS), (S), (C), or (U).

There is no limitation on the length of the abstract. However, the suggested length is from 150 to 225 words.

14. KEY WORDS: Key words are technically meaningful terms or short phrases that characterize a report and may be used as index entries for cataloging the report. Key words must be selected so that no security classification is required. Identifiers, such as equipment model designation, trade name, military project code name, geographic location, may be used as key words but will be followed by an indication of technical context. The assignment of links, rules, and weights is optional.